THE UNIVERSITY OF CHICAGO

UBIQUITOUS ACTUATION

A DISSERTATION SUBMITTED TO

THE FACULTY OF THE DIVISION OF THE PHYSICAL SCIENCES

IN CANDIDACY FOR THE DEGREE OF

DOCTOR OF PHILOSOPHY

DEPARTMENT OF COMPUTER SCIENCE

BY

ALEX MAZURSKY

CHICAGO, ILLINOIS

MARCH 2025

For my Nana, Judy May.

Contents

List of Figures

List of Tables

Acknowledgments

First and foremost, I thank my advisor and mentor, Prof. Pedro Lopes, for his guidance and patience throughout my time at the Human Computer Integration Lab. Pedro's feedback has shaped not only how I approach solving problems but also telling stories. If not for this, I would not have understood the importance of a research vision beyond tackling individually exciting problems. Throughout these years, Pedro always pushed me beyond my comfort zone and that is where all the real growth occurred. Because of his mentorship, I can confidently take with me a greater sense of creativity, critical thinking, and vision. What an immense privilege it has been to have had this opportunity to work together.

I would like to thank my exceptional and understanding committee members, Prof. Ken Nakagaki and Prof. Jin Ryong Kim. Ken's expertise in both actuation and interaction design has been an invaluable perspective, and his vision is a major inspiration of this work. I look forward to watching you create a much more actuated world. My thanks to Jin Ryong for inspiring me with his works in haptics and thermal feedback. On multiple occasions, I would try your lab's demos at conferences and be completely blown away. I remember going back home after conferences and reproducing these incredible illusions on myself and labmates. There was once another version of this dissertation that centered more on thermal, but I was always chasing your work!

Thank you to my fellow PhD students in the Human Computer Integration Lab for all their support, dedication, and feedback: Jas Brooks, Shan-Yuan Teng, Jasmine Lu, Romain Nith, Yudai Tanaka, and Yun Ho. I could always count on you to try my pilot studies and help shoot videos. I'll miss having lunch together nearly every day.

I would not be the researcher I am today if not for the mentors I have been lucky to have over the years. Prof. Jeong-Hoi Koo sparked my interest in research, showed me how to follow my

curiosity while thinking critically, and instilled the value of mentoring others. Prof. Tae-Heon Yang's mechanical intuition, dedicated attitude, and fast-paced workflow inspired the type of researcher I've always aspired to be. Prof. Sarah Sebo supported me experimenting with robot social touch for ~1 year in her lab, where I learned so much from her about rigorous study design and the proper statistics. During my time at Meta, Dr. Priyanshu Agarwal showed me how to break problems down into priorities and address electromechanical challenges swiftly.

Much of these projects were supported by brilliant undergraduate students: Andre de la Cruz, Aryan Gupta, Jacob Serfaty, Beza Desta, Dasha Shifrina, Joyce Passananti, Svitlana Midianko, and Boris Li. If I could teach you a fraction of what you taught me, then great success!

Thank you to the fantastic researchers within HCI that offered valuable input on these projects at key stages: Rob Kovacs, Craig Shultz, and Yasha Iravantchi, just to name a few. Thank you to the many external, anonymous reviewers over the years that strengthened our contributions.

Thank you to the University of Chicago's CS department for providing a space to those of us that do applied work like HCI and hardware. It has been amazing to see our community ramp up over the years. Thank you to everyone in the weekly People and Tech seminars for being a supportive community and for all the feedback on early versions of this work. Thank you to UChicago's MRSEC and CDAC, who helped to fund this work.

Thank you to my family: my mom Lauren and Papa (Dr. Ronald May) for believing in me. Thank you to my sisters and cousins for always providing an outlet to laugh. Thank you to Paul Goetze for always being there to talk shop and bikes.

Finally, my deepest thanks to my wife, Natalie, who embarked on this journey equally with me and never wavered. Looking forward to this next one!

Abstract

As computing has become ubiquitous, transitioning from desktops to mobile devices to wearables, our environments have been augmented with a myriad of sensors (e.g., your home may have dozens of sensors). However, the proliferation of actuators - devices capable of creating physical motion or haptic effects - has lagged behind (how many does your home have?). This is due to a key challenge facing haptic devices: high power consumption. Unlike sensors, which can often operate on just microwatts, actuators require orders of magnitude more power, making it impractical to densely instrument entire environments with them due to battery maintenance. This power constraint has hindered the realization of ubiquitous actuation: the seamless integration of actuated and haptic devices at scale.

To overcome this challenge, we propose engineering actuator architectures and working principles with scale in mind from the start. Notably, we do not add batteries to the environment; instead, we place them on the user to power wearable actuators. These actuators enable scale since they are one-to-many: one wearable actuator can add actuation to many otherwise passive objects and surfaces, transforming them into interactive devices. We apply these principles to present a series of actuators to achieve vibration, friction, and thermal feedback at scale. Along the way, we interrogate and circumvent the limitations of traditional actuators through new materials (e.g., soft and stretchable magnets) and working principles (e.g., microfluidics). Finally, we demonstrate a generalizable approach to actuation at scale through a wearable wireless power transmitter that powers battery-free devices during interaction. Our approach offers a lens into the future in which even any seemingly passive object or surface can respond through actuation, without the constraints that have typically limited actuation at scale.

Introduction

This chapter introduces the motivation behind ubiquitous actuation, our targeted approach to realize it, and the core contributions of this dissertation.

Ubiquitous Computing is Missing Actuation

Computing has become ubiquitous, transitioning from desktops to mobile devices to wearables, steadily realizing Weiser's vision of computation seamlessly integrated into everyday environments [270]. This evolution has enabled environments densely instrumented with sensors—a modern home may contain dozens of sensors monitoring everything from occupancy to temperature to air quality to even touch. However, the proliferation of actuators—devices capable of creating physical motion or haptic effects—has lagged significantly behind. This disparity is striking: while a smart home might contain numerous sensors [301], it typically contains very few actuators for providing physical feedback to users.

This asymmetry between sensing and actuation stems from a fundamental challenge: power consumption. Unlike sensors, which can often operate on just microwatts of power, actuators require orders of magnitude more energy [251]. A typical capacitive touch sensor might consume mere microwatts, while even a small vibration motor requires tens of milliwatts to watts of power [249]. This power gap makes it impractical to densely instrument environments with actuators; the burden of maintaining batteries or power connections becomes inconvenient at scale.

The implications of this power constraint extend beyond mere technical limitations—they fundamentally restrict the realization of truly interactive environments. While we can detect user interactions virtually anywhere through distributed sensing, our ability to provide physical feedback remains confined to specific locations where power is readily available. This limitation

has created an experiential asymmetry in ubiquitous computing: environments that can sense extensively but respond physically only sparingly.

Previous approaches to this challenge have largely focused on reducing actuator power consumption or developing more efficient power delivery systems [105]. However, these efforts, while valuable, do not address the core scalability challenge. The fundamental issue persists: as the number of actuated devices in an environment increases, the complexity and maintenance burden of powering them grows unsustainably. This leads to a practical ceiling on the density of actuated interfaces we can deploy, limiting the broader vision of ubiquitous computing where any surface or object can potentially provide physical feedback.

This constraint has particularly stunted haptic interfaces, which rely on actuation to create physical sensations. While visual and auditory feedback can be provided through centralized displays and speakers, haptic feedback inherently requires actuators at the point of interaction. This locality requirement, combined with the power challenge, has made ubiquitous haptic feedback especially difficult to achieve. The result is that while our environments have become increasingly responsive in terms of visual and auditory feedback, they remain largely "static" in terms of physical interaction.

Addressing this fundamental challenge requires rethinking not just how we power actuators, but how we *architect systems for ubiquitous actuation*. Rather incrementally improving existing approaches, we need new paradigms that fundamentally change the relationship between power sources and actuators in ubiquitous computing environments. This dissertation presents such a shift, proposing and validating new approaches to enabling haptics and actuation at scale.

Our Approach: User-Worn Power for Environmental Actuation

To overcome the power challenge that has limited actuation at scale, we propose engineering actuator architectures and working principles with scale in mind from the start. Notably, we do not add batteries to the environment; instead, we place them on the user to power wearable actuators. These actuators enable scale since they are one-to-many: one wearable actuator can add actuation to many otherwise passive objects and surfaces, transforming them into interactive devices.

This enables new possibilities for ubiquitous actuation. By moving the power source (and associated electronics) to a wearable form factor, we can (1) design passive elements in the environment that actuate only when the user interacts with them (as in *MagnetIO* and *Power-On-Touch*) or (2) overlay virtual sensations on top of passive surfaces and objects in the environment (as in *Stick&Slip* and *ThermalGrasp*). This circumvents the challenge of deploying actuated interfaces: rather than maintaining hundreds of battery-powered devices, we maintain only the user-worn components while allowing the environmental elements to remain entirely passive.

We validate this approach through four distinct technical implementations over the next four chapters, each exploring a different modality of haptic feedback: (1) vibration, (2) friction, (3) temperature, and (4) a generalized approach to power.

Vibration: MagnetIO

First, *MagnetIO* (Chapter 2) demonstrates this principle through vibrotactile feedback. By wearing a battery-powered electromagnetic coil on their fingernail, users can energize passive magnetic patches placed throughout their environment, causing them to vibrate on touch. The patches themselves require no power source or electronics yet provide localized haptic feedback comparable to traditional vibration motors.

Friction: Stick&Slip

Second, *Stick&Slip* (Chapter 3) extends this approach to friction modulation. Rather than instrumenting surfaces with electrostatic or ultrasonic actuators, we use a wearable device to dispense engineered liquids that temporarily modify surface friction. This enables friction-based haptic effects on virtually any non-absorbent surface without requiring power at the point of interaction.

Temperature: ThermalGrasp

Third, *ThermalGrasp* (Chapter 4) applies this principle to thermal feedback. Instead of distributing powered Peltier elements throughout the environment, it places them in wearable locations and uses flexible thermal conductors to transfer temperature changes to points of interaction. This enables thermal sensations while preserving natural interaction with physical objects.

Power: Power-on-Touch

Finally, *Power-on-Touch* (Chapter 5) generalizes this approach beyond specific haptic modalities. By wearing inductive power transmission coils, users can wirelessly power any compatible device during interaction. This demonstrates how the principle of user-worn power sources can extend beyond haptics to enable general actuation at scale.

Contributions

This dissertation advances the field of ubiquitous computing by proposing and validating a new architectural approach to enabling actuation at scale. Rather than placing batteries throughout the environment, our approach moves the power source to wearable devices that can actuate multiple passive elements in the environment. Our key contributions are:

1. **An architectural shift** in how we power ubiquitous actuators. We demonstrate that by placing power sources on users rather than in the environment, we can enable scalable actuation while minimizing maintenance burden. This is validated through four distinct technical implementations.
2. **Novel techniques** for enabling specific haptic modalities at scale:
    a. A method for creating passive yet interactive vibrotactile patches using soft magnetic materials (*MagnetIO*)
    b. An approach to friction modulation using engineered liquid coatings (*Stick&Slip*)
    c. A technique for providing thermal feedback while preserving natural interaction by redirecting heat through flexible conductors (*ThermalGrasp*)
3. **A generalized approach** to power transfer during interaction (*Power-on-Touch*) that extends beyond haptics to enable battery-free operation of both sensors and actuators in ubiquitous environments.
4. **Technical evaluations and user studies** demonstrate that our approach can effectively deliver haptic sensations while being practical to deploy at scale. Our results show that moving power sources to wearables can enable rich interactions without compromising user experience.

Through these contributions, this dissertation provides a foundation for researchers and practitioners to create environments with ubiquitous actuation, advancing us closer to truly interactive ubiquitous computing. To facilitate this, we have open-sourced our hardware and code for others to build upon at: lab.plopes.org

MagnetIO: Passive yet Interactive Soft Haptic Patches Anywhere

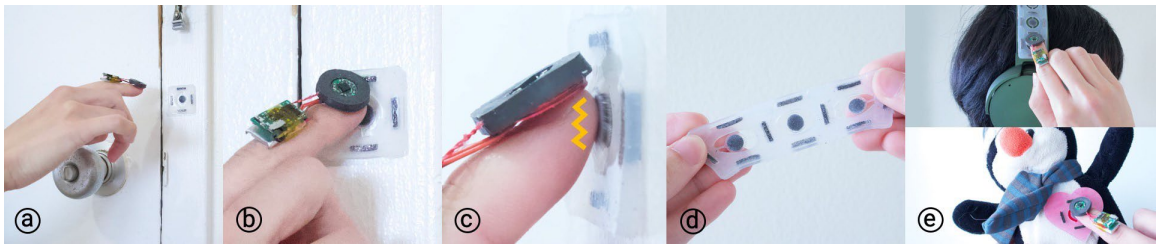

Figure 1. (a) We propose a new type of haptic actuator, which we call MagnetIO, that is comprised of two parts: *any number* of soft interactive patches that can be applied anywhere and *one* battery-powered voice-coil worn on the user's fingernail. (b) When the fingernail-worn device contacts *any* of the interactive patches it detects its magnetic signature and (c) makes the patch *vibrate*. (d) To allow these otherwise passive patches to vibrate, we make them from silicone with regions doped with neodymium powder, resulting in soft and stretchable magnets. (e) This novel decoupling of traditional vibration motors allows users to add interactive patches to their surroundings by attaching them to walls, objects or even other devices or appliances without instrumenting the object with electronics. Photos taken by author unless otherwise stated.

In this chapter, we propose a new type of haptic actuator, which we call MagnetIO [151], that demonstrates vibrotactile haptics at scale.

Introduction

Today's interactive devices increasingly instrument every kind of surface, effectively adding interactive functionality even to passive everyday objects such as walls, tables, and rapidly prototyped objects [56, 138, 273, 302, 303], as well as to the user's body [168, 170, 269]. To enable sensing these interactions, researchers engineered conformable/stretchable sensing devices so that these can comfortably fit around non-planar surfaces, which is the case for everyday objects or the human body. This led to a mature field of on-body or on-object *sensing* technologies that are easy to deploy and ideal for prototyping or enabling interactions in ubiquitous settings.

However, the converse is not the case, while sensing can be done in a distributed fashion around the user and in conformable form-factor, the same is not true for *actuation*. Researchers are still looking for techniques that allow deploying large numbers of actuators without the constraints of power delivery to every single individual actuator, wireless communication across all actuators, microcontrollers, etc. As a result, while we have a range of interactive techniques to deploy sensing "patch"-like devices everywhere, these patches typically do not exhibit any form of haptic response, i.e., they can sense the user's touch (e.g., to turn on/off the user's home-alarm) but they cannot vibrate in response to that touch (e.g., to indicate the alarm is on/off), not at least, without requiring vibration motors or other haptic actuators, which in turn require batteries and circuitry. Ultimately, all these dramatically limit the ubiquitous application of these interactive patch-like devices.

In this paper, we engineered and explored a new alternative for adding haptic feedback to everyday surfaces, which is depicted in Figure 1 (Note: photos in this dissertation were taken by the author unless otherwise stated). Our approach, which we call *MagnetIO*, introduces a new type of haptic actuator that is passive (i.e., requires no electronics, no battery, etc.) until the user's finger, which is instrumented with a wearable voice-coil, touches it, causing it to vibrate.

Our Approach: MagnetIO

MagnetIO is composed of *many* passive interactive patches and *one* nail-worn device, which features a miniaturized and custom-engineered voice-coil, inertial measurement unit (IMU), battery, microcontroller and wireless. MagnetIO's complete voice-coil and circuitry fits entirely on the user's fingernail, thus leaving the fingerpad unobstructed to feel interactions with the user's environment and the vibrations from our passive patches.

The design principle that enables our interactive patches to vibrate is that they are made from silicone doped with neodymium powder, resulting in stretchable magnets that are thus attracted/repelled by the wearable coil. Conceptually, we liken our approach to a linear resonant actuator (LRA, typical vibration element in most commercial mobile devices), which is comprised of a magnet attached on a spring and a coil, which we depict in Figure 2.

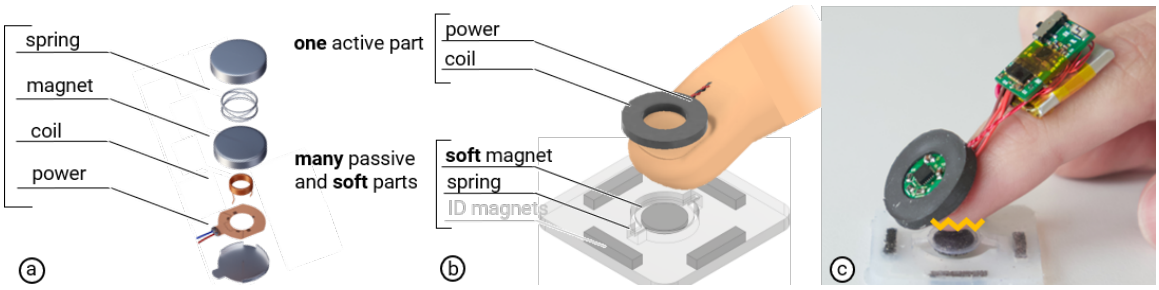

Figure 2. (a) Our device is built from the same principle as traditional linear resonant actuators (LRA), i.e., based on moving a magnetic mass using a coil and a spring. (b-c) However, our device decouples these components into two parts: *one* active element containing the coil, which the user wears on their fingernail; and, *many* passive elements, which are comprised of silicone with regions doped with neodymium powder which together realize a spring & magnet.

To better illustrate our design, we make an analogy to the inner workings of an LRA: when current is supplied to the LRA's coil, it produces a magnetic field which attracts or repels the magnet. By performing this multiple times, the momentum of this *magnet-spring* assembly creates a feelable vibration (Figure 2a).

In our case, our design takes a sharp conceptual turn from that of the LRA as we *purposely decouple* the magnet-spring from the coil (Figure 2b). This allows us to scale up the output by placing *many* spring-magnet pairs everywhere, which are activated when the user's wearable coil contacts them (Figure 2c). The advantage is that our design requires only *one* coil, meaning it also only requires *one* driver circuit, *one* communication module and *one* battery. Furthermore, all our interactive patches are passive since we implement them using silicone, an elastic material that

allows us to achieve the "spring" component; subsequently, some regions are doped with neodymium powder, which allows us to realize the "magnet." Therefore, our soft-magnets realize the "spring-magnet" component typical of LRAs. The result is that MagnetIO patches are easy to place anywhere because they are stretchable and soft, and yet they deliver haptic output to the user, appearing as interactive patches.

Moreover, unlike approaches that attach vibration actuators directly to the user's fingerpad, MagnetIO can trigger vibrations whenever a user touch any of our haptic patches, while simultaneously leaving the user's fingerpad free (thus, minimizing impacts to dexterity).

Note that while our main contribution is *on realizing haptic output* for these soft patches via our soft magnets, we also demonstrate one possible sensing mechanism by using the magnetic signature of the patches themselves, i.e., the user's fingernail-worn device detects the unique ID of each patch by using a 3DOF magnetometer to read each patch's unique 3D magnetic field (see details in *Implementation*). Naturally, there are several other possible passive implementations, each with their idiosyncratic pros/cons, such as RFIDs [66, 179, 267], acoustic IDs [78], optical (barcodes [88], QR codes [229, 246], Anoto pen-like patches [231]), etc.

Related Work

The work presented in this paper builds primarily on the fields of ubiquitous interfaces, especially instrumented interactive surfaces, and haptics, with emphasis on soft and magnetic-based actuators.

Adding Input to Everyday Objects and Surfaces

To enable the vision of ubiquitous computing [271], many researchers have engineered techniques that add input to everyday objects and surfaces. A common approach to adding input to objects is

to apply a flexible resistive or capacitive sheet to the surface [174, 218, 303]. For example, PrintSense [56] utilized an network of electrodes printed on a flexible substrate to add input to surfaces. Electrick [302] combined conductive materials with Electric field tomography to achieve touch input on a wider variety of objects, such as tools and toys. Similarly, ObjectSkin [60] used hydroprinting to transfer sensors and circuits onto irregular objects. Sprayable User Interfaces [273] enabled large-scale interactive surfaces via spray-on sensors. Additionally, many other techniques are available, even acoustic techniques have been used to add touch input to objects [175].

Passively Adding Input to Everyday Objects and Surfaces

The key issue with the previous approaches is that they all add electronics onto the objects they are enabling. As such, we quickly reach a limit to the vision of ubiquitous interfaces, as all objects require batteries, circuits, etc. As an alternative to this, researchers have investigated *passive* input techniques. Passive input is advantageous in that it does not require instrumenting the object with electronics, but instead, typically instruments the user with sensors, such as cameras, etc. For instance, computer vision can be used to detect interaction with surroundings, as demonstrated by early works like Light Widgets [52] and more recently with depth cameras as in WorldKit [282]. Acoustic techniques can also be used for passive input: Acoustic Barcodes [78] and Scratch Input [77] both utilized the physical surface roughness of objects to detect input. Furthermore, electrical techniques are another popular method for passive input; notably Touché [216] realizes gestural detection on any electrically conductive surface and time-domain reflectometry adds multitouch to wires [277]. Finally, 3D printed ferromagnets have been used to encode information directly in 3D printed objects; allowing users to scan the object with a magnetometer, like how one would

scan a conventional barcode. Here, users swipe their smartphone's magnetometer across the surface of the object to read out its unique magnetic identifier [96].

Adding Haptic Output to Everyday Objects and Surfaces

When it comes to adding haptic output to everyday objects and surfaces, the most common technique to instrument objects with haptic feedback is to simply embed actuators within the device, as we do with mobile phones [192, 194, 292]. However, this approach tends to lack haptic fidelity and design flexibility. One versatile solution to this challenge was put forth by *Magtics*, which introduced a tactile array of rigid actuators inside a flexible casing that could conform to curved objects [182]. *Tactlets* also explored a flexible form factor for adding electrovibration feedback to everyday objects [59].

Evidently, when compared with adding input to the environment, adding haptics is far less explored. The limitations that we discussed for active sensing (i.e., it requires electronics & batteries on every object) become dramatic for haptic output, because haptic actuators require even more power than their sensing counterparts. To overcome this limitation, MagnetIO takes a sharp conceptual turn with respect to the traditional design of a haptic device, it decouples the device into two parts: *one* active that the user carries and *many completely passive parts*, that can be attached to objects and surfaces without the need for electronics.

Conceptually, our proposal relates to Sekiguchi et al.'s "Ubiquitous haptics" vision, in which any interactive device around the user's environment, be it a surface or an everyday object, was not only added with input capability but *also displays haptic feedback* [220]; they proposed realizing vision this using active haptic devices based on motorized actuators. We build on this concept but allow this to scale to practical uses with *many* devices. This is only possible because, instead, our concept uses *passive* patches applied ubiquitously in the user's environment, rather

than requiring batteries & electronics inside every surface or object the user interacts with. For our passive patches to produce actual haptic feedback, we were inspired by two hardware techniques: (1) soft actuators and (2) magnetic actuators, which we discuss below.

Soft Actuators

Advances in materials science and mechanical engineering brought soft actuators to interactive devices. A wide range of soft actuators have been developed based on different working principles: pneumatics [4, 247, 261], hydraulics [72, 74], acoustofluidics [5], electroactive polymers [25, 44, 295, 304], twisted and coiled polymers [68], gels [156], and electrorheological and magnetorheological fluids [97, 147, 148, 208, 228, 287]. Many have been adapted to realize deformable devices, shape-changing output, and so forth [6, 23, 199]. For instance, HapBead [74] added a bead in a soft microfluidic channel around the finger pad to generate tactile sensations caused by the bead moving around. HapSense [295] demonstrated a wearable electroactive polymer for tactile feedback. MagnetIO differs from the approach in *HapSense* by its decoupling between the active and passive components. Additionally, MagnetIO is made from softer materials (silicone vs. PVDF), allowing it to conform to more irregular objects and body parts.

Recently, researchers in soft robotics have become particularly interested in soft magnetic materials for sensing and actuation (note that in these mechanics-focused works, and in this paper, "soft" refers to the low-modulus of the materials involved, rather than the magnetic properties). Unlike electrically-controlled or fluid-driven systems, magnetic materials lend themselves well to *untethered* operation because they may be sensed and actuated without contact. For example, magnetic microrobots may be steered within an environment by controlling an external magnetic field [89, 285]. Additionally, magnetic skins have been used as tactile and wearable sensors with minimal need for wiring [7, 80]. Research on fabrication has demonstrated the ability to design

soft magnets with custom polarity by manipulating the applied magnetic field during curing; this allows for tunable behavior when the cured magnet is exposed to a field, resulting in programmable shapes and locomotion [89, 140, 285].

Magnetic-based Haptics

Magnets have been used to convey haptic feedback across a wide range of applications. Permanent magnets have been identified as a passive actuator (no electrical power required) for providing haptic feedback [236, 289–291, 305, 306]. However, permanent magnets lack control; they cannot be turned off and the intensity of their feedback can only be changed by physically displacing them. Thus, many interactive devices rely on electromagnets so that the output magnetic force is controllable [235, 255].

Many of the proposed systems are based on 2D electromagnet arrays. For example, *FingerFlux* utilized an array of electromagnets with a nail-mounted permanent magnet to provide haptics on tabletops [272]. Similarly, Actuated Workbench used magnets to move tangibles on a table [257]. More recently, *M-Hair* proposed coating the body's hair in iron powder so that it may receive haptic feedback from electromagnets moved on top of the user's skin [24]. However, the arrays of electromagnets used here are extremely bulky and prevent wearable, mobile and/or scalable form factors.

To make magnetic actuators more mobile, many devices rely on custom electromagnetic coils. For instance, *Magnetips* designed a single coil worn on the back of mobile devices for delivering feedback to a nail-worn permanent magnet [153]. *Magtics* created a flexible haptic device based on the hybrid of hard electromagnetic actuators in a flexible case [182].

Unfortunately, prior approaches to magnetic-based haptics do not easily scale to many applications because: (1) they require power; (2) the magnets are rigid, so they cannot conform to

objects or the human body. To address these issues, MagnetIO uses *one* wearable coil and *many* interactive patches made from flexible silicone and stretchable magnets. The result is the first *one-to-many* system for ubiquitous vibrotactile haptics.

Walkthrough: Adding MagnetIO Patches Everywhere

To give the reader a complete picture of how MagnetIO allows a user to control their environment with ad-hoc interactive haptic patches, we describe a walkthrough via the example of a user in their home, using our MagnetIO patches to control a wide-range of interactive appliances such as internet-of-things (IoT) devices.

Figure 3a shows our user, wearing our wearable voice-coil on their index finger, walking into their home. Figure 3b shows that as they walk in, they tap a MagnetIO patch that has been attached to their door. In response to tapping the patch, they feel two consecutive vibrations (*tzzz*, pause, *tzzz*) confirming that their home-alarm is now disabled, which is depicted in Figure 3c. Note that this user can also perform this action *in the dark* (i.e., eyes-free, which we did not illustrate for the sake of visual clarity) because our MagnetIO patches are inherently haptic interfaces designed to vibrate on touch.

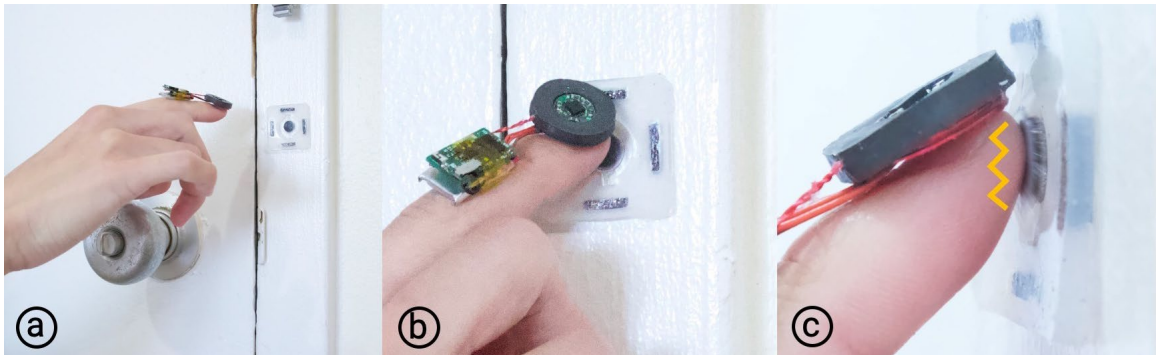

Figure 3. (a) Our user at home, wearing our coil, surrounded by surfaces with interactive patches. (b) They tap their wall, which has a passive patch that controls their home alarm. (c) The user feels the patch vibrate to indicate that their alarm is now disabled.

Now that we depicted an interaction with MagnetIO from the user's perspective, let us examine what is happening from the device's perspective. In other words, we will describe how our patches work to deactivate the user's IoT home alarm. Figure 4 depicts the principle behind MagnetIO interactions. First, as depicted in Figure 4a, as the user taps on the patch to deactivate their home-alarm, the wearable-coil approaches the patch and senses its ID, i.e., the wearable-coil recognizes that the particular patch the user is touching is the "home-alarm" ON/OFF patch. To sense the ID of a patch, the wearable-coil makes use of its inertial measurement unit, which includes a 3DOF magnetometer. Using the magnetometer data, the wearable-coil detects the patch that the user is interacting with by comparing the current reading to pre-trained magnetic signatures. These magnetic signatures are just an example of one many possible ways our system could sense the ID of each patch (refer to *Implementation* for details). Alternatively, our system could utilize a wide variety of sensing mechanisms, such as RFIDs [66, 179], acoustic IDs [78], optical IDs [229, 246], etc. After the wearable-coil has identified that the user touched the "home-alarm" patch, it communicates to the user's IoT home-alarm via its Bluetooth module, informing it to switch to the "OFF" state. Finally, as depicted in Figure 4b, the home-alarm confirms the new state by sending a message to the wearable-coil, which the wearable device renders *haptically* by energizing the coil in a vibrotactile pattern. This creates a magnetic field which in turn attracts the magnetically-doped region of the interactive patch, making the patch vibrate under the user's finger.

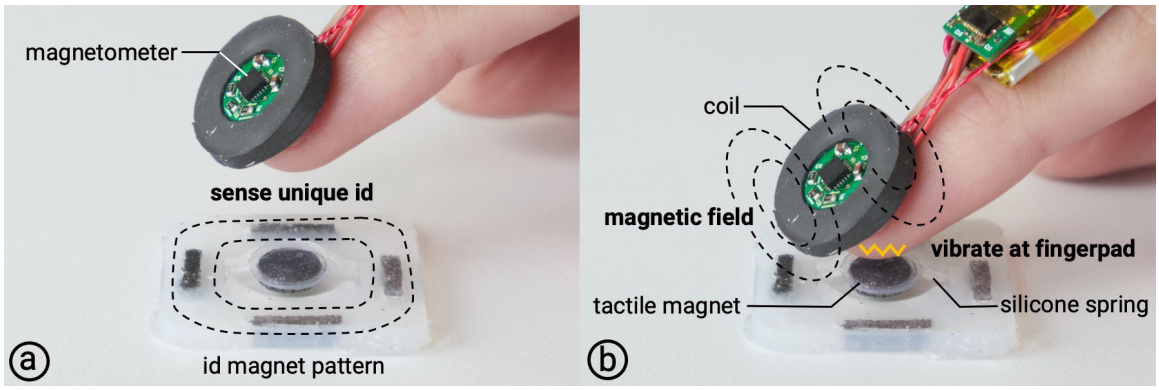

Figure 4. (a) When the user's finger approaches an interactive patch, its magnetometer reads and recognizes its unique 3D magnetic ID and (b) activates the wearable-coil, generating a magnetic field that vibrates the patch under the fingerpad.

Next, as depicted in Figure 5a, the user taps on another patch on the wall to adjust their thermostat. Figure 5b, depicts how the user slides their finger across the patches, at each step, they feel a short vibration that haptically signals each temperature level. However, as depicted in Figure 5c, when they cross the middle patch, they feel a strong vibration (a haptic detent) that indicates that this is the last used setting.

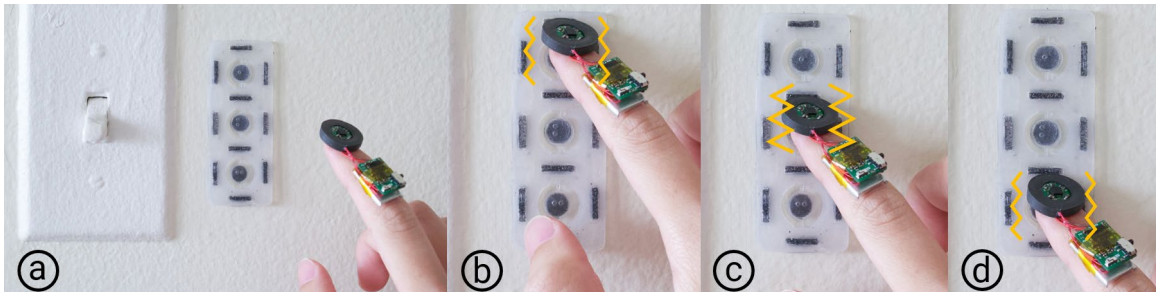

Figure 5. The user touches the top magnet and slides their finger down to the middle magnet where they feel the strongest vibration, indicating the last setting used and continue to slide down to the bottom to reset the thermostat to the lowest setting.

MagnetIO patches are versatile because they are *passive*, made from stretchable silicone. Figure 6a illustrates how our user detaches a patch from the wall and attaches it to new objects. These patches are sticky as their underside is made of a layer of skin safe adhesive, making our

patches also suitable for ad-hoc on-body interfaces. In fact, MagnetIO patches are even weather-proof. For instance, Figure 6d depicts a user washing their smart kettle instrumented with an interactive patch. Because MagnetIO's patches operate via magnetism alone (for both sensing and actuation, no circuitry is inside the patch), the interaction will not be affected so long as the wearable coil remains dry.

Figure 6. (a) The user peels off the patch. Because our interactive patches are *passive* and *soft*, they can be applied to a variety of objects: (b) smartwatch bracelet, (c) water bottle, (d) and even washed (still works while wet).

Besides our sticker patch, we also implemented a strap-like patch, depicted in Figure 7, that can be wrapped around objects, such as handles, bottles, etc. These types of patches are ideal for cylindrical objects such as the gaming controller depicted in Figure 7a. In Figure 7, our user stretches the patch around the grip of the controller, which enhances its functionality by allowing them to mode-switch in their game, while keeping their eyes on the game menu; again, an eyes-free interaction.

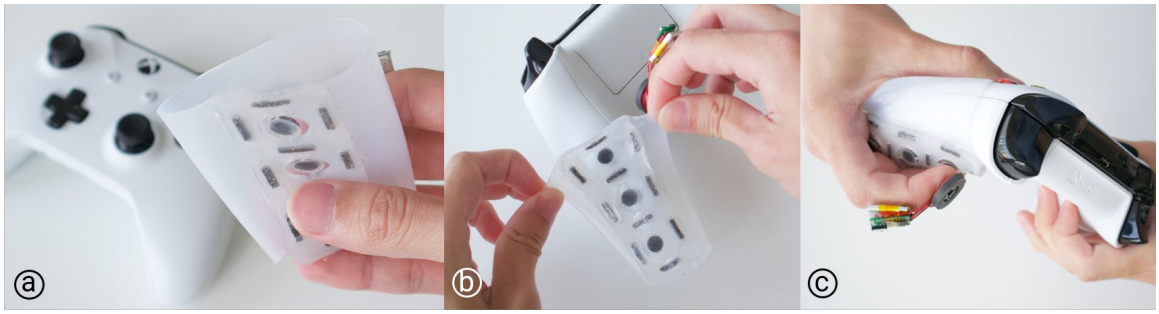

Figure 7. (a) The user holds a strap-like patch and (b) stretches it around their gaming controller, enabling (c) an eyes-free I/O space for controlling modes and menus.

Now, the user's partner, who is Blind, walks into the room. Despite being visually-impaired, their partner also makes use of MagnetIO patches to control their home. Since MagnetIO are interactive *haptic* patches, they can serve as useful interfaces for visually-impaired users. Especially, because MagnetIO patches are simply cast from silicone, one can add *tactile bumps* that encode messages in Braille, as depicted in Figure 8. This allows our visually-impaired user to use the thermostat interface by adding a side patch with Braille annotations. The user then feels the Braille to know which patch this is e.g., "thermostat" or "setting 1", and so forth (Figure 8b), and then make use of MagnetIO's vibrations to know they have selected a setting on the interface (Figure 8c). Alternatively, this information can be embedded into simple haptic vibration patterns.

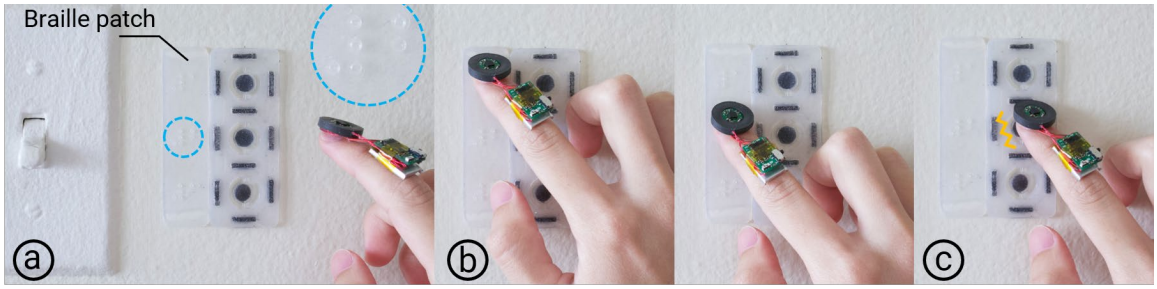

Figure 8. Since our interactive patches are made from silicone, they may easily include Braille to assist Blind users.

While our walkthrough exhibits the key principles behind how MagnetIO allows to deploy haptic patches everywhere, these do not depict an exhaustive list. We designed MagnetIO to be

attached to many more objects and believe that it will inspire researchers to use, or even create, passive haptics patches that can be anywhere.

Contribution and Limitations

Our key contribution is that we propose, explore, and engineer conformable interactive patches that can be placed ubiquitously to provide touch input and more importantly haptic feedback. The conceptual result of MagnetIO is the first *one-to-many* system for ubiquitous vibrotactile haptics.

Our approach has the following benefits: (1) while traditional actuators each require their own power supply/electronic-circuits, MagnetIO decouples the powered coil component from the passive magnetic elements, allowing us to actuate *many* interactive patches using only *one* active component, resulting in haptics patches that scale; (2) our interactive skins offer a conformable I/O space that can adapt to many shapes and body parts that pose challenging to existing, rigid actuators (LRAs, etc.); (3) our nail-worn device leaves the fingerpad free to interact with one's surroundings, yet haptic sensations are still delivered directly to the fingerpad; (4) our fabrication technique enables customizable geometries, magnetic fields and even aesthetics; (5) in contrast haptic devices based solely on permanent magnets, the use of our wearable coil allows us to program custom tactile waveforms and/or turn off haptic sensations only-on demand, i.e., these are truly interactive.

Our approach is limited in that: (1) the use of soft elements has its downsides, as our actuators are subject to mechanical losses from hysteresis and yield a reduced magnetic field strength when compared to rigid, sintered magnets; (2) our approach only generates haptic sensations when the wearable-coil is on top of the soft patch, i.e., these patches cannot vibrate by themselves, which is why we believe they are useful for adding vibrations to touch based-interactions; (3) the object being instrumented with our interactive patches must be larger than the patches themselves; lastly,

(4) as our approach is based on magnets it is not advised for instrumenting ferromagnetic objects, as these attract the magnets and dampen the resulting vibrations.

Implementation

To help readers replicate our design, we now provide the necessary technical details and fabrication process. Furthermore, to accelerate replication, we provide all the source code for our implementation.

MagnetIO devices have two principal components: (1) *many* of our silicone-based interactive **passive patches**, which have regions doped with neodymium powder ($Nd_2Fe_{14}B$) and can be attached to surfaces; and (2) our **nail-worn device,** which can make our patches vibrate via its electromagnetic coil; the latter is entirely self-contained, i.e., it has input (via a 9DOF IMU), output (electromagnetic coil), processing, battery and wireless.

Mechanics of our Passive Patches that can Vibrate

The key behind the design of our patches is that they embody the same mechanics that allow a linear-resonant actuator (LRA) to vibrate, yet they are stretchable and passive. In other words, they implement a mass and spring, depicted in Figure 9, that respond to applied magnetic field. Because of silicone's intrinsic elasticity, it naturally behaves like a spring. To allow the soft magnet to achieve amplitudes needed for "feelable" vibrations, we designed the spring mechanism as a long and slender beam (3.75 mm length, 0.5 mm thickness). Furthermore, we found that an optimal 1 mm for the beam-spring's width maximized feelable vibrations (see *Technical Evaluation* for details).

Moreover, as depicted in Figure 9b, we designed the hollow cutout at the center of each patch with a diameter of 9 mm, which is slightly smaller than 10-14 mm of the average fingerpad

diameter [42]. Thus, as the fingerpad lands on the center of the patch, it is mostly supported by the silicone walls outside the cutout. This allows the magnet to vibrate freely in the airgap and contact the fingerpad even when the finger pushes down.

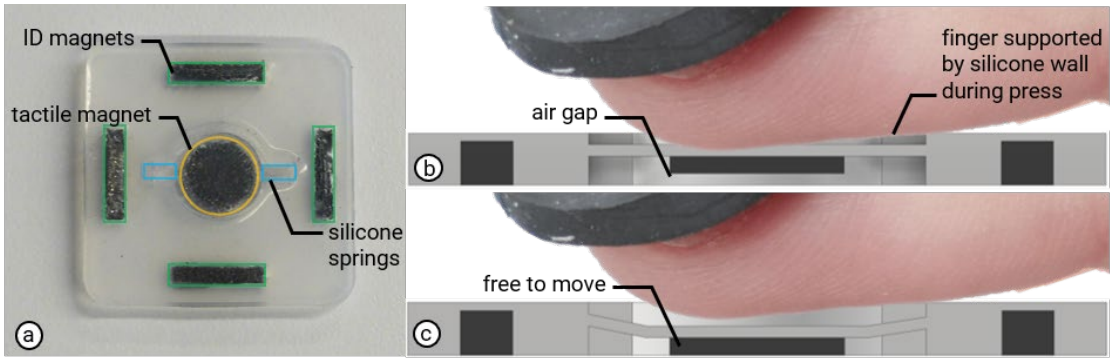

Figure 9. The key mechanism behind our soft magnets: (a) this thin beam act as a spring that connects the magnet (dark region at center) to the base (silicone around it, with cut-outs). (b, c) Schematic side view depiction of our mechanics that allow the magnet to vibrate even as the user presses down; note that as the fingerpad lands on the center of the patch, it is mostly supported by the silicone walls outside the cutout.

Fabrication of our Soft Magnets: Doping Silicone with Magnetic Powder

Our passive patches are made of two parts: a soft stretchable magnet made of silicone mixed with permanent magnetic powder ($Nd_2Fe_{14}B$) adhered to a flexible silicone mechanism that enables vibration.

Prior to the start of the fabrication, the magnetic powder is filtered through a 200 µm mesh. Smaller particles allow for more stretchability, as we validated in our *Technical Evaluation*.

Figure 5 illustrates our fabrication process. First, we fabricate our 1.5 mm soft magnets by mixing the silicone (Dragonskin FX Pro) and NdFeB powder. The mixture is hand-stirred for 10 minutes and cast to a 3D printed mold to shape the magnet; the process is the same for the tactile magnet (that sits at the center of our patches) and the ID magnets (that sit at the edges of the patch, solely for the purpose of shaping its magnetic signature).

The mold is held between two strong permanent magnets (N52 0.75” x 0.75”, K&J Magnetics). This strong magnetic field (~1.1 T) magnetizes and aligns the polarities of the individual particles. This process results in a composite with a strong, permanent magnetic field, while remaining flexible due to the silicone holding it together. With a goal of maximizing magnetic field strength to produce strong vibrations, we use an NdFeB weight concentration of 80%.

Next, the rest of the patch, which embodies our spring-mechanism, is cast using pure silicone. For the spring mechanism, Dragonskin FX Pro silicone is used for its elasticity. The magnets and mechanism may be cured at room temperature (which takes ~40 minutes for Dragonskin FX Pro) or inside a dehydrator in a few minutes.

After both the silicone mechanism and soft magnets have cured, the interactive patch is assembled by adhering the magnets to the mechanism with silicone glue (Sil-poxy). The total thickness of a patch is 2.5 mm.

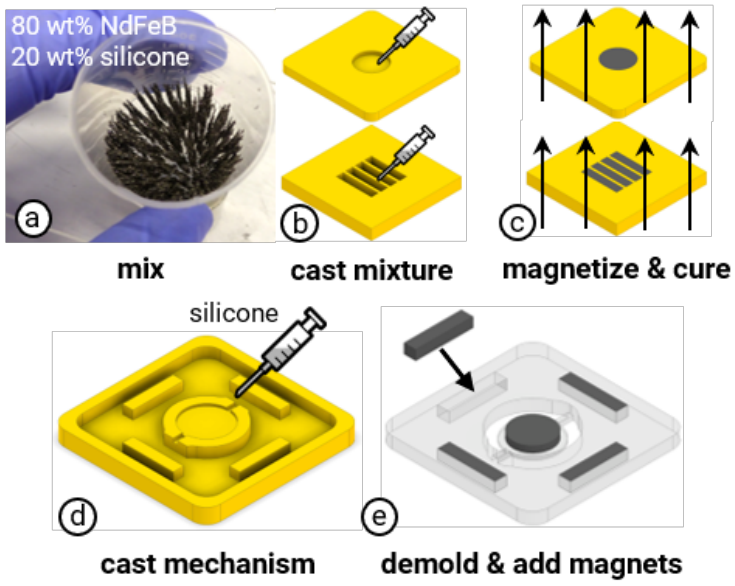

Figure 10. We fabricate our devices by: (a) doping silicone with magnetic powder, (b) casting the doped silicone mixture into 3D printed molds of desired shape, (c) curing the mixture in a strong, external magnetic field, (d) casting our mechanism out of silicone, and (e) adhering the soft magnets to the silicone mechanism.

We designed MagnetIO patches to be attached to a wide variety of objects of different shapes, textures, and sizes. To adhere our patches to surfaces such as walls, objects and even skin, we add a final layer of sticky silicone adhesive (*Skin Tite*) to the back of our patches. Other types of patches can be made with longer straps of silicone (as used in Figure 7 around the gaming controller) or even in custom shapes (e.g., smartphone sleeve made from silicone with our magnets embedded or a beating heart for a child's toy, shown later in *Envisioned Examples*).

Engineering our Nail-worn Device

Our nail-worn device is comprised of a voice-coil and PCBs for processing sensing and actuation, shown in Figure 11. Our voice-coil is optimized to provide strong magnetic forces while maintaining a compact, lightweight footprint that does not occlude the user's fingerpad, allowing the user to still touch objects and feel the haptics of their surroundings.

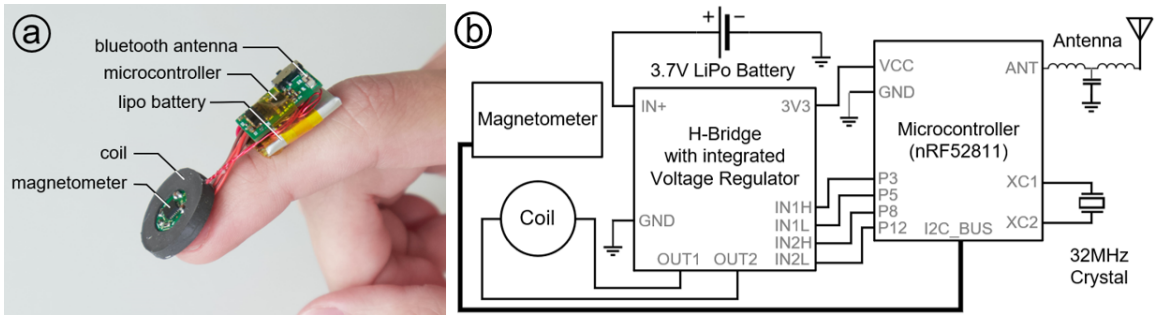

Figure 11. (a) Components used in our device; (b) Circuit diagram of our implementation.

The coil in our voice-coil is made from copper enameled wire (28 AWG wound for 42 turns. To concentrate the coil's magnetic field, we designed a ferromagnetic core to fit around the windings. To make the core comfortable to wear and to bias its magnetic field downwards to the fingerpad, we designed a computationally-optimized ferromagnetic core made from silicone doped with iron powder (70 wt% iron powder, 30 wt% silicone). We describe this optimization process in our *Technical Evaluation*. The final coil design weighs 2 grams.

We engineered a custom PCB for MagnetIO's finger-worn device, as shown in Figure 11. At the center of the coil, we place a 9DOF IMU (MPU-9250, 3-axis magnetometer, 3-axis gyroscope, and 3-axis accelerometer) to read the local magnetic field and sense proximity to any patch.

On the user's finger, we place our PCB that houses our motor driver (DRV8850, Texas Instruments), Bluetooth enabled microcontroller (nRF52811, Nordic Semiconductor), and battery (40 mAh). The motor driver can provide up to 5 A of current, but typically 1 A is sufficient to cause a haptic patch to vibrate. With this one small battery, our device allows for only ~100 haptic interactions. Yet, one can triple its battery-life by adding a second 80mAh battery on the first finger phalanx. The complete finger-worn device including battery weighs **only 4 grams.** The coil measures **18.25 mm** in diameter and 3 mm thick, while the wearable controller and battery measure **17 mm x 11 mm** with 7 mm thickness.

Sensing by Detecting the Magnetic Signature of a Patch

While the focus of our paper *is on the vibrations produced by our novel soft patches*, these only become interactive when the loop is closed, i.e., only when they exhibit both output and input. We acknowledge that detecting touch and/or the ID of the interactive patch that the user's finger is contacting with can be achieved using a variety of methods previously explored, such as radio [66, 179], acoustic [78], or optical [246, 246] IDs.

However, for the sake of completeness, we also implemented an input identification technique that relies solely on the magnetic properties of a patch. To achieve this, as depicted in Figure 12, we added four small bar magnets (which we call ID magnets) around the main vibration magnet, which we call the tactile magnet. All four rectangular magnets are also soft and were produced using the same method as the tactile magnet. The purpose of these rectangular magnets is to encode

an *ID* by means of shaping the 3D magnetic field such that each patch exhibits a different magnetic field when read by the 3DOF magnetometer, which is featured on our wearable nail-worn coil.

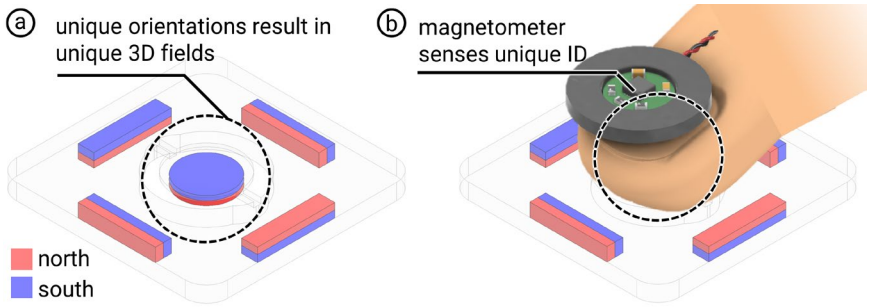

Figure 12. (a) Each patch has one central tactile magnet surrounded (the one that vibrates) and four small bar magnets whose orientation shapes the 3-D magnetic field. (b) When a user touches a patch, the magnetometer reads the patch's unique magnetic field to recognize; thus, enabling the input side of the interaction.

The principle behind our encoding system is as follows: by varying the orientation of the ID magnets, unique 3D magnetic fields can be produced; the number of combinations achieved by this technique is obviously limited but other sensing techniques are also possible. Furthermore, the tactile magnet can also exhibit two polarities, which contributes to a larger number of combinations. Each of the four ID magnets may be oriented in one of four ways (north facing up, down, left, or right). The magnetic fields of each individual magnet interact at the center of the patch and the net magnetic field is read by the magnetometer. As we demonstrate in detail in our *Technical Evaluation,* we can reliably identify eight patches at 99.06% accuracy just using simple threshold-based identification (if-then-else) based on the physical principles that guide magnetism. Certainly, one could alternatively feed the magnetometer data into a more sophisticated classifier (e.g., SVM, DNN, and so forth) to potentially expand both in accuracy and sample size or even fuse the 9DOF of the IMU for more rich data.

Technical Evaluations

We characterized the performance of our proposed device in five technical evaluations. To aid the reader in understanding the different validations we performed, we present an overview of our evaluations with a preview of their respective results:

1. Impact of particle size on elasticity: we found that our choice of doping silicone with small particles (<200 μm) improved stretchability, a key feature since we want our patches to stretch and conform around objects.

2. Measuring & optimizing the vibration response of our soft patches: we found that (1) a 1 mm spring width and (2) a magnet diameter of 7.5 mm optimizes the resulting vibrations to the feelable range of the human skin; and (3) that placing magnets at least 5 mm apart from each other minimizes any interference from the magnetic field of adjacent magnets.

3. Measuring & optimizing the magnetic field of our coil: we found that we could tune the shape of the magnetic field of our coil by (1) computationally simulating it; and (2) adding an iron-doped silicone. The result is that unlike conventional magnets that radiate in a symmetric pattern, our field is biased towards the fingerpad. We also found that most of MagnetIO's vibrations happen at the patch, which vibrates 16x stronger than the coil.

4. Comparing MagnetIO's vibration to a Linear Resonant Actuator: we found that our device vibrates with a similar intensity as an LRA driven at 4V with a wider frequency bandwidth due to its soft spring.

5. Identifying patches by means of magnetic signatures: while the entire focus of our paper is on the haptic vibrations we produce via our soft patches, for the sake of completeness, we also evaluated our straightforward sensing method that identifies patches based on their magnetic signature. We found that this can identify eight patches with an accuracy of 99.06%.

Technical Evaluation 1. Impact of Particle Size on Elasticity

To enable our patches to fit around different surfaces, especially those that are non-planar such as the everyday objects or the human body, it is critical that they allow for deformation, i.e., these should *stretch*. Our choice of implementing our interactive patches from silicone allows this. However, as one dopes the silicone with neodymium powder to enable them to vibrate as a response to our coil, it decreases the elasticity (i.e., an increase in elastic modulus as found by [7]). Thus, to maximize the elasticity of our soft magnets, we explored refining the neodymium powder particle size using a simple mesh filter. Figure 13 depicts the results of a simple elongation test of two soft magnets with comparable properties (size, volume, mass, 80 wt% particle concentration) under 25 grams of load, except that the soft magnet represented by the orange data is made by doping silicone with particles <200 µm; conversely the other soft magnet is made from particles >200 µm.

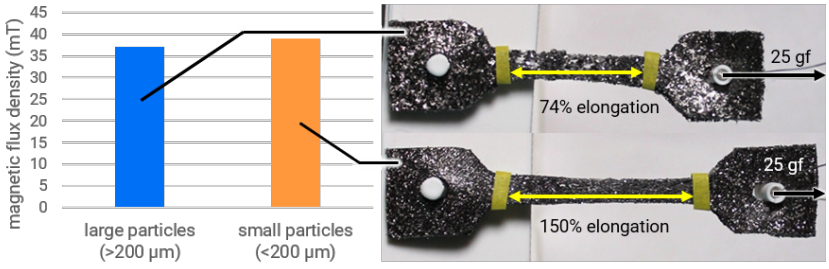

Figure 13. Comparison of soft magnets made with large (>200 µm) and small particles (<200 µm): magnetic flux density (left) and elongation under 25 grams of load (right).

Our results show that fabricating soft magnets using particles smaller than 200 µm allows elongation up to 150% of the original size. Furthermore, not only a smaller particle size improves elasticity, it also slightly increases the magnetic field, which in turn increases haptic performance. As a takeaway from this evaluation, we recommend researchers and practitioners use our approach

to quickly improve the quality of their devices by refining the neodymium particle size using a simple mesh filter.

Technical Evaluation 2. Measuring & Optimizing the Vibration Response of our Soft Patches

To understand the haptic response of our soft magnets we conducted an experimental evaluation aimed at measuring the impact that each design factor has on the resulting vibration. We measured the impact of: (1) the width of our beam-springs, (2) the magnet's diameter, and (3) interference from any adjacent magnets. To measure the vibration generated, we placed a piezoelectric vibration sensor (AB1070B-LW100-R) below each patch. The coil was held stationary directly above the patch at 6 mm away. Data was recorded at 3300 Hz and processed using a Fast Fourier Transform to examine the frequency response. In our plots, "magnitude" denotes the actual analog reading as measured by our piezoelectric sensor.

Impact of the spring's width on resulting vibration profile

In all our haptic patches, the *spring width* is a major factor that determines the amount of resulting vibration over a range of frequencies. As such, we measured the vibration of four of the same magnets (8 mm diameter, 1.25 mm thick, 34.1±3.2 mT measured at surface) when attached via four different spring widths (1 mm, 2 mm, 4 mm, and 6 mm). To gather insights about a wide range of frequencies, we swept our coil in a square wave pattern from 0 to 500 Hz in steps of 20 Hz. Three repetitions were performed for each magnet.

Figure 14 depicts our results for the measured magnitude of the vibrations of these four different spring widths, over a wide range of frequencies (0-500 Hz). By examining the resonant frequencies (sharp peaks in the response) we found that increasing the spring's width increases the resonant frequency. This is in line with simple vibrational theory, where increasing the spring

constant increases the natural frequency. We found that the thicker springs (4 mm or 6 mm) dampen the resulting vibrations. Conversely, we found that the thinner springs (1 and 2 mm) result in a strong vibration. In fact, the 1 mm spring exhibits a maximum vibration a lower frequency peak of ~100 Hz when compared to the 2 mm spring, which resonates maximally at ~300 Hz.

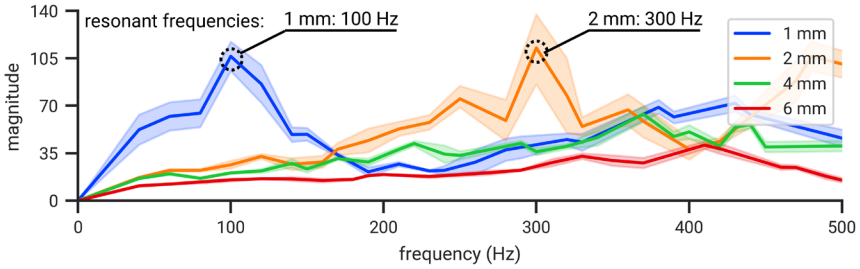

Figure 14. Magnitude of vibrations of the *same* soft magnets but with four varying spring widths. Frequency was swept between 0 to 500 Hz (in 20 Hz steps). Shaded regions depict a 90% confidence interval.

As a takeaway from this evaluation, we recommend researchers and practitioners use a spring width of 1 mm, resulting in a soft magnet design with a resonant frequency at ~100 Hz. From here on, all our soft magnets will utilize a spring width of 1 mm. Note that, depending on the type of application, it might be also worth utilizing also the 2 mm spring which vibrates maximally at a higher frequency of ~300 Hz.

Impact of the magnet's diameter on resulting vibration profile

The next factor that impacts the resulting vibration is the *diameter* of the magnetic region doped with neodymium. As such, using the same apparatus, we measured the vibrations of four soft magnets with varying diameters (6 mm, 7 mm, 7.5 mm, and 8 mm). We fixed the spring width at 1 mm according to the findings of our previous experiment.

Figure 15 depicts the results for the magnitude of the vibrations of these four magnets with varying diameters, as they vibrate over a wide range of frequencies (0-500 Hz). This is again aligned with what is expected by vibrational theory, where increasing the mass decreases the

natural frequency. We found that the larger diameter magnet at 8 mm provides mostly only one resonant mode, i.e., it vibrates maximally at ~100 Hz. Then, for diameters below 8 mm, we found a wider range of frequency modes, i.e., these magnets have a few frequencies at which they can vibrate strongly. For instance, soft magnets with a diameter of 6 mm or 7 mm vibrate the strongest at ~400 Hz. Lastly, at a diameter of 7.5 mm, the soft magnet's strongest vibrations occur at 240 Hz and 310 Hz.

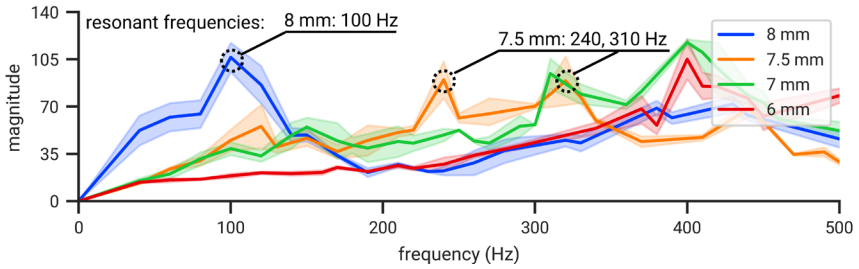

Figure 15. Magnitude of vibrations for four soft magnets with varying diameters of the region that is doped with neodymium (same spring widths of 1 mm). Frequency was swept between 0 to 500 Hz (in 20 Hz steps).

As a takeaway from this evaluation, we recommend researchers and practitioners to use a diameter of 7.5 mm, resulting in a soft magnet design with a resonant frequency at ~240 Hz, which leverages the fact that the human skin is very sensitive at those frequencies [263]. From here on, all our soft magnets will utilize a diameter of 7.5 mm with spring width of 1 mm. Note that, the larger 8 mm diameter might be worth exploring for applications requiring a lower frequency ~100 Hz. However, we advise against using soft magnets with diameters below 7.5 mm for haptic applications (with 1 mm spring width), as these resonate at higher frequencies (~400 Hz) at which the human skin is not particularly sensitive [263].

Impact of adjacent magnets in resulting vibration magnitude

Next, because our approach allows users to easily attach these soft interactive patches to objects and the environment to create simple interfaces, the soft magnets may end up neighboring each

other. Since this meant that adjacent magnets could potentially interfere with each other's magnetic fields and decrease the vibrations, we decided to measure it. We utilized the same apparatus as in our previous experiments, but attached three consecutive magnets separated by 5 mm. As we were interested in measuring the impact of each magnet's field on the adjacent magnet, we attached the magnets to individual stands connected only at the base; allowing us to measure the impact of the field strength independently of vibrations that propagate through the apparatus (these depend on the material that the magnets are attached to and is a known problem in any vibration-based interface [46]). Then, we proceeded to vibrate, using our coil (at the resonant frequency of 240 Hz), each magnet, one at a time, but measured not only the magnitude of this magnet but also its two adjacent neighbors.

Figure 16 depicts our results of the magnitude of the vibrations (normalized to the maximum) of the soft magnet being excited as well as its two neighbors. As expected, the adjacent magnets exhibit a minute vibration, since their permanent magnetic fields interact with that of the coil and vibrate in response. However, we also found that these vibrations are very small, i.e., ~10% of the maximum at the nearest neighbor and less than 1% of the maximum at the further neighbor. A straightforward empirical test (placing another person's finger over the adjacent magnets) did not reveal that one could confidently feel these vibrations in adjacent magnets.

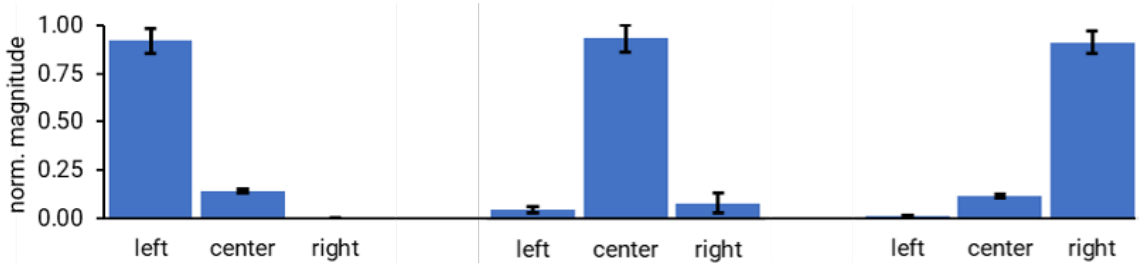

Figure 16. Magnitude of vibration (at resonant frequency) of three adjacent soft magnet placed at 5 mm of each other. As observed, there is very little influence of permanent magnetic field of the adjacent magnets

As a takeaway from this evaluation, we recommend researchers and practitioners to keep adjacent soft patches at least at 5 mm of each other.

Technical Evaluation 3. Measuring & Optimizing the Magnetic Field of our Coil

While in our previous evaluations we characterized the vibration of our soft magnets to precisely optimize their frequency/intensity, we now turn our attention toward optimizing & evaluating our wearable coil. The objective is simple: maximize the field strength at the user's fingerpad without increasing the coil size. First, we performed finite element simulations to design an iron-doped core with a geometry that concentrates the field at the user's fingerpad. Then, we experimentally confirmed that it improved the magnetic field strength by 40%.

Impact of an iron core on the resulting magnetic field

Electromagnets are comprised of a coiled wire spun around a magnetic core made from a ferromagnetic material such as iron [154]; this ferromagnetic core concentrates the magnetic flux and results in a more powerful magnet. This is commonly seen in various types haptic devices, e.g., DC motors, solenoids, etc. Inspired by this principle, we engineered our wearable coil to benefit from a ferromagnetic core. However, because our electromagnet is nail-worn, a pure iron core would be heavy and not ergonomically follow the shape of the fingernail. Therefore, we engineered a silicone doped with iron, which increases magnetic field, yet is soft.

We evaluated the effect of an iron-doped silicone core by means of: (1) a simulation, which enable us to determine in detail the advantages of our design; and (2) an empirical validation with a Gaussmeter, which we present later, that provides confirmation of the advantage but displays less resolution than the former simulation.

First, we performed a finite element method (FEM) simulation to compare the magnetic flux density between our initial coil design against our coil design with an added iron-doped core. As with any other materials of this paper (e.g., software, firmware, circuits, 3D models) the simulation files are provided to assist researchers with replication or building on top of our design[1]. All our simulations were conducted using *Finite Element Method Magnetics* (FEMM), a computational solver for magnetics, electrostatics, etc., widely used in physics [14]. Our simulations were set to match our physical coil and are defined as follows: inner and outer diameter of 11 and 16.75 mm, respectively; thickness of 2.5 mm, which provided enough space for 42 turns of 28 AWG enameled copper wire. The coil was excited with 4.8 A to match our benchtop power supply. For the iron-doped silicone core model, the coil was encased in a composite (70 wt% iron powder, 30 wt% silicone) and a magnetization curve for the material was imported to capture the core's ferromagnetic behavior [283]. Since our coil's geometry is symmetrical, we simulate only its cross-section (Figure 17a).

Our simulation results are depicted in Figure 17b,c, as a slice of the cross-section. We confirmed that adding a silicone-iron core increased the magnetic field produced by concentrating the flux within the core.

Impact of core geometry in the shape on the resulting magnetic field

Having confirmed that adding a ferromagnetic core concentrates the magnetic field, we explored whether the ferromagnetic core's geometry would allow us to design a wearable electromagnet that exhibits an asymmetric magnetic field, i.e., concentrates the magnetic field *at the fingerpad*, where it is needed for haptic interactions.

Our resulting design is a "pot"-shaped ferromagnetic core (Figure 17d). By means of FEM simulation, we found that leaving one of the faces open "forces" the magnetic field lines to "jump

the gap", thus concentrating the field along that face. This effectively biases the magnetic field to one side, making it asymmetric towards the user's fingerpad.

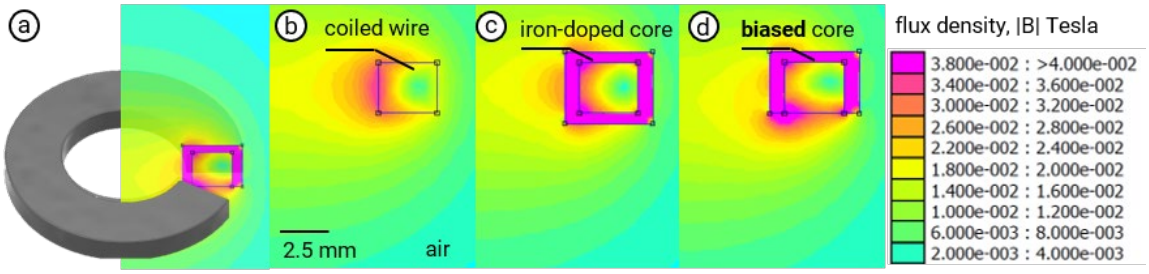

Figure 17. (a) Our simulation is run as a slice of the coil. The magnetic flux contour was calculated for (b) a coil without a core (c) the same coil with a silicone-iron composite core and (d) the same coil but with a core that biases the field to one face of the coil.

Experimental validation of core design

Finally, we empirically evaluated our coil design by fabricating two coils: a coil with our silicone-iron doped core and pot-shaped geometry; and he same coil but without a core (baseline). Then, we powered the coils by connecting them to our MagnetIO device one at a time. Using a gaussmeter (TD8620) mounted on a caliper, we measured the magnetic field strength as a function of distance (from 0 mm to 12 mm away from the coil; <12 mm being the thickness of a typical finger [265]. Because we hypothesized that the field in our custom coil is asymmetric (biased towards the fingerpad) we measured the field strength in two locations: (a) at the center of the coil, and (b) at the edge of the coil, where we expected the field to concentrate.

Figure 18 depicts our results of the magnetic field strength (in mT) measured at increasing distance from the surface of the coil where the field has been biased. Overall, we found that at any distance, our custom coil (with its soft-iron core and asymmetric magnetic field) produces stronger fields, which is critical since magnetic force rapidly decays over distance. Importantly, when measured directly at a finger's thickness away (12 mm) at the center of the coil, the field strength is 40% greater for the coil with a ferromagnetic core compared to no core.

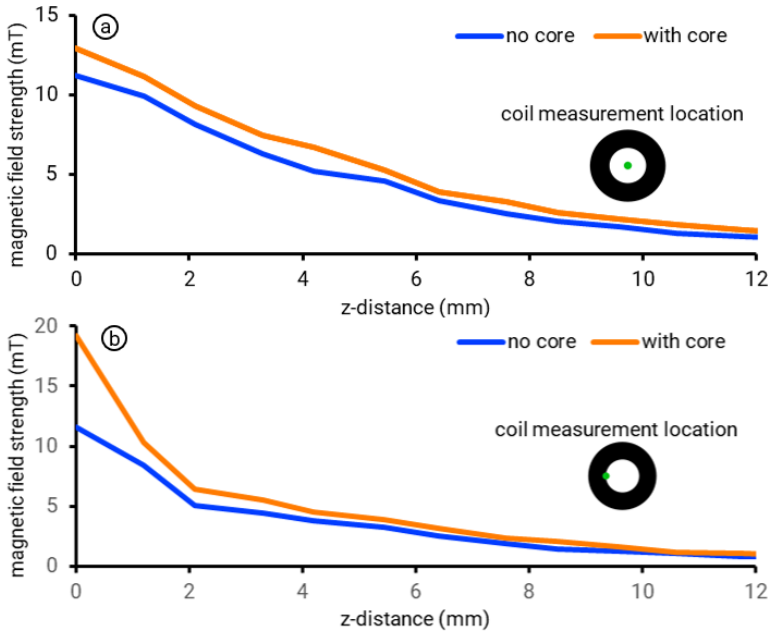

Figure 18. The addition of a ferromagnetic core increased the magnetic field strength at (a) the coil's center as well as at (b) the coil's inner diameter.

As a takeaway from this evaluation, we recommend researchers and practitioners to optimize their wearable electromagnets to direct the magnetic field where it is most useful for the haptic effects. We have not seen this much in the design of interactive devices and believe it might enable improvements in existing interactive devices that are based on electromagnets, such as Magnetips [153] or Magtics [182] just to cite a few.

Measuring the vibrations at the patch vs. vibrations at the coil

Last, since the electromagnetic forces act equally and opposite to each other on the interactive patch and wearable coil, *both* the patch and coil vibrate when excited. To determine the degree to which the coil and magnet vibrate, we placed a piezoelectric sensor beneath each of them and excited the patch at its resonant frequency. We found that the patches vibrate 16x more than the coil, likely due to the coil's greater mass and constraints. Thus, we found that the tactile sensation is greater at the patch, as intended for any haptic application.

Technical Evaluation 4. Comparing MagnetIO's vibration to a Linear Resonant Actuator

To put our results into perspective, we compare our chosen soft magnet (1 mm spring width; 7.5 mm diameter) with a conventional linear resonant actuator (LRA). As we established, the LRA is the most similar haptic device to our approach, except that its inner workings are rigid and thus not stretchable. For this comparison we used the C10-100, which was driven using a function generator and its driver at a nominal 4 V.

Figure 19 depicts our results for the magnitude of the vibrations of our soft magnet vs. the LRA, as they vibrate over a wide range of frequencies (0-400 Hz). As expected, the LRA resonates at 150 Hz, which is consistent with its specifications. Also as expected, our soft magnet (with 7.5 mm diameter and a spring of 1mm) resonates at both 240 Hz and 310 Hz. Surprisingly, when comparing the magnitudes of each device at their resonating frequency, these are comparable, i.e., our soft magnets vibrates as much as an LRA. Note that our device does this while remaining stretchable. Furthermore, our interactive patches operate consistently over a wider range of frequencies than an LRA; this may be attributed to the larger degrees of freedom that arise from the fact that our patches are made from soft materials [22].

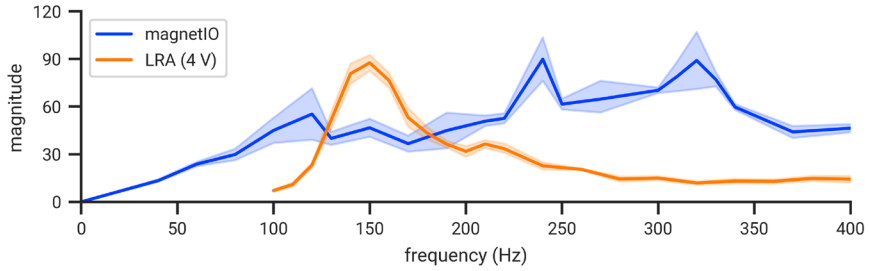

Figure 19. Magnitude of vibrations for our soft magnet design (MagnetIO) vs. a traditional LRA (C10-100 at 4 V).

Technical Evaluation 5. Identifying Patches' ID via Magnetic Signatures

Lastly, to test the accuracy of our simplistic identification based solely on magnetic signatures of the patches, we fabricated eight interactive patches, each with a *random* orientation of their ID magnets. It is extremely important to note that these patches were not custom made. We simply fabricated 32 bar magnets (the small ID magnets) and randomly placed these on each patch without even checking their orientation; this depicts the worse-case scenario for our simple approach. Then, while wearing our nail-worn device with magnetometer, we recorded the 3-axis magnetic field when touching each patch. The readings were converted into a simple rule-based classifier (if-then-else) that classified each patch based on the incoming magnetometer readings. Then, to evaluate the sensing accuracy, one participant touched each patch in a previously randomized ordering (320 touches, 40 touches per patch). For each touch, we recorded the ID predicted by our classifier.

Figure 20 depicts the resulting confusion matrix. We found the overall accuracy across all trials to be 99.06%. This is a sufficient result for simple interactive use, despite using random orientations of the small ID magnets.

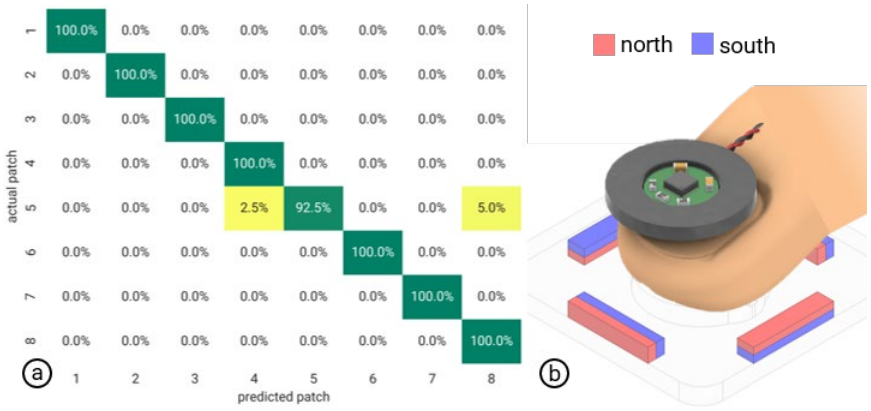

Figure 20. Interactive patch confusion matrix across 320 trials.

While this approach to identifying the interactive patch is relatively simple, i.e., a series of rules based on the physical principles that shape magnetic fields, one could alternatively feed the magnetometer data into a more sophisticated classifier (e.g., SVM, DNN, and so forth) to potentially expand in accuracy and sample size. Lastly, note that we purposely used *only* the 3DOF of magnetometer data for identification to understand the magnetic-only approach; however, our IMU provides an extra 6DOF (3DOF from gyroscope and 3DOF from accelerometer) which can be fused with the magnetometer data for a more sophisticated identification approach.

Envisioned Applications enabled by MagnetIO

To illustrate the versatility of our approach we demonstrate a wide range of applications, where we utilize MagnetIO patches attached to a variety of objects to propose new interactions with haptic feedback. Broadly speaking, we organize our proposed applications into four categories: (1) ad-hoc & ubiquitous haptics; (2) eyes-free use; (3) adding interactivity to everyday objects; and (4) adding interactivity everywhere, even to outdoor objects, exposed to weather conditions.

Benefit#1: Scalability—Enabling Ubiquitous ad-hoc Haptic Interfaces

Figure 21 depicts an example of how a user might instrument their living room using six MagnetIO patches, to create ad-hoc interfaces that fit their own needs, such as (a) haptic buttons for their e-reader; (b) haptic controls for their smart-dehumidifier, (c) volume control with haptic detents on their armchair; (d) additional settings with haptic feedback on their smart thermostat; (e) haptic feedback as they touch their plant's pot to select the amount of water from their watering system; and, (f) controls for their fan with haptics when they touch the "eco" setting.

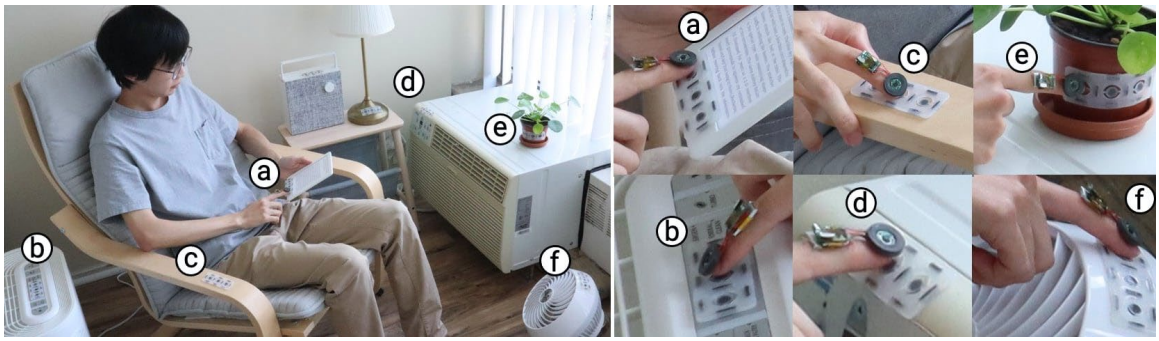

Figure 21. An example of an envisioned ad-hoc interface created by a user for their living room using six patches .

Additionally, MagnetIO patches can weave interactivity into playful everyday objects. Figure 22 shows how patches can (a) add dynamic interaction to a children's coloring book; (b) add tactile cues to board games; and (c) add play, stop, record buttons with haptic feedback for their guitar's looper.

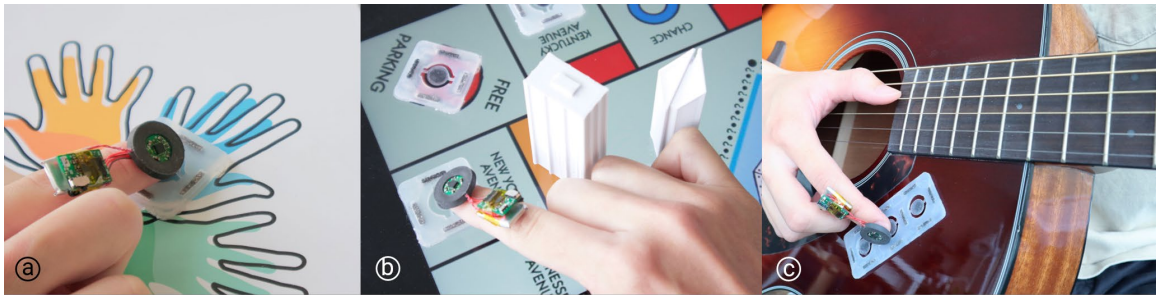

Figure 22. Examples of how MagnetIO can enhance everyday objects by creating an ad-hoc I/O space; these objects can now sense touch interactions and vibrate in response.

Benefit#2: Conformability—Adding MagnetIO Patches to Non-planar Objects, Outdoors, etc.

Furthermore, we believe MagnetIO patches are especially useful for realizing interfaces attached to objects that are not planar, which is depicted in Figure 23. For instance, (a) music player control on their headphones; (b) additional buttons with haptic feedback for a gamepad; and (c) added to one's favorite toy to feel its heartbeat.

Figure 23. Examples of how MagnetIO patches can conform to objects of various shapes.

More interestingly, Figure 24 depicts how our patches can provide interactions in extreme environments, such as contexts where significant forces are applied or drastic weather changes. Figure 24a depicts a user who has instrumented their bike handle with MagnetIO patches to receive turning signals from their phone's GPS navigation application. When the user wants to check driving directions, they place their fingers on a MagnetIO patch that buzzes once or twice, in response to the navigation-application's messages, to notify them to turn on the next intersection to the left or right, respectively. Here, the MagnetIO patches survive adverse weather conditions because they are completely *passive*.

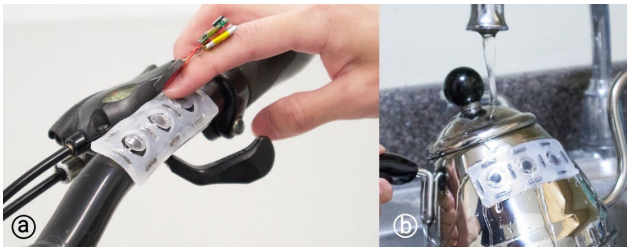

Figure 24. Two examples of applying MagnetIO patches in extreme contexts with significant forces or weather changes, such as this bike's handle; however, because our patches are passive and soft, they resist these adverse conditions.

Conclusion

We presented MagnetIO, a new type of haptic actuator comprised of two parts: *one* battery-powered voice-coil worn on the user's fingernail and *many* of interactive soft patches that can be attached onto any surface (everyday objects, user's body, appliances, etc.). When the user's finger

wearing our coil contacts any of the interactive patches it detects its magnetic signature via magnetometer and makes the patch vibrate, adding haptic feedback to otherwise input-only interactions. To allow these passive patches to vibrate, we fabricated them from silicone with regions doped with polarized neodymium powder, resulting in soft/stretchable magnets. This form-factor allows our patches to be wrapped to the user's body or everyday objects of various shapes.

It is this novel technical implementation, based on decoupling the mechanics of a linear resonant actuator, that gives rise to MagnetIO's unique feature, it is a *one-to-many haptic device*, i.e., *one* active part (an electromagnetic-coil worn the fingernail) powers *many* passive actuators. We demonstrated applications that make use of MagnetIO's patches to realize ubiquitous haptics, i.e., surfaces and objects around the user can now exhibit interactive behavior upon touch.

Furthermore, in our technical evaluation, we demonstrated that our interactive patches can be excited across a wide range of frequencies and can be tuned to resonate at specific frequencies based on the patch's geometry. Furthermore, we demonstrate that MagnetIO's vibration intensity is as powerful as a typical linear resonant actuator (LRA); yet, unlike these rigid actuators, MagnetIO's patches operate as springs with multiple modes of vibration, which enables a wider band around its resonant frequency than an LRA. Future work may examine deeper into the psychophysics of these patches, for example, user studies on vibration strength and pattern recognition. Additionally, while this implementation presented vibration in a single axis, this approach may be adapted to other feedback modalities such as shear.

We tend to think of MagnetIO not as an end-product but as a hardware & fabrication technique that will inspire the creation of a new type of passive-haptic interactive devices that can even unlock new use cases. As such, we published the detailed fabrication process, hardware schematics and code as open-source to accelerate future research (see Chapter 1, Contributions).

Stick&Slip: Altering Fingerpad Friction via Liquid Coatings

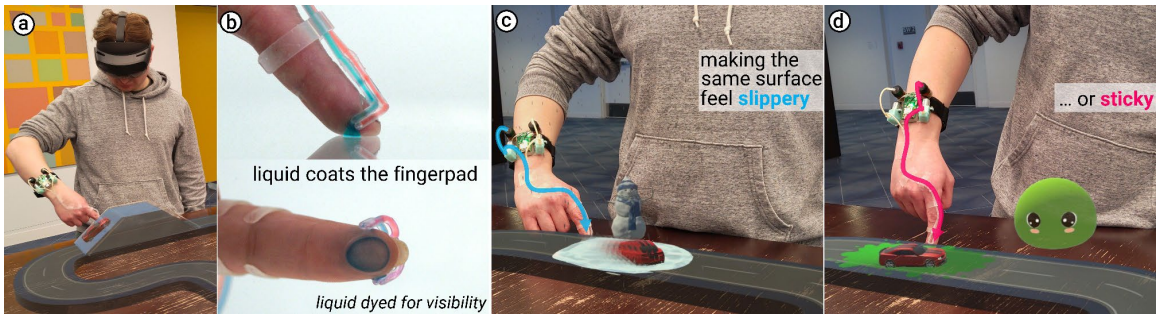

Figure 25. We propose Stick&Slip, an approach to friction modulation that works by coating the user's fingerpads in sticky or slippery liquids, making it possible to alter the friction of nearly any non-absorbent surface, regardless of its geometry. (a) A user plays a racing game in mixed reality, driving the virtual car over real-world surfaces, such as a table and a small ramp. (b) To alter the friction of the user's finger movements on real surfaces, our device deposits liquid droplets onto the user's fingerpad, forming an interfacial layer between the two, which allows us to modulate surface friction corresponding to the virtual events, such as (c) the ice feels slippery to the user's touch, and (d) the green-goo left by the opponent feels sticky while driving the car on the surface.

In this chapter, we introduce Stick&Slip [150], our approach to scaling friction feedback to many objects and surfaces within the environment.

Introduction

Touch plays a vital role in our interactions, providing valuable information about the objects we contact [3, 43, 99, 116]. In fact, a crucial tactile property that guides touch and grasping, is perceived *friction* between a surface and fingerpad [276]. When we feel that an object has lower friction, we intuitively know it requires a stronger grasp to prevent slipping [62]. Given the importance of friction to our tactile perception, many researchers have engineered devices that use surface friction as a feedback modality [18, 159, 172].

Unfortunately, while many other haptic cues (e.g., pressure, vibration, or kinesthetics) have seen a plethora of methods developed over the last four decades, this is not the case for friction. For example, to implement pressure rendering, haptic designers can choose from a variety of

approaches (e.g., motors [249], pneumatics [297], magnets [183, 262], smart materials [198], electrotactile [215, 294], etc.), each offering different pro/cons regarding wearability, power consumption, scalability to real-world objects, etc. However, the haptic domain of friction rendering has not experienced this abundance of research approaches—in fact, only two key approaches to modulating surface friction have been deeply explored: ultrasonic vibration and electrostatic adhesion. Ultrasonic vibrations reduce friction as a finger slides over a surface by vibrating the surface such that it only contacts the finger intermittently [278]. Electrostatic adhesion increases the friction by means of attractive (electrostatic) forces between surface and finger [223]. These two working principles may seem limited in that neither can *both* increase and decrease friction, but this can be overcome by using these techniques in conjunction [95]. Moreover, of greater *conceptual* significance, implementing these approaches requires researchers to *instrument surfaces* around the user—e.g., either adding vibration actuators or coating the surface so that it can be electrically attracted to the user's finger. This need for surface instrumentation prevents achieving the goal that Bau et al. set for the field of augmented reality haptics in their seminal work "[to] only require the augmentation of the user, not the entire environment" [19]. In fact, besides *REVEL* [19] (which requires objects to be electrically grounded to the user and metallic) and a vibrotactile device by Asano et. al [10], the majority of friction devices are implemented on top of touchscreens or tabletops [1, 20, 34, 223, 278], rather than everyday surfaces.

To explore a novel, alternative, technique that circumvents these limitations, we propose Stick&Slip, a wearable device that can modulate the friction between the finger and *many*, *everyday* objects. We achieve this by depositing liquid droplets onto the finger to form an interfacial layer between the fingerpad and surface. By tuning the lubricating and adhesive

properties of the liquid coating, we can either increase *or* decrease the coefficient of friction by up to ±60%. Importantly, we identify liquids that influence friction, yet leave behind only minimal residue (such as alcohol which rapidly evaporates). While we acknowledge that depositing liquids onto the skin is an unconventional approach to haptics, it provides an alternative method that circumvents many of the limitations associated with prior work, enabling friction modulation of a *wide* range of objects and surfaces. To illustrate the applicability of our novel approach, we demonstrate how it adds friction-feedback in virtual/mixed-reality or, even, while using everyday tools. As the first work exploring the use of liquids for interactive friction modulation, we identify not only the benefits of this approach, but also the limitations (e.g., onset times, residues, etc.) via technical evaluations and a user study. Finally, we distill our findings into recommendations based on the benefits and limitations of this approach and discuss areas for future exploration.

Ultimately, we see Stick&Slip as an exploration of alternative approaches for friction haptics—an area that unlike pressure or force-based haptics, has not seen a plethora of technical alternatives.

Our Approach: Stick&Slip

Stick&Slip alters the friction of real-world objects by interactively applying liquid coatings onto the user's fingerpad. We use liquids because they can alter the surface friction of nearly any non-absorbent surface, enabling a wider range of augmented surfaces than possible with prior approaches.

Working principle of Stick&Slip

Figure 26 shows the working principle of Stick&Slip. When the user's fingerpad contacts a surface, they immediately perceive its surface friction [276], which depends upon surface characteristics like roughness, surface energy, temperature, etc. [21, 191]. To alter the surface friction, we deposit a *thin liquid coating* between the fingerpad and the surface from a nail-worn

droplet generator, which acts as a *physical buffer*. We specifically mixed liquids that can decrease friction ("slippery") or increase friction (which we refer to as "sticky"). Our slippery liquids (typically acetone and IPA) decrease the coefficient of friction by forming a lubricating layer that fills the space and irregularities between the skin and the surface, allowing the finger to glide smoothly over the surface with less friction than in a dry condition. In contrast, our sticky liquids (honey mixed with IPA) increase the coefficient of friction by forming an adhesive layer between the skin and the surface, causing the finger to feel more resistance when sliding over the surface.

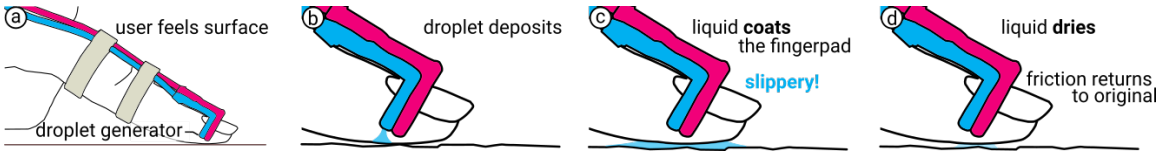

Figure 26. Our approach modulates surface friction via a (a) wearable droplet generator that (b) deposits slippery and/or sticky liquids, which (c) coat the fingerpad to form an interfacial layer that the finger glides on, altering the coefficient of friction. Moreover, (d) these liquids were engineered purposefully to, over time, evaporate and let the surface return to its original friction.

Notably, for surfaces *coated* with liquids, the friction *is almost independent of surface material* [191]; therefore, the liquid coating influences the user's perceived sense of friction *regardless of the surface* touched by the user. This is a key advantage of our approach: unlike prior approaches (electroadhesion and ultrasonic vibration), our liquid-based approach enables changing the friction of *practically any non-absorbent object* touched by the user. Finally, to fully maximize our novel method of interactively altering surface friction, we selected & evaluated liquids that either evaporate entirely (e.g., mixed with alcohol) or which have residues that can easily be washed away with an antagonist fluid (e.g., sugar dissolved with water). Though our skin naturally leaves behind oil residues on surfaces we touch, our selection of fluid aims to reduce any additional residue (see *Technical Evaluation*).

Walkthrough: Stick&Slip in a Mixed Reality Application

We demonstrate our concept in a mixed reality (MR) experience where the *friction* of *real* surfaces is altered. As shown in Figure 27, a user is wearing our wearable device in which thin tubes (mounted on the fingernail) deposit liquid droplets onto the fingerpad, which are pumped from reservoirs worn on the user's wrist. Our device is self-contained (i.e., battery-powered, and wireless) and communicates with the HoloLens 2 headset via Bluetooth.

Figure 27. Our user in MR wears our friction modulation device and interacts with real surfaces and objects.

This user experiences a MR racing game where their index finger controls a car driving around a track on their table. Because our wearable does not cover the user's fingerpad, they can feel the texture of their table and the different objects. For example, when the user slides their finger over 3D-printed props corresponding to speedbumps in the game, they feel their ridged texture. As the user drives the virtual car with their finger around the track, in-game events trigger changes in surface friction. As shown in Figure 28: (a) a cloud rains on the track, leaving a virtual puddle. When, (b) driving through the puddle, they *feel* that the table is *slippery* and see their car spin out of control. This change in friction is caused by our device delivering slippery liquid to the user's fingerpad, leading to a better match between virtual & physical sensations (see *User Study*). Our fluids rapidly evaporate and the surface friction returns to normal (e.g., on following laps, the table no longer feels slippery in this location).

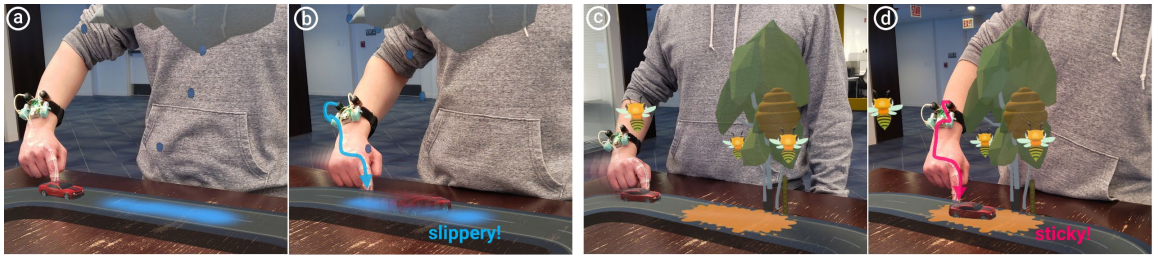

Figure 28. (a) The user drives their car through a rain puddle and (b) our device deposits slippery fluid as their car spins out. (c) The user then quickly rounds a corner, but (d) slows down dramatically sliding through virtual honey as the user feels sticky feedback.

Figure 28 (c) depicts as the user rounds a corner, a beehive drips honey onto the track; thus, (d) as the user drives through the virtual honey, they *feel a resistance* to sliding. This increase in surface friction is caused by our device delivering sticky liquid to the user's fingerpad. Like how one feels after getting fruit jelly on one's skin, our sticky liquids use dissolved sugars to increase the friction between the finger and surface via adhesion. However, unlike jelly, our sticky liquids are designed to quickly evaporate. As our liquids evaporate, they leave behind a thin film of adhesive residue. Importantly, this residue is significantly lower in sugar (i.e., ~2-30wt% compared to 70wt% in jelly) and its stickiness decreases over time (dry sugar is not sticky). Moreover, any sugar residue can be easily dissolved using water, which our device can also deliver (see *Experiments*).

The user keeps racing and experiences more stick & slip effects, as depicted in Figure 29: (a) slowed by an opponent that sprays virtual green goo onto the track, or (b) losing control of their car due to virtual ice on the road.

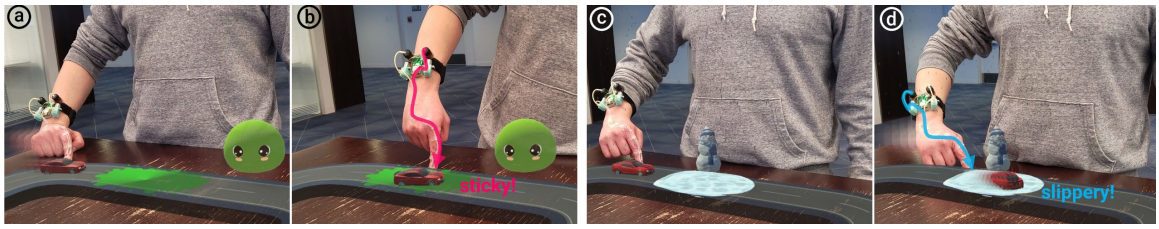

Figure 29. Surface friction effects rendered by our device, e.g., slowed down by resistive slime or losing control on slippery ice.

Importantly, our approach enables friction modulation on nearly any non-absorbent surface, allowing us to alter the friction of everyday objects (without instrumenting them with actuators). Figure 30 depicts this: (a) a virtual boost effect (slippery fluid) makes it feel easier to glide up the physical ramp prop, while (b) a virtual wind effect (sticky fluid) makes the physical speedbump props feel more obstructive.

Figure 30. Our device alters the friction of everyday objects, such as on top of this toy ramp or speedbumps.

Related Work

Our work builds upon devices that provide friction feedback. With a goal of haptic ubiquity, we focus on wearable approaches, especially those that can overlay haptics on real-world surfaces (e.g., [8, 258, 279]). Additionally, we reflect on recent alternatives to traditional actuators (e.g., liquid chemicals), which aligns with Stick&Slip's ethos.

Non-wearable Friction Devices

The most traditional approach to achieving friction feedback is by adding actuators to surfaces. There are four methods that have been commonly used.

Mechanical devices have long been used to generate resistive forces like those presented by friction. For example, the Haptic Tabletop Puck presented a tangible with a retractable rubber stopper that increased friction when dragged on a surface [144].

Vibration devices are commonly used for tactile feedback and simulating surface properties, typically integrated into flat surfaces and tablets. By vibrating the surface at high frequencies, the finger only intermittently contacts the surface, leading to a reduced coefficient of friction [128, 278].

Electroadhesion devices increase friction by electrostatic adhesion [155, 223, 224]. TeslaTouch [20] popularized this approach, using an electrostatic charge on a touch panel to increase attraction between the surface and finger. Others combined electroadhesion with ultrasonic vibration to achieve both increasing and decreasing friction [95]. Haptidrag [157] used a novel electrode arrangement to augment tangibles with electroadhesion friction feedback on real surfaces, although its underlying principle limits the surface materials, e.g., no metals or plastics.

Temperature-triggered mechanisms for friction changes have recently been explored. StickyTouch [94] is a surface with variable stickiness from temperature-sensitive tape that undergoes a dramatic increase in adhesion above a transition temperature. Others found that the friction between skin and glass can be controlled by simply heating certain regions, due to the skin's temperature dependent viscoelasticity and moisture content [34].

Considering the goal of ubiquitous haptics, non-wearable approaches face a particular challenge: *adding actuators* onto every object is impractical due to cost, size, and power consumption [151]. While these approaches lend themselves well for use in tablets and other standalone devices, they do not easily scale to the demands of haptics for mixed reality. As such,

a more pragmatic solution to scaling haptics may be to instrument the user (rather than the environment) so that the actuator accompanies the user *anywhere* that haptics is needed.

Wearable Friction Devices

Wearables offer a solution to providing haptics at scale because they are always with the user and do not require further instrumentation. The common approaches use similar actuators to their non-wearable counterparts.

Mechanical wearables include devices like Frictio [75], a ring with motor-controlled rotational resistance as an eyes-free information display. Similarly, FrictShoes [254] proposed wheeled shoes with brakes for simulating the sensation of walking on surfaces with different frictions in VR. Some have simulated the sense of friction via skin stretch on the fingerpad by placing motors around the finger and end effectors on the pad [197, 209, 219].

Vibration wearables include devices like HapCube [111], which generates tangential pseudo-forces (that can be interpreted as friction to users) by means of asymmetric vibrations [166, 203].

We take inspiration from wearable approaches to rendering friction but identify a key challenge: in most cases, the body is instrumented with actuators that impair interactions with real-world objects. While these approaches work well in VR, these cannot *overlay* friction onto real-world objects, a key goal in MR haptics [11] and also our focus. To solve this, we need devices that leave the fingerpad free to feel *both* physical *and* virtual sensations.

Fingerpad-Free Friction Devices

REVEL [19] laid out the vision for friction modulation in MR by expanding electroadhesion to be applicable to everyday applications outside of using tablets (e.g., mixed reality, tangibles, etc.). REVEL proposed reverse electrovibration, where rather than charging the surface, charge is applied to the user, enabling feeling friction changes when interacting with metallic, grounded

objects. REVEL scales to objects in one's surroundings, as long as the objects have been coated in layers of conductive electrode and insulation. We draw inspiration from REVEL's approach while aspiring to eliminate all object-side instrumentations.

Alternatively, Asano et. al [10] developed a vibrotactile device that leaves the fingerpad free and modulates roughness of real surfaces, which is related to surface friction. Because this approach is based on tactile masking of the real-world, the technique requires *strong* vibrations that the authors note to interfere with the "natural fusion of real and artificial stimuli" [10]. Our work is motivated by this challenge and aims to build upon wearable and scalable haptic devices by improving upon the sensory consistency between real and artificial stimuli.

Both REVEL and Asano et. al made great conceptual strides towards friction modulation anywhere. However, we speculate that to go beyond the capabilities of conventional actuators, a less conventional route may be needed. Thus, we explore friction modulation on a wide range of surfaces via *coating the user's fingerpad with liquids*.

Chemicals as Alternatives to Traditional Actuators

In recent years, there has been a push to experiment with different approaches to influencing perception, such as with chemicals, to overcome challenges of traditional actuators [27, 70, 101]. For example, Chemical Haptics proposed using liquid stimulants as an alternative to Peltiers, vibromotors, and electrotactile stimulation [139]. We draw inspiration from the ethos of these works when we explore using liquids as opposed to traditional actuators for friction modulation.

Water as a touch medium has been investigated in HCI [69, 187, 206]. However, to the best of our knowledge, liquid *lubricants* and *adhesives* have not been investigated within an interactive context. While unconventional, we demonstrate that carefully chosen liquids can circumvent many

of the limitations associated with prior approaches to variable friction, enabling friction modulation of a *wide* range of objects and surfaces.

Benefits, Contributions, and Limitations

Our key contribution is that we propose, explore, and engineer a new approach to friction modulation based on liquid droplets that coat the fingerpad. Our approach provides three key benefits: (1) It enables altering friction on a wide range of surfaces and geometries, making it possible to modulate *nearly* any non-absorbent surface; (2) Since our device is a wearable, friction modulation easily scales to *many* objects in the environment; (3) It can *both* increase and decrease surface friction using a single hardware device. Ultimately, we see Stick&Slip as an exploration of alternative approaches for friction haptics, an area that unlike pressure or vibrotactile haptics, has not seen many alternatives.

Our approach is not without limitations: (1) Liquids are ineffective in absorbent materials (e.g., fabric); similarly, there are edge case materials that resist our approach (e.g., "non-stick" surfaces such as PTFE onto which not even a gecko can adhere [84]) or are incompatible with solvents (e.g., acetone can strip some surface finishes [204]); (2) Because our sticky fluids are diluted to enable faster evaporation, they first feel slightly slippery to the user before increasing in friction as their solvent evaporates; (3) While our approach delivers small droplets, their wetness can be noticed in some use cases. That said, we strive to characterize these limitations so that we can reduce them and improve the overall interaction experience. Further insights into understanding these limitations, best practices, and areas for ongoing investigation are detailed in our *Recommendations and Future Work* section.

Finally, we are not proposing to replace existing friction modulation techniques such as electrostatics and vibration, but rather we aim to widen the range of objects and surfaces that can be modulated with a new approach.

Implementation

To help readers replicate our design, we now provide the necessary technical details. The key components of our haptic device are the finger-worn droplet generator, the pumps, and the control electronics, as shown in Figure 31. Our wearable device uses its pumps to draw liquids from their reservoirs (worn as a bracelet around the wrist), through tubing, and then to the holes that generate droplets on the skin.

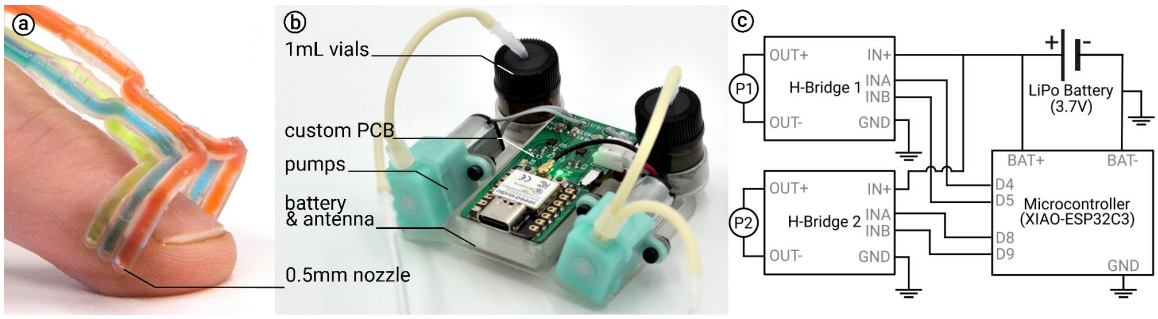

Figure 31. (a) Our nail-worn droplet generator. (b) Our bracelet device and its components. (c) Electronics schematic of our PCB.

Finger-worn Droplet Generator

We wrap y-split channels around the sides of the finger, there the channels narrow from 1mm to a 0.5mm nozzle that pinches the fluid into a droplet (droplet size: ~15uL). These droplets run down the side of the finger and coat the fingerpad. The nozzle diameter is small enough such that shaking the device or touching a surface does not cause leakage. Importantly, our droplet generator keeps the user's fingerpad free to feel real surfaces—even if fingers are slightly wetted from friction modulation, they still feel some of the surface's texture [65]. The droplet generator weighs 0.35

grams and is adhered to the fingernail with double-sided tape. We use silicone tubing for sticky liquids and PTFE tubes for slippery liquids (to prevent evaporating through silicone).

Pumps, Sensors, and Microcontroller

At the core of our device is an ESP32C3 microcontroller (Seeeduino Xiao), which communicates with external applications (e.g., MR experiences) via Bluetooth LE and is responsible for controlling the micropumps. Our entire wearable device weighs 60 grams including filled liquids. We also piloted a three-channel version by adding another pump, tubing, and y-split in the droplet generator to include a channel for depositing water to wash away sugar (as shown in Figure 31a). For the sake of miniaturization, our final device uses just two channels (sticky/slippery).

Pumps. We use peristaltic micropumps (Takasago RP-Q) to pump our liquids from their reservoirs to the droplet generator. These specific pumps were chosen for their siphon prevention (i.e., liquid cannot be shaken or sucked out preventing accidental fluid discharge, unlike piezoelectric diaphragm pumps). We run our pumps at 3.7V via DRV8837 H-Bridges and control fluid volume based on timing (adding thermistors or flow meters to close the loop is possible, but we found in pilots that these pumps are consistent even in open loop). We found that 1 second of pumping is sufficient to coat the fingerpad, which is what we use in typical interactions. Given our 1mL fluid reservoirs and our pump flow rate of 1mL/min, our device enables 120 interactions (60 droplets x 2 channels). This number is proportional to the reservoir size (e.g., a 2mL reservoir will double interactions).

Battery life. Our 350mAh battery fits directly under our custom PCB. Since our pumps are low-power (3.7V x 80mA = 0.3W), the battery life is >4 hours of continuous pumping. However, as outlined above, we only need to pump fluid for ~1 second to coat the fingerpad. Therefore, our battery tends to last a full day of on-demand use.

Latency. The total latency of our device is ~200ms as measured by a highspeed camera, i.e., from a keyboard trigger in Unity to a droplet beginning to dispense. This overall latency includes Unity/OSC/BLE communication (~40ms), microcontroller (<10ms), and pump (~150ms).

Developing our Friction-Modulating Liquids

There are two primary factors that influence a fluid's frictional characteristics: viscosity and surface energy. Increased viscosity leads to greater resistance to flow, while increased surface energy leads to greater adhesion and cohesion [61, 238]. As such, we experimented and selected a set of liquids with various viscosities and surface energies aiming to find fluids that induce sticking and slipping. As a subgoal, we uniquely want fluids that can either *quickly evaporate away* or whose effects can *be negated by another fluid*, so that we may interactively switch between frictions. As this is a first work in using liquids for interactive friction modulation, we detail the rationale for selecting candidate fluids: (1) We chose only from fluids deemed skin-safe (i.e., found in commercially-available healthcare products), which ruled out UV-curable resins and chemically corrosive fluids. (2) We selected only fluids that are relatively clean to deposit into environments, which eliminates fluids that cause miscoloring such as liquid metals—all our fluids are clear and were colored only for visibility in photos. (3) We chose only from fluids that can be easily pumped, which rules out very viscous fluids like pure honey or silicone damping fluids. (4) We did not choose fluids that require hardware beyond pumps (e.g., skin-safe super glue requires a closing mechanism to protect it from curing in air). (5) We did not choose liquids that are not liquid at room temperature (e.g., hot glue). This yielded the following set of initial fluids that we evaluate later:

Isopropyl Alcohol. While not commonly regarded or studied as a lubricant, isopropyl alcohol (IPA: 99.9% v/v) acts as a slippery liquid while also offering a rapid rate of evaporation. This is

highly desirable for our use case—IPA can lubricate a surface to make it feel slippery and then evaporate away without a trace. If the user touches the surface after the liquid has evaporated, it will feel as though it had never been lubricated. IPA is skin-safe under normal use [83, 115], but can lead to dry skin when the skin is exposed to high volumes of fluid for a long time (e.g., 20mL for 1 hour [115]); this exposure level required for extreme dryness is considerably higher (>1000x the volume) and longer than that of our droplets, which evaporate in minutes as shown in *Experiment 2*. Moreover, widespread clinical studies have found IPA to be *less irritating* to the skin than hand washing with detergents [134, 244]. Thus, it is commonly found in hand sanitizers, cosmetics, and household cleaning products. Similarly, isopropyl alcohol is compatible with a wide range of surfaces spanning metals, glass, electronics, and most plastics. It should be noted that some plastics and surface finishes are degraded by alcohol and are thus incompatible with IPA [135].

Acetone. Acetone is a solvent that can act as a lubricant, but with a faster rate of evaporation than IPA. This makes it a great candidate for interactive applications in which the friction must only be briefly reduced. Acetone, like IPA, is skin-safe under normal use. While acetone is commonly thought to lead to dry skin [141, 309], studies in dermatology have found that it does not disrupt the skin barrier, even when exposure is much greater and longer than used in our application (e.g., a cotton ball soaked in acetone applied for >12 mins continuously) [2, 207]. It is commonly found in nail polish remover, often accompanied by additives such as glycerin to ensure skin moisturization [31, 171]. While acetone has the advantage of rapid evaporation, it should be noted that it is a stronger solvent than IPA [204]. Thus, if a material is incompatible with acetone, IPA may be used as an alternative.

Honey-IPA Solution. Honey is well-known for its viscosity and stickiness owing to sugar's hydrogen bonds with water [266]. Unfortunately, honey's viscosity makes it difficult to pump. Therefore, to create a sticky liquid, we dilute honey with IPA to reduce its viscosity. Importantly, honey's stickiness remains despite being diluted (as we show in our *Technical Evaluation*, just 2wt% honey can cause a 50% increase in static friction). Because we dilute honey with a solvent, the honey can effectively coat the fingerpad. As the IPA evaporates, it leaves behind a thin, adhesive film on the fingerpad. Importantly, we chose honey because it is water-soluble; thus, it can simply be washed away with water after use, returning the fingerpad and surface to their original friction. Note, we chose IPA (IPA: 70% v/v, water: 30% v/v) as the solvent rather than acetone because sugar water is insoluble in acetone. This is beneficial: slippery liquids that do not rehydrate sugar residue prevent accidental stickiness.

Thickened Water. Water can be made into a viscous gel with a very small amount of thickening agent (e.g., 1 wt% of Xanthan gum, a food-grade polysaccharide). Despite the small concentration of thickening additive, it feels adhesive to the touch while very little residue behind.

Additional safety measures. We exclusively applied our liquids in small droplets (~15 uL) to the fingerpad, with brief exposure times enabled by rapid evaporation. This approach mitigates potential side effects, notably dry skin. Moreover, the small volumes employed, coupled with the direct delivery of droplets to the side of the fingerpad, not only ensures immediate coating but also minimizes the risk of inhalation or application to other skin areas.

Experiments 1-4: Fluid Friction and Practicality

To understand the effects of our candidate liquids on friction as well as their practicality (i.e., how long do their frictional effects last?), we performed four technical experiments. We then apply these findings to our user study where participants experienced our approach in an interactive

context. To our knowledge, these experiments have not been performed in related work. Thus, we designed these to focus on our specific application of temporary friction modulation between a finger and surface.

To aid the reader in understanding the four technical experiments we conducted, we present an overview of their results: **In experiment 1, we measured the fluid effects on friction coefficients**: we found the greatest friction reduction from oil, IPA, and acetone, and the greatest friction increase from sugar water, 30wt%, and 2wt% honey in IPA**; In experiment 2, we measured the fluid evaporation rates**: we found that acetone, IPA, 2wt%, and 30wt% honey in IPA evaporated the fastest, and we eliminated oil, water-based lube, water, and sugar water for their poor evaporation; **In experiment 3, we measured friction over repeated trials**: we found that acetone and IPA initially decreased friction, then returned to the baseline. We found that 2wt% and 30wt% honey in IPA caused stickiness faster than thickened water**;** finally, **in experiment 4, we measured washing away residue**: we found that water washes away sugar residues, where effectiveness increases with water volume.

Experiment 1: Fluid Effects on Friction Coefficients

To determine the extent to which each of our candidate fluids impacts the coefficient of friction between surfaces, we built a mass-pulley tribometer, as illustrated in Figure 32. By increasing the load of the hanging mass, a sliding mass approximating the finger's frictional properties slides across the surface. The coefficient of friction can be calculated by measuring the block's acceleration along with the hanging mass. For each fluid, 10uL of liquid was pipetted between the testbed surface and the sliding block. We evaluated both the static and kinetic friction coefficients for nine potential liquids: (1) sugar water (66.6wt% sugar), (2) 30wt% honey in IPA, (3) 2wt%

honey in IPA, (4) thickened water (1wt% xanthan gum), (5) water, (6) water-based lubricant (*Shibari*), (7) acetone, (8) IPA, and (9) oil (*3-IN-ONE Multi-purpose*).

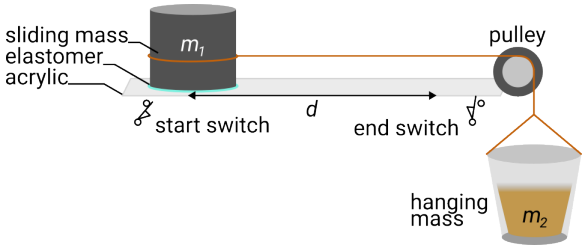

Figure 32. We built a mass-pulley tribometer to mechanically evaluate the effect of our liquids on coefficient of friction.

Our sliding mass approximated the finger's frictional properties during a light, exploratory touch. The sliding mass weighed 25g. To approximate skin, the bottom of the sliding mass was coated in polyurethane (commonly used in mechanical approximations of the skin [41], *Smooth-On KX Flex 40*). The surface area of the block was 20mm^2 to approximate the contact area of a fingerpad under 25g of compression [49]. The testbed was made from smooth acrylic (note that for well-lubricated surfaces, the friction coefficient is nearly independent of the material [191]). Prior work in contact mechanics indicates that the friction coefficient for an index fingerpad on acrylic under 25g and sliding at low velocity is ~1.60 [3, 125]. In our testing, we found our sliding mass to be a reasonable approximation for a finger because its kinetic coefficient of friction on acrylic measured 1.6±0.125 over 25 trials.

Static friction procedure. First, we tested the effect of liquids on the coefficient of static friction, determined by finding the minimum force required to initiate sliding. To do so, the hanging mass was slowly increased by pouring sand into a suspended cup (~1.5grams/sec). Once the mass began to slide, a hardware limit-switch was released, and no more sand was added. The hanging mass was then weighed. The static coefficient of friction is calculated by taking the ratio of the hanging mass to the sliding mass. For each liquid, five trials were performed, and the

apparatus was cleaned between trials; we confirmed the cleaning effectiveness by measuring and comparing it to the no-liquid baseline value.

Static friction results. Figure 33 (a) shows change in static friction coefficient that fluids achieved (relative to a no liquid baseline, the surfaces' original friction). We found greatest reductions in static friction from oil (-62.9±3.3%), IPA (-59.7±2.9%) and acetone (-59.2±4.3%), while the greatest increases in static friction were found from sugar water (83.0±15.7%), 30wt% honey in IPA (78.3±16.1%) and 2wt% honey in IPA (56.1±9.5%). Note that because there is an onset time for sticky liquids, we depicted maximal values (see *Repeated Trials* for a characterization of this onset).

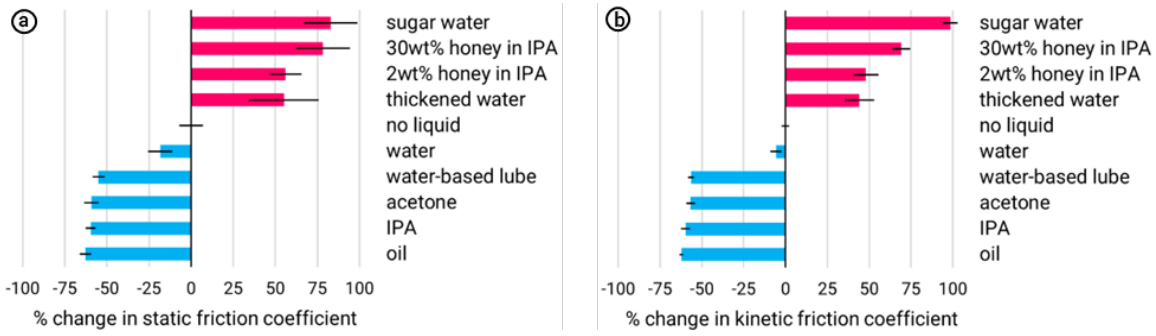

Figure 33. Relative changes in: (a) static friction, and (b) kinetic friction for each fluid.

Kinetic friction procedure. As we are interested in sliding interactions, we measured the kinetic friction coefficient, which can be determined by finding the acceleration of the sliding block. To do so, we apply a hanging mass equal to the average mass that initiated sliding for each fluid in our earlier static experiment. When the mass begins sliding, the start limit switch is released and the block slides into the end limit switch. The distance (6cm) and time difference between triggering the switches is used to calculate the block's acceleration ($a = d/t^2$). The kinetic friction coefficient is then calculated using: $\mu_k = (m_2 g - (m_1 + m_2)a)/m_1 g$.

Kinetic friction results. Figure 33b shows the relative change in kinetic friction coefficient for each liquid. As shown, the overall trend held between the static and kinetic friction tests. Considering that friction coefficients span a small range (i.e., typically from 0.0 to 4.0), even a ±30% change is dramatic.

Experiment 2: Evaluating Fluid Evaporation

With a goal of using liquids to alter friction interactively, we aim to choose liquids that not only alter sensation, but are also *practical*, i.e., evaporate quickly and leave minimal residue so that we may design applications that can switch easily between sensations. Thus, we measure the weight of a fluid droplet over time, to characterize its evaporation.

Procedure. To measure the rate of evaporation, we pipetted a 10uL droplet onto a plastic weigh tray and placed it inside a lab-grade scale (Mettler Toledo, 0.0001g precision). The droplet weight was recorded every 30 seconds.

Evaporation results. Figure 34 shows the relative remaining droplet mass after five and 60 minutes (only two points depicted for clarity, measurements taken at 30s intervals).

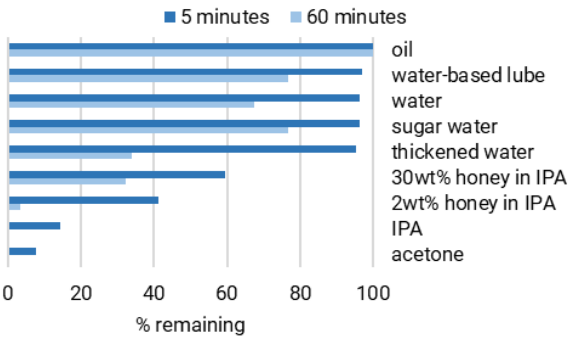

Figure 34. Fluid evaporation at two points (5 and 60 minutes).

We found that solvents like acetone and IPA evaporated the fastest and left behind no residue. The second fastest evaporating group of fluids were solvents containing honey, where a lower concentration of honey resulted in faster evaporation. Notably, the solvents evaporated out of these

mixtures leaving behind residue of approximately the mass of the honey contained within the mixture along with retained water (after 60 mins, 2wt% honey had 3.4% remaining mass and 30wt% honey had 32.4% remaining mass). Water-based liquids evaporated slower than solvent-based liquids, where thickened water evaporated faster than water, which itself evaporated faster than water-based lubricant. Finally, oil showed no signs of evaporation in 60 minutes.

Eliminating unsuitable fluids. At this point, we found that oil, water-based lube, water, and sugar-water do not evaporate rapidly (i.e., the four slowest evaporations in Figure 34). Moreover, given that we found that solvents had comparable lubricating properties in our previous experiment and that these solvents evaporate rapidly, we deem oil, water-based lube, water, and sugar-water as no longer fluids of interest. That said, these may still have niche use cases, which we elaborate upon in *Recommendations and Future Work*.

Experiment 3: Fluid Friction over Repeated Trials

Having characterized each fluid's maximal effects on friction along with their evaporation rates, we now look to characterize friction and evaporation in conjunction over multiple sliding motions. Additionally, we aim to shed light on the timing (onset and offset) of each fluid's effects.

Procedure. We used the same apparatus and procedure described in *Static Friction*. However, instead of cleaning the testbed and sliding block after a single trial, we placed the sliding block back on the starting position and tested the static friction again. After a droplet was placed on the block, sliding was repeated 10 times. Each time, the block slid 6cm, for a total distance of 54cm.

Repeated trial results. Figure 35 shows the relative change in friction for each fluid over the sliding distance (each point represents the average of 5 trials). We found that all our fluids cause an initial reduction in the static friction, with solvent-based fluids being the most lubricating. Acetone and IPA return to approximately the no-liquid baseline as the fluid evaporates. The fluids

containing honey and xanthan gum result in increased friction after sufficient spreading of the fluid during sliding and evaporation.

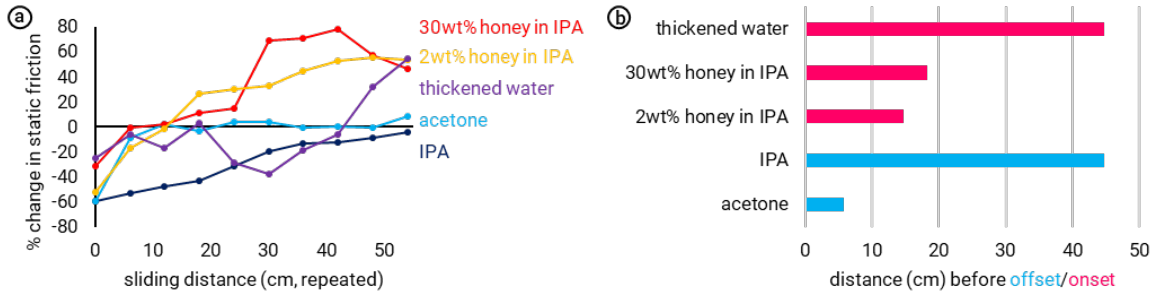

Figure 35. (a) Fluid friction over repeated trials (distance in cm); and (b) offset/onset distance (i.e., the sliding distance required for a slippery sensation to disappear or a sticky sensation to appear).

On/offset results. To understand how the onset/offset times of friction changes affect perception, we contextualize them within psychophysics literature by comparing to established just-noticeable-difference (JND) values. Specifically, the Weber fraction for surface friction is known to be ~11% [63]. Therefore, we can determine the sliding distance required for a change in friction to be felt, as depicted in Figure 35b. All tested liquids initially reduce friction greater than 11% and thus immediately feel slippery. In the case of liquids that intentionally are slippery, we aim to select for those that can quickly return to within 11% of the baseline friction coefficient (determined with linear interpolation), i.e., the slippery effect has disappeared, and the surface feels unaltered. In the case of IPA, we found that after 44.7cm, the change in static friction returns to within 11% of the original. Acetone exhibited a faster return to baseline friction, at just 5.7cm. This suggests that acetone is better for brief lubrication, while IPA can provide a sustained sensation for the same dispensed volume (while still disappearing over time). While sticky liquids initially reduce friction by a small amount, after some sliding and evaporation, they dramatically increase friction. Therefore, we are interested in how long it takes for sticky liquids to perceivably increase the friction by more than the 11% JND. We found that 2wt% honey in IPA took the

shortest distance (14.7cm), followed by 30wt% honey in IPA (18.2cm) and thickened water (44.7cm).

These are conservative estimates. We discuss the implications of these timings in *Recommendations* but it is important to note that mechanical analysis results in very conservative estimates of performance: (1) we slid the block repeatedly over the same path as opposed to one continuous long slide (worst-case scenario); (2) our elastomer skin does not absorb any fluid unlike actual skin [139]; and (3) our sliding block is at room temperature, while our skin is significantly warmer which aids in fluid evaporation [160].

Eliminating unsuitable fluids. Because thickened water has a long onset time to increasing friction, we eliminate it, but discuss other potential uses for it in *Recommendations*.

Experiment 4: Washing Away Sticky Residue

As we found in our second experiment (Figure 34), sticky liquids leave residue behind due to sugar content. Moreover, our third experiment (Figure 35) found that, in the short-term, this residue increases friction as long as it retains water (dry sugar is not sticky). While waiting for this stickiness to naturally dry might fit some applications, we argue that understanding whether this process can be sped up is of value for a wider interactive application of our concept. To tackle this, we propose using water to dilute and dissolve away sugar residue. To this end, we conducted an experiment.

Procedure. On sticky liquids, we performed static friction tests until the friction reached within 5% of the peak reported in our first experiment (Figure 33). Then, we added 10uL or 20uL of water and continued performing static friction tests.

Washing stickiness results. We found that without washing, the friction decreases over time for both 30wt% and 2wt% honey in IPA. Adding water causes an initial decrease due to lubrication.

Then, the water dissolves the sugars, and the friction decreases toward the baseline condition, where more water led to greater reduction in friction. Moreover, we also confirmed that using acetone and IPA as wash fluids also reduced the stickiness immediately, but the stickiness eventually rises back to peak values as the solvents evaporate without having diluted the sugars.

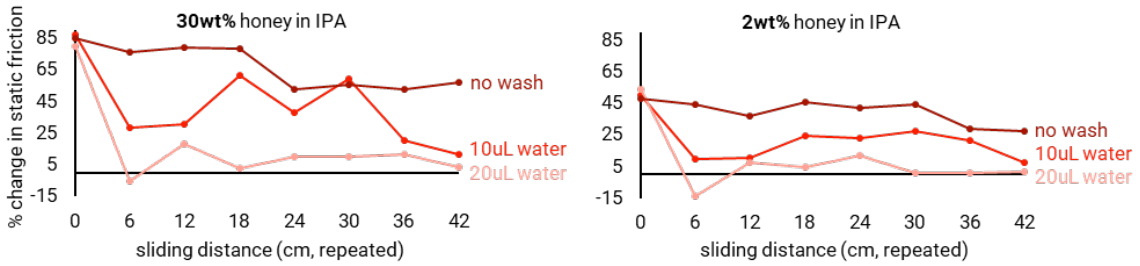

Figure 36. Applying water to sticky surfaces reduces friction.

Summary of Findings and Narrowing the Best Liquids

Our four experiments characterized fluids based on their ability to modulate friction and their practicality. While all fluids we investigated offer unique properties which we discuss in *Recommendations*, we optimize for our applications (requiring strong modulation changes while being easily removed). As such, we selected **30wt% honey in IPA as our sticky** fluid and **acetone as our slippery** fluid for all our interactive applications.

Experiment 5: User Study on Interactive Use

While our first experiments examined our fluids' effects on friction along with their evaporative properties, our final experiment focused on observing our approach in an interactive application. Specifically, we assess the extent to which our approach influences the sense of immersion and enjoyment in a mixed-reality experience with physical surfaces and props. Our main hypothesis for this study was that the MR experience with Stick&Slip would feel more immersive and enjoyable than a baseline without our device because of the haptic experience.

Conditions. Participants experienced two interface conditions in counterbalanced order: (1) Stick&Slip (worn on the right-hand index finger and wrist) and (2) a no-haptics baseline in which participants did not wear our device. We chose this baseline rather than depositing a "neutral" fluid because any fluid, even water, still causes changes in friction, as found in our experiments and literature [173]. Additionally, the baseline depicts the current state of MR with passive props. Wearable devices offer the benefit of always-available haptics, often at the expense of, to some extent, encumbering the user. To assess whether adding our liquid-based friction haptics to mixed reality justified this encumbrance, we compared between *our device* and a *no-haptics* baseline.

Participants. We recruited twelve participants (seven identified as female, five as male, average age of 23.4 years old, SD=3.3). Participants received $10 for their time.

Apparatus. We built a prop-based MR experience to evaluate our device as shown in Figure 37. Specifically, as informed by our prior experiments, we tested this experience using **acetone** as a slippery liquid and **30wt% honey in IPA** as a sticky liquid. In the experience, participants wore a Microsoft Hololens 2 MR headset. The table was made of acrylic to minimize issues with the Hololens' hand-tracking.

We designed the timings of pumping our liquids based on the results of Experiment 3: (1) **Slippery sensations produced by acetone:** Because there is no onset time for slippery liquids to reduce friction, we pump for one second immediately when a user's finger enters a slippery zone. (2) **Sticky sensations produced by 30wt% honey in IPA:** Sticky liquids have an onset distance due to time required for fluid to evaporate and leave behind a sticky film. Informed by Figure 35, we designed our experience to begin pumping 30wt% honey in IPA approximately 18cm before the effect appears so that it feels sticky when the user reaches it.

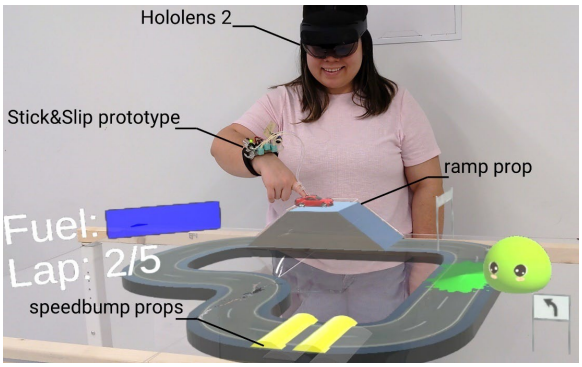

Figure 37. Study 2's apparatus: a mixed reality experience with physical props (image taken from 3rd person perspective).

Procedure. We utilized our MR racing experience, in which participants drive a virtual car on a track by dragging their finger (the same application described in our *Walkthrough*). In this version of the MR racing game, participants experienced eight surface haptic events (rainfall, ice, slime, and honey—each was presented twice). Each trial took ~10 minutes and participants were interviewed between trials. Interviews consisted of Likert ratings (1-7 scale) of the experience (immersion, enjoyment, sensory engagement [226, 251]) along with open-ended questions regarding what contributed to their experience. Participants' fingers were cleaned with soap and water before each trial. Finally, besides these virtual effects, participants also experienced physical props, such as the texture of the table, 3D-printed speedbump props and an acrylic ramp prop.

Results. Figure 38 presents our main findings. After testing the Likert data for normality, we used a Mann-Whitney test (two-tailed) to test our hypothesis that Stick&Slip leads to improved experience. We found significant differences between the two interface conditions, where Stick&Slip received greater ratings than the baseline for immersion ($p<0.001$), enjoyment ($p<0.001$), and sensory engagement ($p<0.001$). Moreover, all twelve participants indicated that they preferred the Stick&Slip condition over the no-haptics baseline. Altogether, this supports our main hypothesis that Stick&Slip improves the experience.

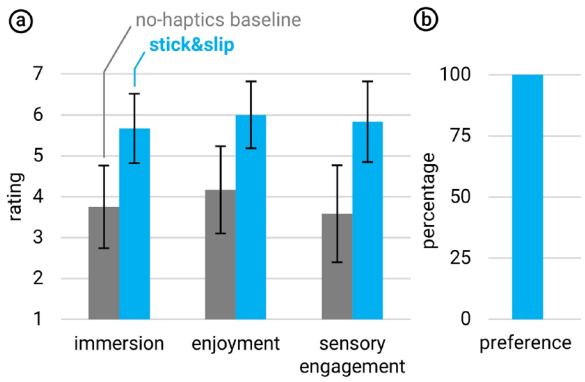

Figure 38. (a) Participants' ratings for both conditions. Error bars show standard deviation. (b) Participants' preference.

Qualitative Feedback. We analyzed all responses to our questionnaire. First, all participants felt that friction haptics added to the experience. To illustrate this, P10 stated "when touching one single surface, you don't feel much but now with different road situations its quite interesting." P2 & P6 both stated that the device made them want to explore tactilely and P9 expressed that it "sparked more childish excitement." While one may expect some potential novelty effect, all participants preferring Stick&Slip gives some indication that participants felt the fluids were not unpleasant and added to the experience; for example, the liquids "added a whole other dimension to the game through sensations" (P6 & P4). This suggests that the gain in immersion was worth the cost of wearing our device.

Beyond adding haptics, five participants expressed a desire for "the digital and physical to correspond" (P11). P5 explained "seeing the visuals line up with the feeling led to better immersion". P7 noted that "the ice felt slippery" and that their "finger went faster than expected". Similarly, P9 stated, "if I were driving through ice, it's how I'd expect it to be". Along this line, P8 recalled that "[I] felt a sense of traction going through honey effect".

Our haptics also influenced how participants experienced props on the track. For example, P1 felt that it was harder to go up the ramp after going through slime. Similarly, P3 & P9 felt the ramp was more slippery after it had rained.

Finally, our approach is not without limitations and participants' responses also indicate opportunities for further research. First, two participants (P1 & P9) noted feeling that the ice and rain felt cold, likely either from acetone's evaporative cooling or from a pseudo-haptic effect driven by the visual suggestion (P1 noted the ice felt colder than the rain, despite identical actuation parameters). Second, three participants noted that they felt a delay between the sticky visuals and the sticky sensation. Third, only two participants noted feeling any residue, despite us opting not to use any wash fluid during the MR experiment, suggesting that once the sugar has dehydrated, it is no longer perceived as sticky. No participants commented on any odors originating from the fluids, which suggests that no odors were perceivable (e.g., from possible vapors of the liquids as they evaporate). Finally, no participants reported any dry skin or irritation.

Further Applications for Stick&Slip

To illustrate the versatility of our approach, we implemented two additional and unique applications in which we use Stick&Slip to enhance user experience via variable friction.

VR using Static Props with Dynamic Friction

Figure 39 depicts a VR escape room experience in which the user needs to repair three pipes to open the next door. When a pipe cracks and sprays water, the user must place their hand on the crack to stop the water, which will now feel slippery via our device rendering the virtual water with real water droplets. To patch the pipe, the user turns around, dips their finger into virtual sealant putty, and returns to rub it over the crack. The user then discovers that another pipe has

rusted and feels the rust's roughness rendered by our sticky fluid. To remove the rust, the user sprays a dissolver and rubs the pipe until the rust sheds off, feeling the pipe's surface return to its smooth texture as our device washes this stickiness with water.

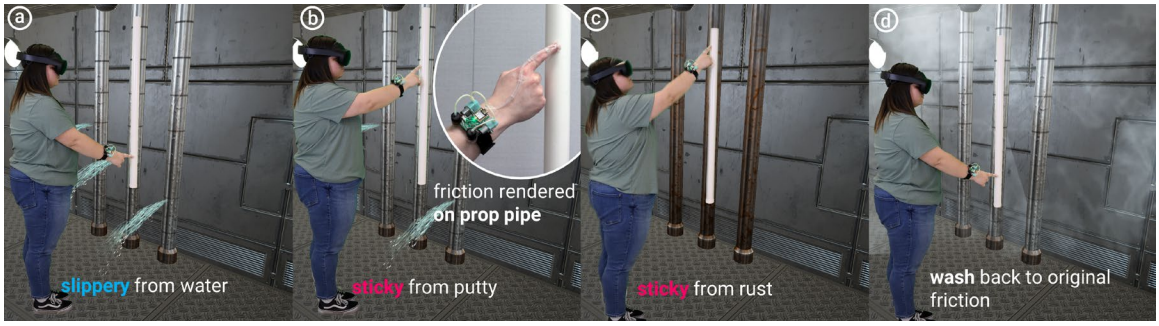

Figure 39. Stick&Slip adds friction feedback to VR with props.

We use this example of enhancing VR with props to demonstrate a key benefit of Stick&Slip: no existing technique can *both* increase or decrease surface friction on a prop of this size and material (not electrically conductive).

Augmenting Friction of Everyday Tools

We leverage liquid lubricants and adhesives because they modulate the friction of nearly any non-absorbent surface without the need for any surface instrumentation. Therefore, our approach can alter the friction of everyday objects and tools. Figure 40 (a-b) demonstrates our first example of how Stick&Slip can alter friction while interacting with everyday tools. Here, a user is tightening a nut with a digital torque screwdriver (Figure 40a). When they reach the maximum allowable torque, our device deposits slippery liquid, causing the user's fingers to slip off the tool and stop tightening (Figure 40b). This provides an additional haptic cue when maximum torque is reached.

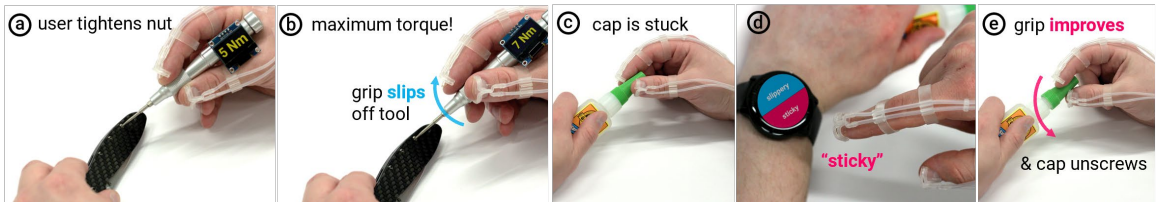

Figure 40. Stick&Slip with tools: (a) A user tightens a nut via a digital torque screwdriver. (b) At the maximum torque, our device pumps slippery liquid to provide an additional haptic cue. (c) A user unsuccessfully tries to open their glue. (d) The user activates on-demand stickiness, which increases friction and improves grip, (e) which assists the user to unscrew the cap.

Figure 40 (c-e) depicts a second example of altering the friction of everyday tools. Here, our device can improve users' grip. The user tries to unscrew a stuck glue cap but is unable (Figure 40c). They activate Stick&Slip on-demand via their smartwatch, which coats both their index and thumb's fingerpads (Figure 40d). This improves their grip on the cap, assisting them to ultimately unscrew the cap with less effort Figure 40e).

Each of these examples demonstrate that our device can augment everyday tools with variable friction, providing cues and aid to the user. This highlights another benefit of Stick&Slip: it would be impractical to augment these tools with any other existing approach (i.e., coating/grounding every tool for electroadhesion).

Recommendations and Future Work

We now condense our recommendations based on the benefits and limitations of our approach, as informed by both our technical evaluation, user study, and pilots.

Timing. Because our sticky fluids are diluted with solvents like IPA to enable greater evaporation, they first feel slightly slippery to the user before their dramatic increase in friction as the solvent evaporates. Therefore, it is important to design with this in mind. We conservatively characterized this delay in our *Experiments* and used it to design our MR experience. For example,

depositing sticky fluid on top of the ramp prop in anticipation of an upcoming sticky event did not interfere with immersion because participants felt that the initial slipperiness corresponded to sliding down the ramp. Similarly, we investigated liquids with a range of evaporation rates. While we implemented further studies and applications using fluids with rapid evaporation, there is opportunity considering liquids that *intentionally* leave a trail of liquid as a feature of the interaction.

Residue. Sticky liquids may leave residue in proportion to the added sugar. Once water has evaporated from this sugar, it is no longer sticky, but this is slower than desired for most interactions. Thus, based on our technical experiments, performance can be improved by either adding a third channel or opting to use a water-based liquid as the slippery liquid, which can also serve the dual purpose of acting as a washing fluid.

Wetness. Our approach to friction modulation might also be accompanied by a sensation of wetness. Surprisingly, only two participants mentioned this (and could be due to pseudo-haptics from visual suggestions of ice/water puddle). Still, we recommend designing with this user expectation in mind. For example, in our user study, we used visual effects that would not feel out of place if the participant experienced wetness.

Mixing liquids. As the first exploration of interactive liquid friction, we selected liquids that both alter friction and are *practical* to use, which yielded simple mixtures. It is likely possible to synthesize more advanced liquids. Because this is an early exploration, it is likely that future works may identify liquids that alter friction with fast onset and offset times but are entirely inert when interacting with skin and sensitive materials (e.g., surface lacquers). In the meantime, we can draw inspiration from products that contain our liquids (nail polish remover, hand sanitizer, etc.), but also include common additives like glycerin for improved practical long-term use [31, 171].

Moreover, liquids offer a wider design space than just friction, such as affective responses (e.g., pleasantness), which offers opportunity for further investigation [64, 65].

Conclusion

We proposed, engineered, and validated Stick&Slip, a new approach to altering everyday surface friction by coating the user's fingerpads with liquid. Unlike traditional actuators such as vibromotors or electroadhesion, which are confined to specific surfaces, our method uses liquid lubricants and adhesives. These substances can modulate the friction of nearly any non-absorbent surface without requiring specific surface instrumentation, resulting in a more universally applicable friction modulation.

We demonstrated the versatility of our technique in various applications, including mixed reality, virtual reality with props, and everyday objects. Our approach was validated through four technical experiments and a user study.

Stick&Slip points towards a new direction in HCI, in which engineered materials/chemicals offer alternative methods to achieve haptic sensations. Having shown that liquids can both modulate friction and be improved in their practicality, we hope to inspire future research exploring the use of liquids for haptics beyond friction modulation. Ultimately, we hope to provoke alternative strategies in areas of haptics that may otherwise be limited by traditional approaches.

ThermalGrasp: Enabling Thermal Feedback even while Grasping and Walking

Figure 41. (a) We propose a new approach that enables thermal feedback devices to provide realistic temperature sensations while still allowing users to grab or step on real objects—not only can virtual objects display a temperature, but users can also feel and grasp real objects, such as props. Our approach is different from traditional thermal interfaces, in which Peltier devices are applied to the user's hands to render the temperature of virtual objects. Unfortunately, attaching a Peltier element and its cooling unit (fan and heatsink) directly to one's palm prevents users from also grasping real-world objects. Similarly, existing thermal interfaces cannot be applied to feet soles (as one would need to step on the cooling unit). The result is that existing temperature interfaces are restricted mostly to virtual interactions (hands-free, no props). With ThermalGrasp, (b) we explore a flexible thermal mechanism that allows the cooling unit to be moved away from the user's palms or soles—enabling them to grasp and step on objects.

In this chapter, we describe ThermalGrasp [145], our approach to thermal feedback that is still compatible with grasping real objects and walking on real surfaces.

Introduction

Haptic feedback improves user experience in virtual reality (VR) and mixed reality (MR) by providing physical sensations that complement the immersive audiovisuals. Haptics research has led to a remarkable range of wearable haptic devices for delivering tactile (e.g., vibration [39, 110,

111], pressure [112], skin stretch [71, 104]) and force feedback (e.g., exoskeletons [36, 37, 85, 167] or electrical muscle stimulation [48, 136, 137]).

More recently, researchers explored stimulating senses beyond forces and tactile cues, such as providing thermal feedback [165, 186]. At the same time, researchers also demonstrated the compelling use of real-world props as proxies for virtual objects and virtual terrains because they provide cheap yet hyper-realistic haptic feedback [33, 86, 296].

Unfortunately, wearable thermal actuators and props are at odds. This is because typical thermal actuators are inherently bulky or fragile; thus, applying wearable thermal actuators to the user's hands or feet prevents users from grasping or stepping on physical objects (e.g., props or terrains). For example, some recent thermal devices create hot and cold sensations by pumping water through flexible tubes worn by the user [67, 73, 190]. While the tubes' flexibility allows them to conform better to the body, this is also their limitation: any kink in the tubing cuts off the liquid flow and halts the thermal sensations, which happens when a tube is compressed, like if gripped or stepped on.

As such, the most popular approach to wearable thermal feedback is still the *Peltier* element [307]—a thermoelectric material that, when powered, heats up on one side while cooling down on the other. This makes them appealing for wearables because of their simple electrical control and lack of moving parts or fluids. More recently, even emergent flexible Peltier materials have begun development [127] (price is still prohibitive at 100x the cost of a rigid Peltier, and their flexibility is limited to <12 repeated folds or very small angles). Despite the benefits of Peltiers, to sustain *both hot and cold sensations* (especially lasting more than a few seconds, e.g., rendering temperature of objects and terrains), Peltier elements, both rigid and flexible, *require additional cooling from heatsinks and fans* to remove excess heat from the hot side [91]. Without these bulky

cooling units, Peltier elements quickly saturate, i.e., heat leaks from the hot side to the cold side—cascading into a positive feedback loop of undesirable heat.

This requirement for cooling units prevents Peltier elements from being applied to body parts that *contact real objects*, such as the user's palms or soles. In fact, interactive systems based on attaching Peltiers and their heatsinks to users' palms and soles will not allow users to *grasp objects nor walk on top of surfaces*.

To tackle this challenge, we introduce *ThermalGrasp*, an engineering approach for wearable thermal interfaces that enables users to grab and walk on real objects with minimal obstruction. To realize this, our approach moves the Peltier and its cooling unit to areas not used in grasping or walking like the top of the foot or back of hand. We then use thin, compliant materials to *conduct* the Peltier's heating or cooling to the palm or sole. Unlike existing approaches, our thin materials enable grasping and walking on real objects while enjoying thermal feedback. For example, Figure 41 depicts a user walking in a VR desert at dusk, feeling *both* the *sand's texture* and the associated (virtual) *decrease in temperature*.

Our Approach: ThermalGrasp

ThermalGrasp devices consist of three components, depicted in Figure 42: (1) a thermal element (typically a Peltier but others are possible), (2) **a thermally-conductive yet flexible material** (e.g., heat pipes, sheet metal, etc.), and (3) insulation (e.g., foam, plastics, etc.). The thermally-conductive materials contact the surface of the thermal element (in this case, a Peltier element) and channel the heat flow. Thus, when the Peltier element warms up, heat conducts through the conductive material. By wrapping the channel in insulation, we improve the heat transfer efficiency. The user feels heat at the correct location because we expose the target area's

skin to the conductor, while insulating all its other surfaces. Similarly, when the Peltier is cooled, heat is conducted away *from* the user, giving the sensation of cooling.

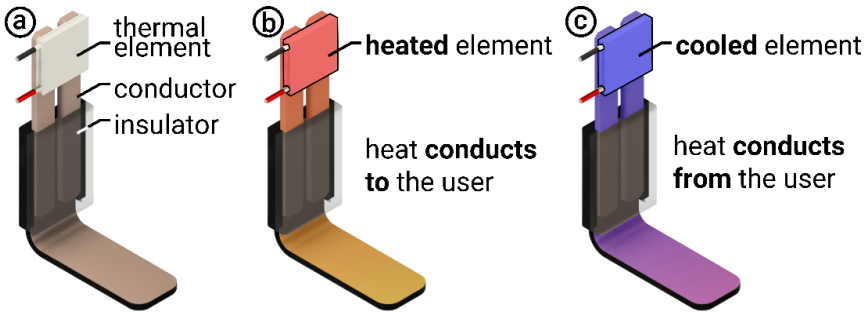

Figure 42. The key technical elements that comprise our approach, i.e., flexible thermal conductors to transfer heat.

ThermalGrasp's approach is different from the traditional approach (which we map in Figure 3)—placing Peltiers *directly* on the user's palm/soles to deliver thermal feedback (e.g., [57, 124, 177, 200]—to cite a few palm devices). Unfortunately, without cooling hardware (heatsinks and/or fans), Peltiers cannot provide sustained cooling for more than a few seconds before residual heat bleeds into the cold side, cancelling out the cooling effect [117]. While brief temperature changes can be effective for feedback like notifications, they cannot provide realistic temperatures needed to render the sense of walking on a gradually cooling floor in VR (e.g., stepping on desert sand that cools as the sun sets, which we demonstrate in *Study 2*). Again, even flexible Peltiers require added cooling to hold cold temperatures [13, 38].

As depicted in Figure 43, our technique **balances** thermal realism and haptic realism from props. While placing a Peltier directly on the palm/sole maximizes thermal realism (sensations are at the palm/sole), one cannot step on or grasp objects with cooling units directly on the palm/sole. Conversely, one could try to place the Peltier element on the backside of this limb to keep the palm/sole free (as in [163] or tactile devices that leave the palm free [8, 195]); however, the thermal realism is now drastically reduced because the sensation is felt at wrong location (opposite-side of

palm/sole). Instead, our approach delivers thermal feedback at the palm/sole while only minimally impeding upon real-world interactions, thereby optimizing for *both* thermal *and* real-world haptic realism.

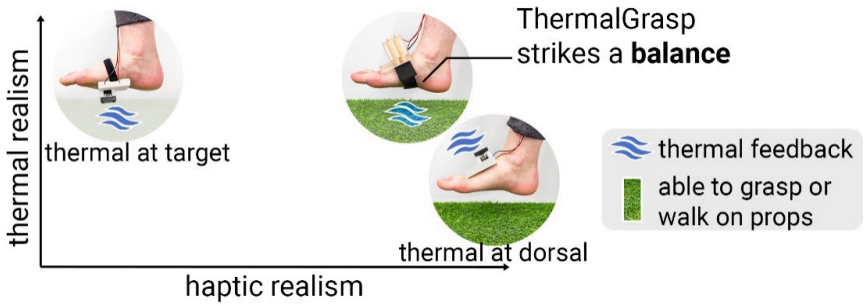

Figure 43. ThermalGrasp balances the realism of virtual temperatures and the realism of haptic props by conducting temperatures from Peltiers using flexible conductive channels, which enables to step or grasp at the application point.

To strike this balance, our approach relocates the bulky yet necessary cooling hardware away from body parts involved with grasping or walking, such as the palms of our hands and the soles of our feet. Then, using robust yet flexible & thin thermal conductors it transfers thermal feedback to the center of the palm/sole. These flexible materials can withstand large forces and wrap around the body—enabling thermal feedback while grasping or walking.

Finally, we tend to think of the devices that we engineered not as end-products but as artifacts of the ThermalGrasp approach—these depict some instantiations of our approach. In the process of creating these devices, we created four additional variations using different types of conductors, which are depicted in Figure 44. Namely, conduction using a copper mesh, a copper netting, a copper tape, and a silicone doped with liquid metal (EGaIn). While in our early technical pilots we found these to have reduced thermal efficiency compared to our final devices using thin flexible copper sheets, these can still be used or serve as a source of inspiration for future thermal devices that also allow grasping and walking.

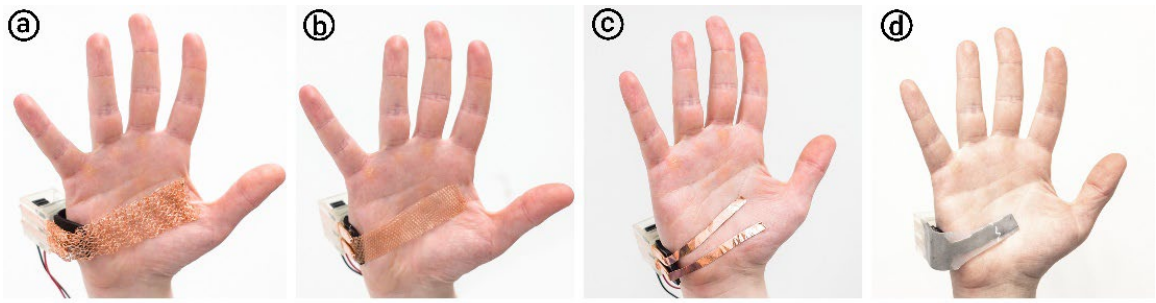

Figure 44. We also explored other conductors: (a) copper net, (b) copper mesh, (c) copper tape, (d) silicone doped with liquid metal.

Related Work

The work presented in this paper builds on the field of wearable haptics, with emphasis on devices that allow users to also feel real-world sensations and devices that render thermal feedback. Finally, we succinctly review prop-based passive haptics in VR since these are the key application domain for our technique.

Wearable Thermal Feedback = Attaching Thermal Actuators to Target Area

Researchers have been exploring how to miniaturize thermal actuators into wearable form factors. The most common approach to this challenge has been commercially-available thermoelectric Peltier elements. When electrical energy is supplied to a Peltier, it acts as a heat pump, transferring heat from one side of the device to the other—one side cools while the other heats, depending on the current's direction. This simple electrical control has made Peltier elements easy to deploy in wearable form factors, as shown by *ThermoVR* [185], *LiquidReality* [184], and *TherModule* [142].

However, while Peltier elements are inexpensive and easy to control, they pose disadvantages when applied directly on the user's hands and feet: (1) Peltier elements tend to be thick (~4-6mm typically); (2) Peltier elements are typically rigid (they do not conform well to the body); and more importantly (3) Peltier elements tend to require additional cooling (e.g., large heatsinks and fans).

While some wearables have used Peltiers without fans and heatsinks, these are limited to quick notifications [165, 186, 307], and cannot sustain realistic temperatures that are desirable for VR. This is because without cooling, Peltiers can only reliably perform cooling for a few seconds before residual heat from the hot side bleeds into the cold side, which cancels the cooling effect [117]. As such, most interfaces that aim to reproduce the thermal properties of touching an object use dedicated cooling hardware [35, 205]. This limitation has prevented thermal feedback from being applied, for instance, to the sole.

While recent research has led to the advancement and initial commercialization of flexible Peltier elements, these too require fans/heatsinks to deal with their residual heat during/after cooling. Take the Asahi Rubber DK-TEM es-02 [311] flexible Peltier element: its thermal performance was still characterized while attached to a fan and heatsink (3x the area of the Peltier). Moreover, flexible Peltiers remain both expensive and fragile. For example, [311] currently costs $240 a unit (100x a normal Peltier) and has a maximum bending angle of just 115 degrees (i.e., 50 mm bend diameter), which is smaller than even simple human joints, like closing the palm (which folds over itself when making a fist [245]) or curvatures like the arch of the foot (bending angle of 152 degrees while standing [32]).

As an alternative, other types of thermal elements have been explored, such as nichrome wire and conductive fabric [114, 256, 274], which provide resistive heating in a thin form factor but cannot create cooling sensations, thus missing half of our spectrum of thermoception. Some research has instead examined pumping hot and cold fluids for feedback [123, 190, 298]. For example, *HydroRing* [73] delivered temperature-controlled liquids to the fingerpad. Similarly, *Therminator* [67] developed a hydraulic system for thermal feedback on the arm in VR. Finally, *ThermAirGlove* [28] presented a pneumatic glove for grasping *virtual* objects to feel their thermal

properties. Thus, while these approaches address the rigidity downside of Peltier elements, they come with their own challenges: (**1) putting moderate forces on a tube will stop the liquid flow** (e.g., if one steps on it, it halts the thermal feedback); and **(2) temperature-controlled fluid tanks have yet to be made wearable**. Faced with the power consumption challenges, others have instead turned to using liquid chemicals to induce illusions of temperature change by chemically stimulating skin receptors to trigger pseudo-temperature changes [27, 139]—still, these chemical approaches are at an infancy (e.g., slow and coarse) compared to expressive and time-tested thermal feedback from Peltier elements and other devices.

In addition to each approach's individual limitations, all these approaches share a conceptual limit: they all apply some form of *thick thermal actuator* (be it a Peltier or a tube) *directly to the area of the user's skin* at the target they wish to stimulate. Here, we observe a conflict with our original goal: to provide thermal sensations yet minimize obstruction to the target area. The closest approach to tackle this is generating phantom heat sensations at the midpoint between two thermal elements [176, 213]; while we find this approach promising and draw inspiration from it, it is limited in that, **(1) the thermal sensations may be confusing**—in fact, to measure the illusion, the "*author instructed the participants to indicate the strength of the sensation perceived on their fingerpad* ***regardless*** *of their perception on the finger side*" [213]—users will feel a spatial mismatch since the sides are hotter than the illusion point, and **(2) the thermal actuators need to be close to the point of the illusion** (e.g., 14 mm; so close that they only add actuators to the side of the fingers in [213], not larger body parts).

Solving this challenge of enabling thermal feedback in conjunction with grasping and walking has, to the best of our knowledge, never been addressed. As such, we looked for inspiration in how

researchers have approached this challenge in other haptic modalities, namely those that attempt to provide tactile sensations while keeping the user's hands free.

Wearable Strategies towards Haptic Feedback while Preserving Real World Sensations

This tension in preserving haptic sensations while interacting with objects is not unique to thermal feedback; in fact, recent research in tactile feedback has focused on engineering devices that minimize encumbering the sensitive areas we use for manipulation, especially the hands [90, 106, 151, 164]. We cluster these strategies, including examples of thermal instantiations, in three categories: (1) *relocated actuators*; (2) *foldable actuators*; and (3) *thin actuators*.

Relocated actuators. One way to preserve tactile sensations is to move the actuator away from the area that will contact an object—this approach is often referred to as *relocated haptics* [211]. The key concept is to still deliver a haptic sensation but not in the location where it is expected to happen. For example, Ando et al. [8] and *Haplets* [195] placed vibrotactile actuators on the fingernail to render feedback that should be felt on the fingerpads. Another example, *Tasbi* [188], moved the actuators even further from the hand by placing them on the wrist. This idea of relocation has been applied to thermal feedback. ThermoFeet placed Peltiers on the dorsal side of the foot to provide directional cues [51]. *Altered Touch* placed its Peltier element on the nail to give thermal feedback while leaving the fingerpad free [163]. Similarly Sato et al. placed its Peltiers on the sides of the fingerpad [213]. As a result, these haptic devices excel in minimizing tactile obstructions (hand/sole free to grasp/walk) but sacrifice this for realism, i.e., the sensation occurs in a location where it is not expected—in fact, to measure this illusion of thermal feedback created from actuators away from the fingerpad, in [56] the "*author instructed the participants to*

indicate the strength of the sensation perceived on their fingerpad ***regardless*** *of their perception on the finger side*".

Foldable actuators. A second approach is to use an actuator that provides the haptic effect only when it is necessary but then tucks away while not in use. Examples include a wrist-mounted actuator that taps the palm on-demand [122] and a nail-mounted actuator that taps or *warms up* the user's fingerpad on-demand [248]. Unfortunately, these approaches are only suited for touching either virtual or real objects, but do not allow users to touch both at the same time—this folding approach does not support augmenting a physical object (such as a VR prop) with thermal sensations.

Thin actuators. The third strategy is to *balance* virtual and real feedback by placing an actuator on the skin area that interacts with objects but making it as *thin as possible*, so that it impedes tactile sensations as little as possible (also referred to as "feel-through" [169, 279]). Examples include an electrotactile device for stimulating the fingerpad via a thin film [279], a latex ring for presenting pressure, vibration, and temperature in mixed reality [73], and hand-worn air bladders that can be in/de-flated on demand [248]. Using this approach, the user does not have full tactile acuity but can still feel objects *through* the thin actuator [169], while also enjoying haptic effects. With respect to thermal feedback, this approach has only been explored by recent flexible Peltier devices [113, 127, 181], which again still require cooling to give sustained/realistic feedback, have limited flexibility, and remain expensive [311] (see section 3.1). ThermalGrasp is directly inspired by the latter by proposing a technical approach that places a *thin thermal conductor* that allows the user to feel thermal feedback and *still grasp or walk*.

The Importance of Physical Cues even in VR (i.e., props as highly realistic haptic feedback)

In recent years, the use of physical props as proxies for virtual objects has grown popular because they provide cheap yet hyper-realistic haptic feedback [33, 86, 296]. Key to the rise of haptic props is that they can be low-tech; they don't necessarily require expensive actuation or wearables and can be made from readily-available materials (wood, plastic, etc.), yet they can provide sensations very close to their real-world counterparts, such as the weight of a bat [275] or tool [234]. Often, these sensations cannot be produced by common haptic actuators, such as the vibrotactile motors in VR controllers [275]. For example, Franzluebbers et al. found that replacing VR controllers with a golf club prop was preferred by participants and even led to improved VR golf performance [55]. In our work, we strive to allow thermal interfaces and prop-based experiences (VR experiences that rely heavily on grasping and walking) to finally work together.

Walkthrough: ThermalGrasp in Prop-based Virtual Reality

To help readers understand how ThermalGrasp can present thermal feedback while enabling grasping and walking, we demonstrate it in a prop-based VR desert experience; the user's goal is to survive the night by staying warm. They experience this via physical props, such as tracked handheld props (e.g., wooden logs) or terrain props upon which they can walk (e.g., sand, artificial grass, and a puddle of water). Users wear four ThermalGrasp devices, one on each hand and foot (see Figure 45a).

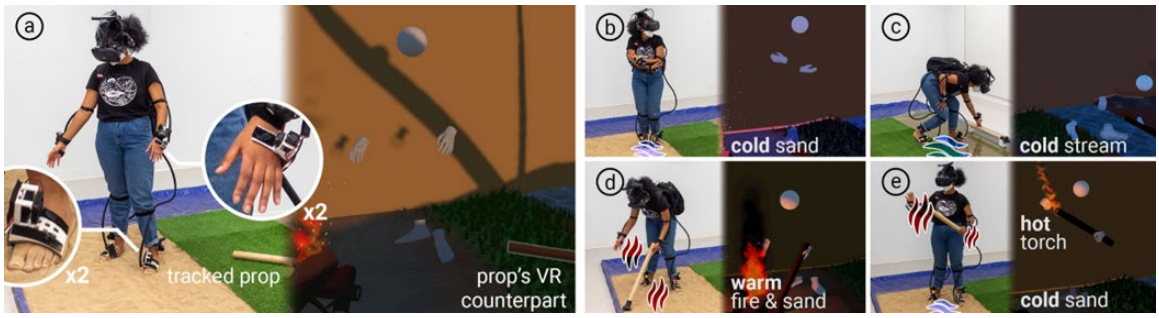

Figure 45. The user immersed in our VR desert survival experience interacts with haptic props such as sand, logs, grass, and water while feeling thermal feedback.

Figure 45b depicts that as the sun sets, the user feels the sand beneath their feet getting cold — using ThermalGrasp, the user walks on the real sand while feeling the cooling sensation from the virtual world—this is an example of our how approach improves thermal realism (as shown in Study 2). Walking on sand is possible because the footworn Peltiers and their required cooling units on top of the user's feet (dorsal side) conduct heat to the soles of the feet via thin, flexible copper sheets.

Now, users must survive the desert night by finding a heat source. Figure 45c-d depicts the user collecting wooden logs into a bonfire—their hands grab haptic props (e.g., the wooden logs) and feel the prop's realistic texture. The user even steps into shallow water to grab a log, which would not be safe with Peltiers on the bottom of the feet, as these could short-circuit.

As the user places logs in the fire, the wind blows out the bonfire, scattering the burning logs. The user must now find a new heat source. They search throughout the terrain, while feeling cold on their soles and palms. Finally, they find a scattered log still burning and repurpose it as a torch, as shown in Figure 45e. Upon grabbing the torch, they feel the prop as warmer because the thermal device on the grasping hand heats up due to the virtual flame—an example of how ThermalGrasp allows users to feel the realism of the haptic prop alongside the accompanying thermal sensation.

Finally, as the sun rises, the user feels the sand increase in temperature, indicating they survived the desert night.

Benefits, Contributions and Limitations

The key contribution of our work is a new method for providing thermal feedback (both hot and cold) in a form that *still* allows for interacting with real-world objects, like grasping props or walking on terrains. The benefit is that this approach **(1) relocates bulky yet necessary cooling hardware to unobtrusive locations**, such as the back of the hands and top of the feet and as a result, **(2) allows users to feel hot and cold sensations and still grasp, walk on, and feel real-world objects**, which is relevant to many interactive domains, such as prop-based VR or AR.

Our approach is not without limitations. First, our approach naturally requires more energy than adding a heat source directly on the target area to reach the same temperature; this is because we conduct the energy over a distance, which requires a thermal gradient where the temperature at the source is more extreme than at the skin. Similarly, because it takes time for the heat to transfer over the distance from the heat source to the target area, our approach is slower than directly placing a heat source on the target area (e.g., a Peltier which can heat and cool at 3ºC/sec [186] vs. ours which is <8x slower at cooling and <6x slower at heating as shown in our *device characterization*). While our primary goal is developing thermal devices that enable walking and grasping, we mitigate this lag as much as possible by using heat pipes with high effective conductivities and insulation to reduce losses. That said, we characterized the time to generate a feelable sensation in Study 1 and found that it fits several applications well where slower thermal feedback is realistic (such as radiative heat from fire, gradual temperature changes as the sun sets and rises, and so forth—such as our application for *Study 2*). This is consistent with findings from prior work on slower thermal feedback [225]. However, these are limitations as much as they are

tradeoffs, as our approach balances thermal realism with the ability to grasp and walk on surfaces. Finally, because our approach is designed around feeling real-world objects, it is important to note that these objects also have their own temperatures, which interact with the temperatures presented by ThermalGrasp, which may influence perception.

Implementation

To help readers replicate our approach, we now provide the necessary technical details.

Materials

Our ThermalGrasp devices consist of three basic components: hot/cold sources, conductors, and insulators.

Hot/cold sources. For hot and cold sources, we use Peltier elements to be able to render both hot and cold (though our principles of guided conduction would hold for guiding heat from hot/cold liquids, etc.). Moreover, to achieve these realistic, sustained cold sensations, Peltiers require cooling units—we too use a heatsink and fan per Peltier.

Conductors. We use thermally-conductive materials to transfer heat between the thermal element and the user. There are three factors that affect heat transfer in our conductors: (1) materials' conductivities (higher is better); (2) source-sink distance (shorter is better); (3) cross-section (larger is better). Thus, we aim to leverage all factors in our final design to minimize power requirements and improve performance.

We explored various metals and thermally-conductive polymers as conductive channels [17, 149]. Notably, copper boasts a high thermal conductivity (k=~400W/(m·K)) among metals while being low-cost. Thus, we centered our explorations around copper. Specifically, *copper heat pipes* are the key to enabling our technique to work across long distances. Commonly found within

computer cooling systems, copper heat pipes consist of a sealed copper tube containing water and wicking material. When one end of the heat pipe is heated, the water vaporizes and naturally travels to the cold end due to the pressure gradient, where it then condenses back into a liquid, releasing the latent heat. The water then returns to the hot end of the pipe via capillary action where the cycle repeats. Notably, this phase change is entirely passive and self-contained (no pumps or fluid in/out)—this gives copper heat pipes an effective thermal conductivity of ~500x that of an equivalent piece of solid copper [50]. While heat pipes are not intrinsically flexible or thin, they are malleable and can be bent into custom shapes. However, heat pipes alone are not sufficient for condensing the bulkiness of Peltier elements into minimally obtrusive thermal actuators. We use them to transfer the heat as far as possible without impeding the user and then transfer the heat into a *thinner conductor*, such as copper sheet metal. To ensure effective heat transfer at all material interfaces, we add thermal paste.

Insulators. Insulation is critical: (1) insulation around the channels reduces losses to the environment as heat travels through the conductive materials, thus boosting our device's efficiency, and (2) insulation prevents the user from feeling thermal sensations at undesired locations. For example, if we wish to cool the palm, we can insulate the conductors at all points except for the desired point of contact with the skin. Our devices use two types of insulators: rigid plastics (such as PLA, k=~0.13W/(m·K)) for giving structure to the devices and soft foams (such as neoprene, k=~0.05W/(m·K)) which leverage closed air cells as an effective insulator for comfortably interfacing with the user [15, 308].

Fabrication

We fabricated devices for the palm of the hand and the sole of the foot, as shown in Figure 46. In both designs, we 3D print a form-fitting shell that attaches to the dorsal side of the hands and feet.

Peltier elements are placed within the shell and springs are used to press the Peltier's surface to the heat pipes, along with a layer of thermal paste for improved heat transfer. The heat pipes connect to sheet metal that wraps around to the opposite side of the hand/foot. To ensure good contact with the skin, the tightness of the device can be adjusted by sliding the heat pipes up/down in their slots. Additionally, we explored three strategies (all possible) to attach our devices to the body (in order of increasing contact reliability): (1) spring-loading the flexible sheet metal against the foot by enforcing a tight bend radius; (2) adhering the conductor to the skin with skin-safe glue; and (3) wrapping fishing line from the tip of the conductor around the body and anchoring it to the 3D-printed shell. For reliability and ease of donning/doffing, we evaluate designs using the fishing line approach.

Specifically, each design uses the following components: Peltier element (foot: TEC12706, hand: CP60231H), flat copper heat pipes (foot: 70W 11.2 x 3.5 x 100mm, hand: 60W 8.3 x 2.5 x 70mm), copper sheet metal (0.2mm thickness), soft neoprene foam (3.2mm thickness, easily compressible), heatsinks (foot: 40 x 40 x 12mm, hand: 20 x 20 x 10mm), fans (foot: 24V, hand: 12V), and 3D-printed shells. The foot-worn device weighs 145g and the hand-worn device weighs 34g.

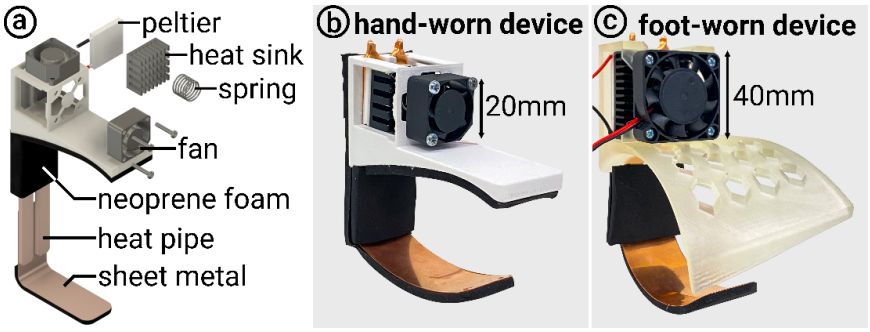

Figure 46. (a) Exploded view and fabricated devices for the (b) hands and (c) feet.

Sensing, Electronics, and PI-controllers

All our wearables feature temperature sensors (100kΩ NTC 3950 thermistors) at the point where the Peltier contacts the heat pipe and where the sheet metal contacts the user—allowing it to monitor the thermal gradient in real-time.

All devices share the same hardware. The Peltier elements are driven by a VNH3SP30 motor controller, which is controlled by an ATmega2560 microcontroller. To combat saturating the Peltier elements in the cooling condition, we use two separate PI tunings for heating (P=75; I=3) and cooling (P=200; I=8). Each controller receives only the temperature at the flexible sheet metal, while the Peltier temperature is used as a safety feature. To achieve rapid temperature change, we use bang-bang control when outside the goal temperature by more than 1ºC in cooling and 2ºC in heating, and the PI controllers when within range of the goal temperature. The fans are triggered programmatically via a MOSFET (RFP30N06LE) when the temperature exceeds the goal. At peak power, one of these devices consumes 25W, which we power via a large LiPo battery worn by the user in a slim backpack.

Characterizing the Performance of our Devices

To characterize the performance of our devices created with the ThermalGrasp approach, we tested the heating and cooling performance while wearing the devices.

Temperature stability. We tested the heating and cooling performance on the example of the device for the sole of the foot, as shown in Figure 47. First, to determine the cooling performance, we drove the worn foot device at full power (25W) for five minutes. As shown, the temperature at the point of contact with the foot decreased from 25ºC to 20ºC. In the following five minutes, our controller drove the Peltier element to heat and maintain 40ºC. Finally, to demonstrate the system's stability, we drove the Peltier for five more minutes to cool from 40ºC back to room temperature.

Thermal camera images (FLIR C3) were taken of the device's externals to determine the effectiveness of the neoprene insulation. As shown, temperature change was observed at the surface of the insulation (22ºC at end of cooling, 33ºC at end of heating). Considering the Peltier's temperature was 16ºC and 52ºC at these times, heat leakage is expected due to the high thermal gradient.

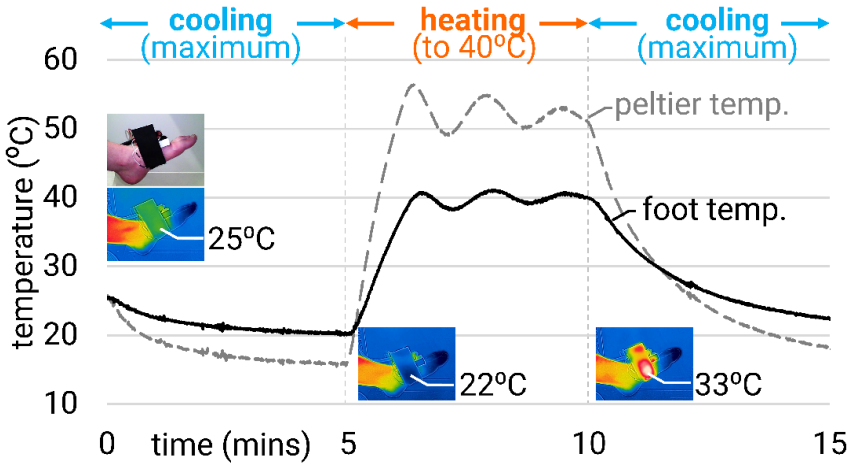

Figure 47. Performance of our ThermalRedirect device for thermal feedback on the sole.

Figure 48 shows temperature over time where our devices contacted the skin. Each device was driven at full power (25W, starting from Peltier at room temperature) for 35 seconds. Moreover, to assist the reader in interpreting this performance characterization, we also show the results of our Study 1, in which we calculated the point at which the average participant felt a temperature change (hand heating and cooling: 11.3 sec, 12.3 sec; foot heating and cooling: 25.2 sec, 16.1 sec).

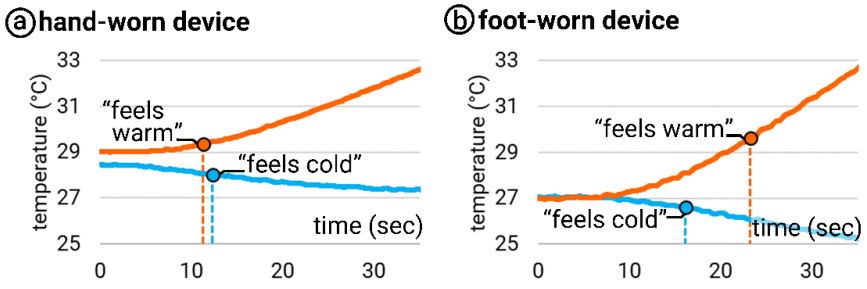

Figure 48. Heating and cooling curves for our (a) hand and (b) foot-worn devices.

It is important to note that while this approach is not as fast as a Peltier directly applied to the skin (i.e., these rates are less than 3ºC/sec exhibited in related works [15]), they are consistent with prior works in which speed is not the goal, yet effective feedback is achieved (e.g., [69]). Instead, our approach generates perceivable temperature changes while still allowing us to grasp and walk on surfaces. Despite this strategic tradeoff, Study 2 demonstrates the value of this approach for conveying realism in VR.

User Studies

We conducted two user studies to validate our technique and its implications in interactive applications, specifically in the case of VR. Our studies were approved by our institution's ethics committee.

In our **Study 1**, **we evaluated ThermalGrasp's performance** by first determining if our devices could effectively transfer thermal feedback to the desired location (by sketching the border of sensation over a blank anatomical diagram [242]). Then, we characterized how long it took participants to notice temperature changes while wearing our devices on their hands and feet. The result of this study demonstrated that our approach effectively transfers hot and cold sensations to the user at the target location (comparable to placing a Peltier directly on the target) and is perceivable within an interactive timeframe.

In our Study 2, we compared the participants' sense of realism in a VR task involving *both* real-world and thermal sensations. We found that ThermalGrasp led to improved realism and sensory engagement in VR.

Study 1: Evaluating ThermalGrasp's Thermal Performance

Our first study focused on characterizing ThermalGrasp's ability to provide thermal feedback. This study assessed (a) the areas of perceived stimulation for both Peltier devices placed on the top and bottom of the foot, along with our foot-worn ThermalGrasp device; and (b) the time it took for the temperature change to be perceivable. Both metrics were evaluated using standardized study designs from psychophysics literature [103, 242].

Study 1a: location of thermal stimulation

We hypothesized that ThermalGrasp provides stimulation closer to the target area compared to placing a Peltier on the dorsal side of the limb but underperforms compared to a directly Peltier on the target area.

Location = foot. We chose to evaluate the foot (rather than the hand) because it represents the more challenging case for existing approaches: (1) virtually no thermal devices can be applied on the soles, since the user cannot step on top of Peltiers and their cooling systems or would otherwise stop the thermal flow for tubes with hot/cold fluids; and (2) the distance from top of the foot to the sole is greater than that of the hand, which pushes ThermalGrasp to its limits more than if we had tested the hand.

Conditions. Participants experienced three interface conditions (in randomized order, across all participants): (1) **direct-peltier** (wearing a traditional Peltier along with heatsinks and fans applied directly to the target area of the sole, the same TEC12706 Peltier as incorporated into the ThermalGrasp design), (2) **dorsal-peltier** (a Peltier applied along with heatsinks and fans to the top of the foot), and (3) our **ThermalGrasp** device (a Peltier on top of the foot, heat transferred via a thin conductor that wrapped from the medial side of the foot to the sole). Thermal contact areas were held constant across all three interface conditions (56 x 27.5mm).

Participants. We recruited eight participants (two identified as female, five as male, one as nonbinary, with an average age of 24.5 years old, SD=1.73). No participants had prior injuries on their feet. Participants received $20.

Apparatus. Participants sat on a chair in front of the experimenter. They could comfortably rest their leg on a stool. Participants were blindfolded so that they could not see the stimulus applied to the foot, nor the thermal device. Participants experienced a cold (20ºC) and hot (40ºC) temperature for each condition. The temperature over time was PID-controlled to follow the same curve for all conditions.

Procedure. When participants felt the 20ºC and the 40ºC stimulus, they were asked to indicate the area where they felt thermal sensations for each stimulus and the point where the sensation was most intense. Participants were provided with a diagram of the foot (sole and dorsal side) and could draw freely; this is a standard method used by prior works [242]. Finally, participants rated the intensity of the thermal sensation (1-7 scale).

Results. Figure 49a depicts our main findings regarding the participants' thermal acuity. For both hot and cold stimuli, **dorsal-peltier** resulted in the area the furthest away from the sole, which implies that dorsal-peltier doesn't present thermal feedback to the sole of the foot. Conversely, **direct-peltier** exhibited the smallest area spread and this area was the closest to the target area (more thermal acuity). While these were expected, it was unknown how **ThermalGrasp** would compare to either of the baselines. We found that **ThermalGrasp** sat between these conditions, exhibiting less thermal acuity than **direct-peltier,** but more than **dorsal-peltier**. This validates our hypothesis. While all participants reported temperature change on the sole during the ThermalGrasp condition, five participants reported sensation on the side of the foot during heating, indicating some heat bleeding through the insulation. Finally, we found no statistical difference

between the intensity ratings across all conditions (p=0.24 for hot; p=0.15 for cold stimuli), which suggests that our apparatus was functioning robustly (all conditions followed the same temperature curves as dictated by our PID controller).

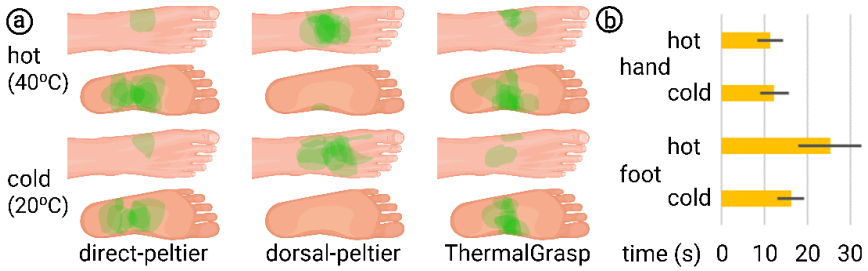

Figure 49. (a) Data (all participants) indicate that participants felt both hot and cold sensations in the desired location of the sole of the foot in the ThermalGrasp condition. (b) Time to notice the change in temperature for both our foot and hand device for heating and cooling. Error bars show standard deviation.

Study 1b: time to perceive thermal stimulation

Having determined that ThermalGrasp could accurately present thermal feedback at the desired locations, we now aimed to find how long it takes participants to experience its temperature feedback.

Conditions. Participants experienced ThermalGrasp on either their dominant hand or foot (counterbalanced).

Participants. We recruited eight participants (three identified as female, five as male, with an average age of 25.1 years old, SD=2.35). No participants had prior injuries on their feet. Participants received $20.

Apparatus. Participants comfortably rested their foot on artificial grass while holding a wooden dowel rod.

Trials. We used two types of trials: **(1) real** temperature, in which our device was actuated to maximum heat/cool, and **(2) placebo** temperature, in which our device was not actuated and stayed

at skin temperature. Participants experienced a total of 24 trials (4x repetitions of 3x sensations (cooling/heating/placebo), on 2x body parts (hand/foot))

Procedure. Participants were notified when a trial began. After the experimenter started the trial, a random delay (0-10 sec) was implemented before power was supplied to the device's Peltier. Participants were instructed to confirm using a keypad upon feeling a change in temperature. We recorded the time difference from powering on to the time participants indicated the temperature changed. If participants could not perceive a change in temperature, they were instructed not to press any keys. If a participant did not indicate a change in temperature, the trial would conclude after 45 seconds. Importantly, we purposely included placebo trials in which no stimulation was presented to ensure that participants were not just pressing confirm without no real sensation. Finally, between trials, we waited for the device to return to skin temperature (measured at the sheet-metal) and room temperature (measured at the Peltier).

Results. Figure 49b depicts how long it took participants to notice a change in temperature. For the hand, we found it took on average 11.3 sec (SD=2.9) to notice heating and 12.3 sec (SD=3.3) to notice cooling. For the foot, we found it took on average 25.2 sec (SD=7.3) to notice heating and 16.1 sec (SD=3.2) to notice cooling.

Discussion. We found that participants could feel sensations in under 30 seconds despite transferring the heat over a distance. While this delayed feedback is a limitation for certain applications, it is also exactly what enables being able to walk and grasp while wearing thermal devices. Using these findings, we hypothesized that for interactive applications in which both real-world and thermal sensations are required, our technique will provide users with an improved experience. In our next study, we investigated this with the example of prop-based VR.

Study 2: Realism in VR

While our first study examined the psychophysics aspects of our approach, our second study focused on observing our approach in an interactive application. Specifically, we assess the extent to which our approach (which allows feeling or walking on props *and* feeling virtual thermal sensations) influences the sense of realism in prop-based VR experiences.

Our main hypothesis for this study was that ThermalGrasp would feel more realistic than a baseline without our devices. Moreover, we were also interested in a range of additional measures typical in studies that evaluate realism of VR experiences, such as immersion (extent to which the experience is inclusive, extensive, surrounding and vivid [226]), enjoyment (taking pleasure in the experience), and sensory engagement (the range of sensory modalities experienced).

Conditions. In this study, participants experienced two interface conditions in counterbalanced order, across all participants: (1) **ThermalGrasp** (four devices, one on each foot and hand) and (2) a no thermal feedback **baseline**.

Participants. We recruited eight participants (four identified as female, three as male, one as nonbinary, average age of 21.8 years old, SD=2.22). None reported injuries on their feet or hands. Participants received $20 for their time.

Task. The VR task mirrored the experience presented in our *Walkthrough*, including all the interactions depicted in Figure 45. The goal for the participants was to find a way to survive the night in this VR desert by building a fire to keep warm. Participants explored this VR experience by walking on the physical terrain shown in Figure 50. The prop-based terrain measured 2.5m x 2.8m with regions of sand, artificial grass, and shallow water. The room was maintained at 22.8ºC. In our experimental condition, participants wore four ThermalGrasp devices, one on each hand and foot. In all conditions, they also wore a wireless HTC VIVE headset, and a backpack with a

battery and our devices' controllers, which communicated using Serial over the VIVE's wireless link. Additionally, participants wore a VIVE tracker on each wrist and ankle to track hands and feet. The remaining physical props (wooden logs) were tracked using VIVE trackers.

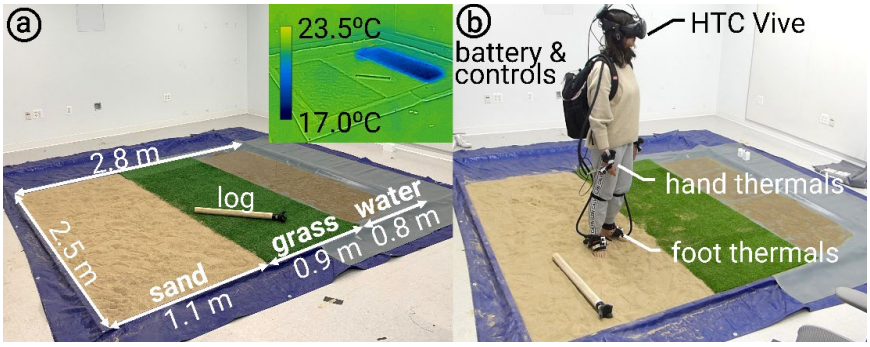

Figure 50. (a) Physical prop-based terrain. (b) Wearable study setup.

Procedure. As participants explored the VR desert wearing ThermalGrasp, their location in the VR world triggered thermal effects. Figure 51 presents the timeline of events alongside the temperatures that participants could experience. The experience's timeline was the same for both conditions, except for the thermal sensations. These timings were designed to ensure a comparable experience across participants and work realistically with our devices' speed. Experimenters added the physical log props into the terrain periodically outside of the participant's field of view, in different locations across conditions. When a participant picked up the log and placed it in the fire, the experimenter "froze" the virtual log's position in the fire and proceeded to move the physical prop to a new location to be collected again. After each trial, participants were asked to report their sense of realism, immersion, sensory engagement, and enjoyment on a 7-point Likert scale, as well as elaborate upon their ratings and the sensations they experienced.

Figure 51. Timeline of events and temperatures (for the ThermalGrasp condition).

Figure 52 presents our main findings. We analyzed our data using a paired T-test (two-tailed). Specifically, **ThermalGrasp** (M=5.63, SE=0.17) was perceived as more realistic (p=0.017) than the baseline (M=4.63, SE=0.30). Similarly, **ThermalGrasp** (M=5.63, SE=0.35) was perceived as more engaging (p=0.009) to the senses than the **baseline** (M=4.63, SE=0.58).

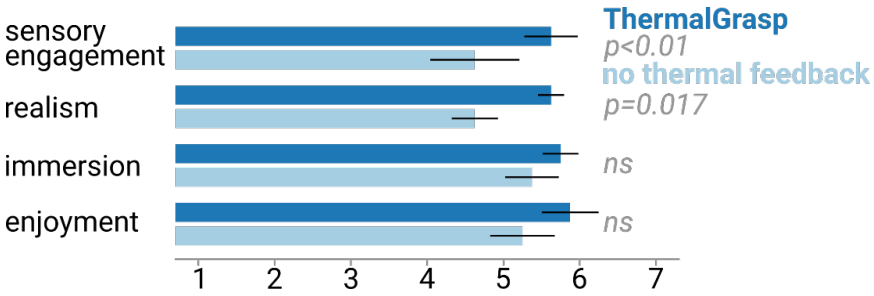

Figure 52. Participants' ratings for both conditions. Errors bars show standard error.

No significant difference was found between the **baseline** and **ThermalGrasp** in terms of immersion (p=0.099; baseline: M=5.38, SE=0.35; ThermalGrasp: M=5.75, SE=0.23) and enjoyment (p=0.090; baseline: M=5.25, SE=0.42; ThermalGrasp: M=5.88, SE=0.37). Finally, five of eight participants reported that they preferred the condition in which they were instrumented with our ThermalGrasp devices.

Qualitative feedback. We analyzed transcriptions of all responses to our open-ended questionnaire. We identified four topics: (1) *thermal referral*, (2) *behavioral change*, (3) *presence* and (4) *preserved grasping and walking*.

Thermal referral. Six (out of eight) participants associated thermal feedback to objects or events in the scene (P1, P2, P5, P6, P7, P8). For instance, P4 reported the temperature of the physical sand being warmer than the grass, even though the sand and grass were at room temperature; it was our device that warmed the feet only when standing on sand. Moreover, participants reported *missing* the thermal feedback when absent: "[baseline led to] a slight disconnect" (P1); "[this experience is] a sensual experimentation and you lose an entire sense [in baseline]" (P7); or "[baseline] felt less like [I was] interacting with the world" (P3).

Behavioral change. We observed behavioral changes in response to the thermal feedback. Notably, heat altered half the participants' relationship to the campfire and its surrounding space (P5, P6, P7, P8). For example, P6 stated "I've got to hold this [torch] so that I'm not near the part that's on fire". P5 also stated that the alignment between the heat and VR situation "feels like something is happening, so you're more encouraged to actually stand by the fire and wait."

Presence. Some participants mentioned their sense of presence increasing based on thermal feedback. P5 remarked that, without thermal feedback, the experience felt like "spectatorship or a loading screen more so than an immersive experience." P3 remarked, "[ThermalGrasp] felt like I was actually taking up space in the environment (…) even though it might seem like a small thing, having that physical feedback […] really affects the experience."

Preserved grasping and walking. Qualitative feedback affirmed that our approach preserves some tactile sensations along with grasping and walking. In both conditions, six participants (out of eight) described the tactile regions in detail (P2, P4, P5, P6, P7, P8). Seven participants (out of eight) reported the textures were unaffected by the thermal devices (P1, P2, P3, P4, P6, P7, P8). P8 detailed their experience by stating, "everything was the same besides adding the heat (…) when I went to pick up the sticks, I didn't have the same feeling on my palm because the device

was in the way." Notably, no participant reported any difficulty grabbing or manipulating the tracked prop, no participants reported temperature change felt on the dorsal side of their hands/feet, and no participants reported any discomfort during the experience.

Discussion

In Study 1a, we found that ThermalGrasp accurately presented thermal feedback at the desired locations; in fact, with similar performance to adding Peltiers directly on target—however, ThermalGrasp works even while grasping or walking. Conversely, in Study 1b we found that, as expected, ThermalGrasp is slower than directly applying a Peltier to the target, since it requires to transfer heat over distances. Remarkably, in Study 2, we found that this tradeoff between speed and realism can be beneficial, as our participants felt that ThermalGrasp was more realistic and engaging in a VR experience that made use of walking and grasping props.

We see ThermalGrasp as not an end-product, but as an approach to make thermal feedback with props more seamless. Transferring heat over distances has weaknesses for interaction, namely, the rate of temperature change, which may explain why immersion was not greater in Study 2's ThermalGrasp condition. As such, future work can enable wider use cases by improving feedback speed. Several potential avenues to achieve this include:

Increased Peltier/power density. Adding a second Peltier to the design (i.e., sandwiching both sides of the heat pipe) or using higher power Peltier elements will lead to a greater thermal gradient between the Peltiers and the skin, thus increasing the heat transfer.

Spatially-divided hot and cold stimuli. Traditional Peltiers encounter a similar need for rapid temperature changes, especially in scenarios simulating the transition between touching hot and cold surfaces. To overcome the lag of individual elements, a common strategy is to arrange Peltiers in a 2x2 grid with dedicated Peltiers for heating and for cooling. This arrangement enables rapid

perceived temperature changes by exploiting two characteristics of human thermal perception: spatial summation and the adapting temperature [214] and has been implemented in various thermal devices [185, 186]. ThermalGrasp can incorporate this arrangement by using multiple Peltiers, each with their own conductive paths meeting in a grid on the skin, to increase the speed of perceived temperature change.

Advanced materials. The bottleneck in our presented hardware is the copper sheet metal. While the heat pipe component transfers heat especially fast, the copper sheet metal has orders of magnitude lower effective thermal conductivity yet is necessary to present the temperature in a thin and conformal interface against the user's skin. Advances in thermal materials may alleviate this bottleneck, such as thin and flexible heat pipes [131, 178, 286].

Beyond this limitation, our work underscores the value of considering thermal latency trade-offs, as our Study 2 found enhanced realism even with this non-instantaneous thermal feedback. Thus, our approach is apt for scenarios expecting non-instantaneous thermal feedback (our Walkthrough/Study 2 used slow thermal feedback, e.g., the sun rising or the flames growing). In our study, we occupied participants (e.g., collecting logs, fire growing visuals) to allow the device time to heat/cool. This strategy is used in haptic displays that require seconds to minutes to actuate, e.g., pneumatic [250] or motor-based [98]. We emphasize that our approach enables an experience that (despite some limitations) is otherwise not possible with traditional approaches: overlaying thermal sensations while grasping/walking on props.

Conclusion

We proposed, engineered, and validated ThermalGrasp, an approach for wearable thermal interfaces that enables users to grab and walk on real objects with minimal obstruction. Our approach moves the thermal device and cooling unit to areas not used in grasping (e.g., back of

hand) or walking (e.g., top of foot). We then use thin, compliant materials to conduct the device's heating or cooling to the palm of the hand or sole of the foot. Unlike traditional actuators and heatsinks, our thin materials uniquely enable grasping and walking on real objects while enjoying thermal feedback. We demonstrated that our technique can be applied to VR experiences that heavily rely on props or tool manipulation.

We believe that ThermalGrasp points to a direction in which interactive devices aim to harmonize as many senses as possible, while minimizing obstruction to real-world manipulation. Here, we demonstrated how to harmonize thermal feedback and physical interactions. Given the rich haptic properties of real-world objects, we argue users should not have to compromise between choosing to interact with *either* real *or* virtually-rendered sensations.

Finally, we tend to think of the devices that we engineered not as end-products, but as artifacts of the ThermalGrasp approach, which may serve to inspire the creation of new thermal devices that enable interactions with real-world objects.

Power-on-Touch: Powering Actuators, Sensors, and Devices during Interaction

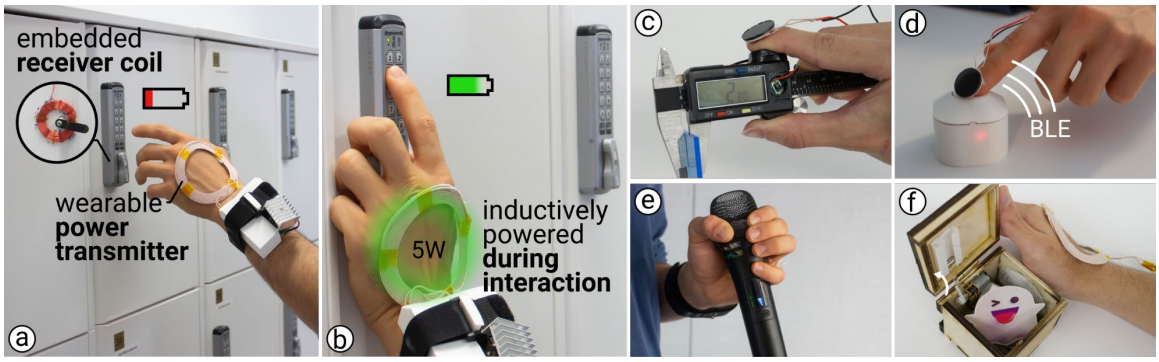

Figure 53. (a) We propose a new method for powering devices only during user interaction. It comprises of two parts: a wearable transmitter-module worn by the user and receiver-tags with coils that can be used to power devices without batteries. (b) When the user interacts with devices with receiver tags, energy is inductively transferred between the user's coil and the device's coil. This energy is sufficient for powering sensors, microcontrollers, and even actuators. (c-f) Our approach offers a new pathway for a greater number and diversity of battery-free devices in ubiquitous computing.

In this chapter, we present Power-On-Touch [146], our generalized approach to actuation at scale.

Introduction

Mark Weiser envisioned a future where computing devices are seamlessly embedded in nearly every object, enabling an era of ubiquitous computing [270]. While this vision is becoming increasingly feasible with advancements in technology, a significant hurdle remains: *power supply*. Currently, most interactive devices rely on batteries, which do not present a major hassle if users just interact with a limited number of devices in a room. However, as the number of interactive objects in a single environment increase, users find themselves requiring charging or replacement of batteries, which becomes impractical if we truly envision potentially hundreds of devices in a single smart environment [270].

In fact, supplying power is one of the primary practical obstacles in ubiquitous computing [81, 87, 217, 230]. There have since been significant strides made in ubiquitous sensing [82, 273, 302, 303], visual displays [76, 189, 201], low-power computers and microcontrollers [260], and even battery-free devices that harvest energy from users and operate intermittently [45]. However, these do not represent the full-power spectrum of interactive devices. While sensors or displays might require less power, most devices that contain actuators are not eligible for most forms of low-powered computing or energy harvesting [252, 284]. In fact, most interactive devices containing haptic actuation, motor-based tangibles, or other power-hungry actuators (e.g., ultrasound, electromagnets, and much more), are not typically featured in research on ubiquitous computing or in visions of this future.

To explore a new technical approach towards these challenges, we propose *Power-on-Touch*, a one-to-many wearable approach designed to power devices on-demand. By eliminating the need for built-in batteries and enabling scalable power transfer, *Power-on-Touch* not only mitigates the maintenance burden associated with batteries but also meets the power required for actuators, facilitating wider adoption of haptic and actuated devices in ubiquitous computing.

Related Work

The work presented in this paper builds primarily on ubiquitous interfaces, particularly instrumented interactive surfaces, and wireless power transfer, with emphasis on wearable approaches.

Adding Output to Everyday Objects and Surfaces

To achieve the vision of ubiquitous computing [270], researchers have developed various techniques to integrate input & output into everyday objects & surfaces—attempting to make these

come alive and become responsive. One main challenge when adding interactivity to objects is how to power the input & output components. Since these objects and surfaces are meant to be scattered around users, powering them with batteries is challenging due to repetitive charging.

In addition to input, researchers have explored adding output to everyday objects and surfaces. For instance, researchers have added visual [76], audio [93], and actuated output [182]. On the haptics side, the common approach to adding haptics is to simply embed a vibromotor in the object [193, 194, 292]. On the actuation side, *Robiot* generated mechanisms for adding actuation to everyday objects, such as augmenting a lamp with robotic movements [129]. Evidently, when compared with adding input to the environment, adding actuation is far less explored, likely a symptom of their limited battery life. This is because actuators require orders of magnitude more power (100-1000x) than their sensing counterparts, making their burden of battery maintenance substantial.

To address this issue, some have argued for making actuators wearable so that a *single* device can overlay sensations onto *many* objects [102, 150, 243]. For example, *MagnetIO* added feedback to objects via passive magnetic patches that vibrate against the user's finger in a magnetic field [152]. These techniques have furthered the scale of haptics; however, they rely on *modality-specific* approaches that limit them to single modalities (only vibration, only friction, etc.).

To overcome this limitation, *Power-on-Touch* takes a *generalizable* approach. Instead of being tied to a specific actuation modality, our device directly addresses the bottleneck of actuation at scale: providing *power* to many devices. This is only possible because our concept uses *battery-free* devices in the user's environment. To power these devices on-demand, we are inspired by and build upon techniques from (1) wireless power transfer and (2) battery-free devices. Such ideas

explore the notion of the user becoming the battery (i.e., bringing power with them for on-demand use).

Wireless Power Transfer

Wireless power transfer denotes transferring energy from a source to a receiver without the need for physical connectors, like wires or cables, making it especially attractive for reconfigurable and mobile devices. Several techniques have been developed for transferring power over a distance, such as electromagnetic [210], capacitive [119], laser-based [237], and ultrasonic [161]. In our review, we group approaches into three main categories: (1) *instrumented environments*, (2) *body-as-wire*, and (3) *encountered-type*, which we summarize and compare in Table 1.

Instrumented environments. Researchers have experimented with stationary transmitters built into the environment for transferring power to devices. For example, *UltraPower* used focused ultrasonic waves pointed at a receiver to transfer up to 50 mW [161]. Similarly, Su et. al combined lasers with photovoltaic cells for powering vibration motors via light [237]. However, these mediums are difficult to integrate into daily life because they require very precise tracking and alignment between the transmitter and receiver. Alternatively, others have used wireless power transfer coils to augment desks [40, 107, 221, 280] and even entire rooms [212] with wireless power. These have the advantage of being able to transfer high amounts of power (>10W) over a large space without precise alignment, but unfortunately require very specific construction, such as encasing entire rooms with metallic cages and poles [30, 212]. As such, it is difficult to scale instrumenting the environment, and there are cases in which it is infeasible, such as outdoors and on-the-go.

Body-as-wire. To make wireless power transfer mobile, others have focused on wearable and environmental transmitters that can send small amounts of current through the skin. Often, this

approach is used to power battery-free wearable devices that are augmented with a receiving electrode [130, 158, 162, 253, 259]. For example, *SkinnyPower* demonstrated intra-body power transfer to transmit power from an electrode on the wrist to an accelerometer worn on the index finger [222]. *Power-Over-Skin* improved upon this approach to intra-body power transfer to scale to powering multiple receiver devices, sensors, and microcontrollers (typically <1 mW, dependent upon electrode size) [118].

Intentio had a similar principle, but for non-wearable, or encountered objects [119]. When a user wearing a transmitter touches an electrode on a receiving object, power is transferred through the skin to the receiving object. However, the user and object must share a common ground, which can require instrumentation and sensitive tuning of the capacitive coupling to ensure efficiency. Unfortunately, for body-as-wire techniques, the power that can be transferred through the skin is limited by the current that can travel through the skin without inducing tactile sensations (typically <0.5 mA [120]). While this is sufficient for sensing and microcontrollers, it is not enough power to realistically drive actuation.

Encountered type. Alternatively, other works aim to power devices that the user *encounters* within their environment. *Meander Coil++* [241] and its predecessor *Twin Meander Coil* [240] leveraged inductively coupled wireless power transfer on the user by embedding coils into the user's t-shirt. This work inspires us with examples of encountered and wearable sensors, LEDs, and a robot. Similarly, *PowerShake* [281] demonstrated using wireless power to transfer energy between users' phones and watches via device-to-device contact. However, the form factors of *Meander Coil++* and *PowerShake* limit interaction, since the user must either contact objects with their torso or tap devices together. Instead, we leverage a more natural channel: *interactions via one's hands*—we use our hands heavily to interact with and manipulate objects in the environment,

and many existing devices are designed around this channel. *TouchPower* [300] shares our vision of powering devices during touch, recognizing that many electronic devices only need to be powered up during interaction (e.g., TV remotes, digital calipers, karaoke microphones, etc.) and that interaction with devices usually requires proximity or contact between the user's hands or body and the target device, forming a natural channel for power transfer. However, *TouchPower*'s working principle is fundamentally different from ours. *TouchPower* is a glove with electrodes, that, when aligned with receiving electrodes, powers battery-free devices during grasping. The downside to an electrode-based approach is that it requires at least two electrodes to be precisely aligned (actual physical contact, no gaps), to connect both power & ground and complete the electrical circuit. Therefore, this technique is only suitable for objects in which the geometry dictates a precise grasp—moreover, it assumes that all users will grasp the object in the same way, i.e., not robust to variations in pose. In contrast, our approach does not require precise alignment, and therefore accommodates a wider range of grasps and interaction poses, as we later show in our *Technical Evaluation*.

Comparing approaches. When comparing approaches, a few trends emerge across the categories. *Instrumented environments* tend to be versatile across spectrums of power and robust to various touch interactions; however, they are intrinsically limited in scale because it is infeasible to implement in *every* environment. In contrast, *body-as-wire* tends to enable scale due to wearables' travelling with the user (with minor drawbacks of requiring common grounds, which necessitates instrumenting objects with electrodes); however, passing current through the skin is limited to low-power devices like sensors and microcontrollers, and is too low for actuation. Finally, *encountered-type* ensures scalability and is generally versatile across power spectrums depending on the working principle. However, to our knowledge, *encountered-type* devices have

not been robust to various touch interactions. In contrast, *Power-on-Touch* is tolerant to alternative touches because inductive power transfer does not require precise alignment to the extent that electrodes do, while leveraging natural touch channels, such as the hands and fingers. Thus, *Power-on-Touch* achieves all three goals.

Table 1: Comparison of *Power-on-Touch* with prior work on wireless power systems. *Power-on-Touch* addresses all the stated design goals to provide a solution to scaling on-demand power through touch (✗: not available, ♦: partially available, ✓: available).

Category	Related Work	Design goals		
		Easy to scale	Versatile across spectrums of power	Robust to various touch interactions
instrumented environments	desk-scale inductive power [40, 107]	✗	✓	✓
	room-scale inductive power [30, 212]	✗	✓	✓
	laser power [237]	✗	✓	♦
	UltraPower [161]	✗	♦	♦
body-as-wire	*SkinnyPower* [222]	✗	✗	♦
	Power-over-Skin [118]	♦	✗	♦
	Intentio [119]	♦	✗	♦
encountered-type	*MagnetIO* [152]	✓	♦	♦
	PowerShake [281]	✓	✓	✗
	Meander Coil++ [241]	✓	✓	✗
	TouchPower [300]	✓	♦[a]	✗
	Power-on-Touch (our work)	✓	✓	✓

[a] *TouchPower*'s efficiency/output were described as very low (46%, 200 mW). We see no reason why they cannot be improved, thus we bumped it up in our rating.

Energy-harvesting and Battery-free Devices

Finally, we draw inspiration energy harvesting and battery-free devices [9, 288, 301]. For instance, *interactive generator* presented a rotary input device that provided haptics with energy entirely harvested from the rotation itself [12]. Teng et. al used a similar approach in a wearable to harvest energy from the user while providing resistance as haptics [252]. While *Power-on-Touch* can transfer high power from the user to devices, we use this to actuate power-hungry devices, which

can lead to intermittent power. Thus, we employ similar strategies to works on intermittent power sources [45].

Our Approach: Power-on-Touch

Power-on-Touch consists of a wearable wireless power unit that enables users to power many battery-free devices as they encounter and interact with them. We augment devices with our custom-engineered receiver-tags so that they can be powered inductively during interactions that require close proximity. The key enabler of our approach is that our device is: (1) encountered-type, which enables scale; (2) versatile across power requirements, which enables powering not only sensors, but also actuators; and (3) robust to various touch interactions due to its non-contact working principle.

Our approach is based on inductive power transfer, not unlike the principle used in common wireless phone or electric toothbrush chargers, as shown schematically in Figure 54a. In these chargers, when a receiving device is placed on a charger in the environment, the transmitter and receiver become inductively coupled, enabling power transfer. However, we take a conceptual turn from typical wireless chargers—we developed a *wearable* power transmitter (Figure 54b). Rather than placing transmitters in the environment for users to bring their devices to (i.e., coupling upon proximity), our transmitter travels with the user to power devices *during interaction* (i.e., coupling during interaction). By turning the user into a mobile power source, devices that only need power during interaction no longer need to have batteries and can instead be powered *on-demand*. Eliminating the need for built-in batteries reduces maintenance efforts while enabling powering actuators, which can broaden adoption of haptic and actuated devices in ubiquitous computing.

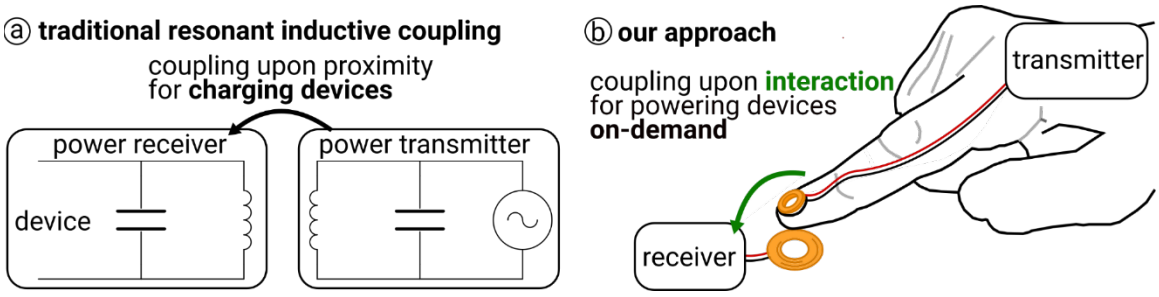

Figure 54. Our approach uses (a) resonant inductive coupling to power devices. (b) However, rather than placing transmitters in the environment to which users must bring their devices to charge (i.e., coupling upon proximity), our transmitter travels with the user to power devices during interaction (i.e., coupling during interaction).

Synergies between our work and other approaches. Powering devices in the environment is a longstanding challenge, and numerous approaches have been proposed. Today, users are typically equipped with mobile and wearable battery-powered devices (e.g., cellphones, smartwatches). Thus, there are increasing opportunities to share power between the user's devices and devices in the environment. For instance, sharing energy between devices like phones and watches is already integrated in some commercial devices [47, 281]. Others showed transmitting energy through the skin from a central battery to power peripheral wearables [118]. There has also been growing focus on new ways to charge wearable batteries, such as through kinetic interactions with objects [288] or harvesting from the user [252]. Rather than *supplanting* these approaches, Power-on-Touch *complements* them, enabling its battery to be charged through harvesting or shared power while also facilitating energy transfer back to devices in the environment on demand.

Contribution and Limitations

Our key contribution is that we propose, explore, and engineer a novel method for powering devices during interaction. Our technical approach enables new ways to scale the number and diversity of battery-free devices in ubiquitous environments, such as going beyond ubiquitous sensing and into the realm of *ubiquitous haptics*.

Our approach has the following benefits: (1) While traditional devices and actuators each require their own power supply, often in the form of batteries or tethered outlet connections, *Power-on-Touch* instead places the battery on the user and augments devices with receiver tags to receive power *on-demand*, resulting in scalability; (2) *Power-on-Touch* is versatile across spectrums of power, enabling not only sensors and microcontrollers to be deployed ubiquitously, but also *actuators*; (3) *Power-on-Touch* is robust to various touch interactions, from hovering to single-finger touch to grasping and resting as it does not depend on direct or perfect contact with devices; (4) *Power-on-Touch* can sufficiently provide power without obstructing the user's palms and fingers (e.g., wearing a glove); instead, coils can be placed on the back-of-the-hand and fingernail, leaving the user free to interact with devices.

Our approach is limited in that: (1) inductive power transfer will never be as efficient as wired power transfer due to additional losses—still, to minimize this, we employ tuning techniques (see *Implementation*); (2) our approach requires proximity between the user and devices, thus it is most applicable to devices that only need to power on when the user is close or touching them; (3) our approach requires modification of existing devices to be compatible with wireless power, which can result in requiring some retrofitting and possible changes to form factor; (4) metallic obstacles (e.g., a metal enclosure) will introduce unintended losses via eddy currents and may interfere with effective power transfer [100, 299]; (5) for our complete vision in which every user can power devices on-demand, all users must be equipped with wearable transmitters/coils. While the latter is a limitation, it can also be a strength and a worthwhile vision for research, as this allows us to explore the goal of a *one-to-many* and *natural* power delivery system, as there are many more devices in the world than there are people [92]. Future work may investigate deeper not only into the *limits of affordances* within Power-on-Touch but also *identify opportunities* in this space.

Implementation

To help readers replicate our design, we now provide the necessary technical details and fabrication process. *Power-on-Touch* consists of two principal components: (1) *many* battery-free devices in the environment that are powered wirelessly with our receiver tags and (2) our wearable wireless transmitter (battery, microcontroller with BLE, voltage booster, switching circuit, and coils).

Achieving Resonant Inductive Coupling

Ordinary inductive charging (e.g., commonly used with electric toothbrushes) is efficient when the transmitting and receiving coils are especially close together and well-aligned. However, as the gap between coils increases or the alignment skews, this efficiency plummets. Therefore, the key to achieving our approach at reasonable efficiencies is to *tune* our transmitting and receiving circuits to *resonate* at the same resonant frequency. This is called resonant inductive coupling, and greatly improves both the efficiency and power transfer over distance/misalignment. For example, early seminal work demonstrated 40% efficiency over a distance of 8 coil diameters [126]. Had these coils not been carefully tuned, this efficiency would be many orders of magnitude lower. Thus, to maximize efficiency, and therefore enable a wider range of interactions (e.g., powering while hovering, stronger actuators, etc.), we carefully tune all our circuits.

Tuning consists of a series of steps. First, each coil has its own *quality factor*, (*Q-factor*) a measure of the frequency at which the coil experiences the lowest losses. In other words, driving our coils at frequencies for which a coil has a high *Q-factor* results in greater efficiency (and lower temperatures). In our *Technical Evaluation*, we use impedance analysis to find coils that have high *Q-factors* at our desired frequency. Then, the coils are tuned to the resonant frequency by placing

a capacitor in parallel. This turns the circuit into an *LC* circuit, which has a well-defined equation for undamped resonant frequency: $f = \frac{1}{2\pi\sqrt{LC}}$. In practice, damping occurs; as such, we hand-tune the capacitor value to ensure resonance at the transmitting frequency. These steps are taken for both our transmitting and receiving coils, and as we show in our circuits, we leave room for multiple parallel capacitors in our PCBs to enable fine-grain tuning. In the future, integrating dynamic frequency tuning may automate this process [210].

Coil Design

We implement and characterize three types of coils in our approach: (1) *large-coils* typically worn on the back-of-the-hand and used in grasping or palmar interactions; (2) *small-coils* typically worn on the fingernail and used in single-finger touches; (3) *spherical-receivers* designed to receive power omnidirectionally. We investigate both traditional spiral coils and spiderweb coils for their low self-capacitance [143]. In general, we recommend pairing the receiving coil's diameter to be close to that of the transmitting coil for maximal efficiency [268].

Large-coils. Large diameter coils are our default coils. The larger a coil's diameter, the further its field travels [227]. Thus, larger coils tend to enable greater magnitudes of power transfer and higher efficiencies. Therefore, we use larger diameter coils when the interaction permits (i.e., the user's body part can accommodate a larger coil, like on the back of the hand, foot, arm, etc.) and when the receiving object can fit a large coil without dramatic consequence to form factor.

Small-coils. In instances where larger coils are unsuitable (e.g., fingernail for power over single-finger interactions), we opt for smaller diameter coils. As shown in our *Technical Evaluation*, this comes at a small cost to efficiency. However, as we also show, the power transfer of smaller coils can be increased by adding ferrite backings that direct the field [232].

Spherical-receivers. To best enable our vision of robustness to various types of touches (e.g., angles, etc.), we wound and characterized spherical coils designed to receive power omnidirectionally— as we show in our *Technical Evaluation*, no matter the direction from which user approaches, power is received, unlike traditional, flat coils, which have dead zones when coils are arranged perpendicularly [58, 108, 109]. We recommend these coils in devices that don't have affordances that suggest directionality, such as cylindrical devices (e.g., microphones).

Coil Wearability. Figure 55 shows three distinct coil materials that we explored, each with their own benefits. First, we engineered rigid coils made from solid copper wire. While these coils prove effective for receivers, their rigidity becomes problematic for wearable transmitter applications, as demonstrated by the difficulty in bending a sample coil in Figure 55a. In contrast, Litz wire presents a more conformable alternative, comprising multiple thin individual wires that enable significantly greater flexibility compared to solid wire of equivalent gauge (Figure 55b) [233]. At the opposite end of the spectrum, we engineered stretchable coils by embedding liquid metal channels within silicone(as in [241]). While these stretchable coils offer superior flexibility (Figure 55c), they did not match the efficiency of our flexible or rigid coils. Ultimately, we found Litz wire to strike a better balance between being *flexible* for wearability and *performance* in our transmitter's frequency range; Litz wire is effective at reducing losses due to skin effect and proximity effects within 100kHz-1MHz [202]. We deliberately chose to wear transmitter coils on body parts that *minimize* interference with manual interactions, such as the back of the hand or fingernail, as opposed to gloves [300]. While we could have placed coils on the palmar side of the hand or finger—which would significantly increase transmission efficiency—this would have correspondingly and dramatically reduced user dexterity. We attached these coils to the user's body using double-sided tape and tacky silicones, though future work might explore alternative

attachment strategies, such as semi-open gloves. Moreover, while our current implementation employs traditional coil form factors, our approach remains compatible with other materials and fabrication techniques. Potential future iterations could integrate coils into knitted textiles [196] or jewelry [239], for improved social acceptance and wearability.

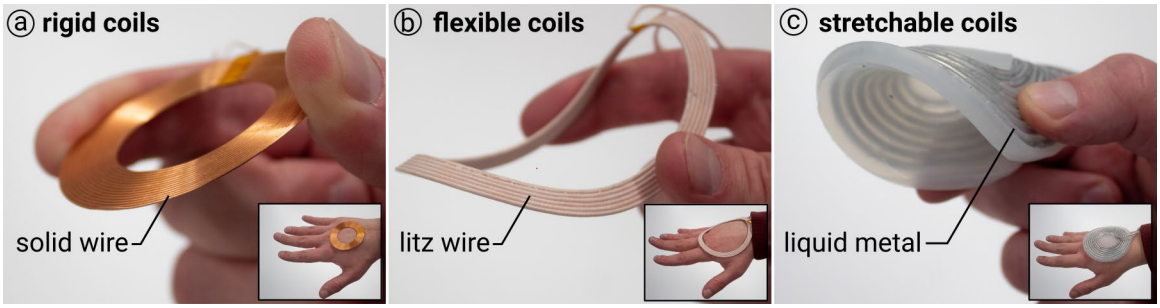

Figure 55. We tested coils made of (a) solid wire, (b) flexible Litz wire, and (c) liquid metal wires (silicone tubing filled with EGaIn).

Engineering our Wearable-Transmitter and Receiver-Tags

We engineered (1) a wearable-transmitter and (2) receiver-tags, as shown in Figure 56 & Figure 57.

Wearable-transmitter. Our wearable transmitter primarily consists of a battery (1200mAh), microcontroller with BLE (Seeeduino XIAO nrf52840), DC-DC voltage booster (XL6009), transmission switching module (XKT-801: 50-900kHz adjustable, Taidecent), and coils worn on the user. We selected this frequency range based on compatibility with the Qi standard (100-200kHz), a common standard in commercial devices [133, 264]. Thus, many commercially-available coils are optimized for this range, enabling prototyping with proven coils. This is just one physical implementation of the conceptual principle of Power-on-Touch, and implementing other standards (e.g., NFC at 13.56MHz) is possible. In fact, higher frequencies may lead to improved wearability, as they afford coils with fewer turns/smaller diameters [132, 293].

The battery powers the microcontroller, which uses a MOSFET (RFP30N06LE) to control the current flow from the battery through the voltage booster, which steps the voltage up from 3.7V to 32V, before being fed into the transmission module. Our wearable transmitter contains a power-monitoring circuit consisting of a current sensor (ACS70331) in combination with the nrf52840's built-in battery voltage monitor to actively sense the reflective load presented by nearby receiving coils. While our implementation of a transmitting circuit is made from individual modules assembled on protoboard, the device can be miniaturized with a custom PCB.

The transmitter's power consumption varies based on its operational mode. During active power transmission for our typical large-coil, the transmitter draws 3.2W (0.85A), and this increases to 4.5W (1.2A) when a receiver coil is nearby. With a 1200mAh battery, the transmitter can continuously emit power for ~1h. However, we conserve battery life by only transmitting at full power when a receiving coil is detected. In standby mode with test-pulses to detect if a receiver is present, power consumption drops to an average of 0.3W, extending battery life to ~9.5 hours.

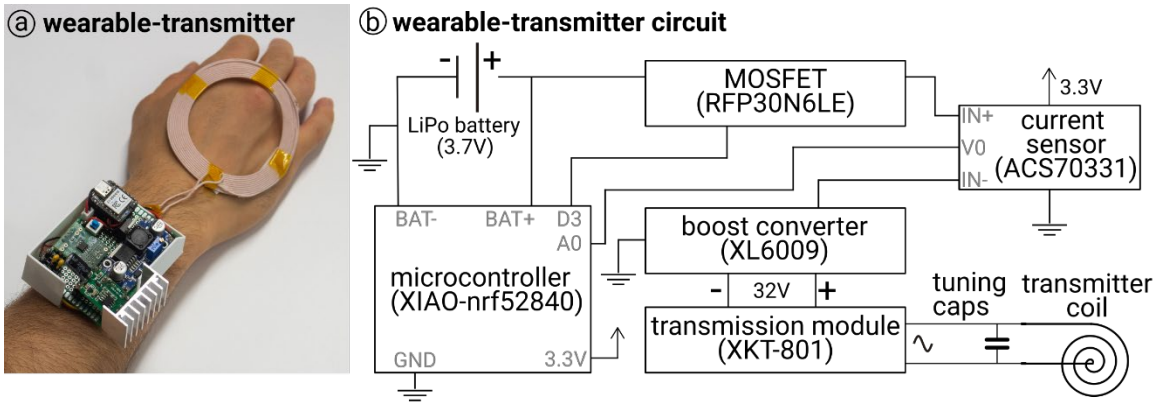

Figure 56. (a) Our wearable transmitter and (b) its schematic.

Receiver-tags. We engineered a custom PCB for our receiver-tags containing a rectifying circuit, a supercapacitor, microcontroller with BLE (Seeeduino XIAO nrf52840), and MOSFETs for controlling high-power devices (actuators, displays, etc.). It can accommodate up to three

receiver coils with various tuning capacitors. The received AC power is rectified through fast-switching diode bridges (1N4148, while we experimented with rectifier-specific diodes, we found fast-switching to be necessary to reduce losses at high frequencies). The rectified DC power is then smoothed through capacitors. Since our rectifiers are wired in series, the voltages from each coil add together. This total voltage is used to charge the supercapacitor (330mF, 5.5V). The benefit is that our tags can accommodate multiple coils for added robustness to variations in touch, as well as our spherical-receivers, which consist of three coils on orthogonal planes.

The supercapacitor directly powers the microcontroller, which was chosen for its fast boot time, low minimum operating voltage (1.7V), and simple footprint for producing and deploying receiver tags rapidly. Our PCB exposes all but two of the XIAO's I/O pins for easy prototyping. Two pins are dedicated to controlling onboard MOSFETs (SIA436DJ). We use these MOSFETs to control high-power components; when the supercapacitor is charging, the MOSFETs remain open until a sufficiently high voltage is reached for actuation. This is especially critical as many high-power devices have an "activation energy" that must be overcome to turn on. Using MOSFETs isolates higher-power components from draining the supercapacitor. Supercapacitors enable our approach to quickly charge with sufficient energy to generate high power actuation and short-term sustained power because, supercapacitors charge faster than batteries, and more importantly, balance energy storage with charge and discharge times. While supercapacitors do not hold as much energy as a comparably sized lithium-ion battery, they trade capacity with power density [121], which allows for fast charging/discharging speed (orders of magnitude faster than a battery of similar capacity). The supercapacitor circuit can be tuned to balance storage (increasing capacity) vs. charging time (decreasing capacity).

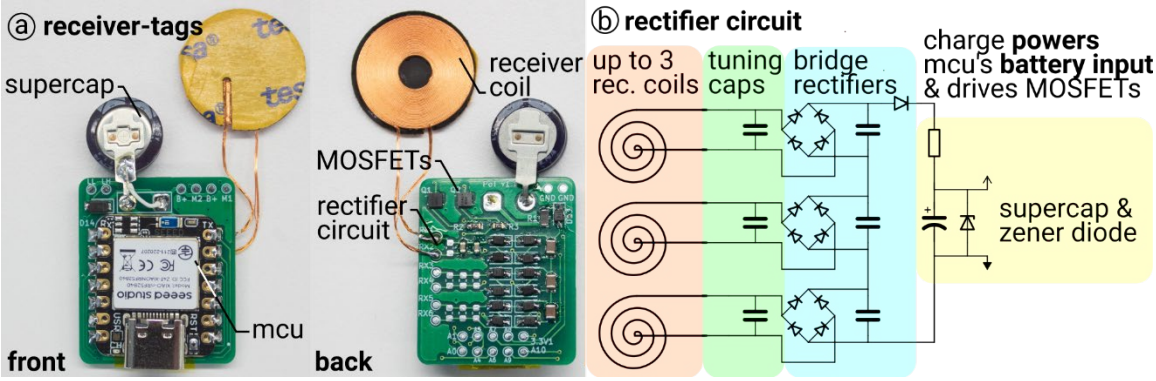

Figure 57. (a) Our custom receiver tag PCB and (b) its schematic.

Detecting Receiver Tags and Communication

While our primary goal focused on implementing a wireless power technique for powering battery-free devices to scale up the number and diversity of devices (including actuators) in ubiquitous computing, we also implemented a basic tag detection and communication schema. Rather than our transmitter constantly emitting power into the environment and needlessly wasting energy, we implemented a simple protocol for detecting when receiving tags are nearby. Our transmitter periodically sends out short (50ms) test pulses at monitored power draw. When a receiving coil is nearby, the transmitting and receiving coils' coupling increases and the receiving coil naturally draws more power from the transmitter during the test pulse. If a test pulse's power draw exceeds our threshold for knowing a potential receiver is nearby, our transmitter switches from test pulses to transmitting at full power. Since our receiver tags feature a BLE microcontroller, upon receiving power, the tag can begin advertising itself as a BLE device to let the transmitter know its specific needs or its supercapacitor's voltage to strategically control transmission for better energy use. This type of reflective load sensing is very similar to how wireless chargers based on the popular Qi standard operate [264].

We acknowledge that there are multiple ways to implement sensing (e.g., RFID). While BLE requires time to pair and energy to stream, it is a simple protocol to demonstrate our full vision with communication. In the future, lower power and faster communication can be established by implementing an ultrasonic chirping circuit (inspired by Sozu [301]).

Technical Evaluation

To characterize the technical effectiveness, and more importantly, seek out improvements to our system, we performed a series of technical evaluations. Specifically, this section aims to find coils that efficiently transfer power so that we can best enable applications that are otherwise not feasible. Since electromagnetic fields decay dramatically over distance, even marginal gains can unlock new interactions and more robustness to variation in touch.

1. First, we measure the quality factor (*Q-factor*) of a variety of coils, both commercially available and custom-made based on prior work. This gives us a view of how efficient each coil is with respect to frequency.

2. Next, we measure the power transfer efficiency for pairs of candidate coils with respect to distance and alignment. This gives us insights into what kinds of devices we can power with different form factors, spacings, and alignments.

3. Additionally, we test the robustness of these coils to changes in the angular alignment between coils. While flat coils are very effective when aligned angularly, their efficiency drops as the angular difference increases [53, 79]. As such, we propose and demonstrate a spherical-receivers that can effectively receive power along all three planes.

4. Finally, to characterize our approach's ability to power real devices during interaction, we tested our approach on three example objects with different form factors and output modalities.

5. We perform a safety and thermal analysis to validate safe levels of electromagnetic field and heat.

In summary, our *Technical Evaluation* demonstrates our approach's ability to transfer a wide spectrum of power while being robust to different types of touch.

Quality Factor Analysis

First, we measure the quality factor, Q, of a variety of coils, both commercially available and custom-made based on prior work. The quality factor is defined as $Q = \frac{2\pi fL}{R}$, where f is frequency, L is inductance, and R is resistance. Since inductance and resistance also depend on frequency, the *Q-factor* is a frequency-dependent measure of where the coil experiences the lowest losses. In other words, to optimize our system's efficiency, we want to select coils with high Q-factors at our transmitting frequency. To perform this analysis, we used an impedance analyzer (Analog Discovery Studio), which gives insight into each coil's resonant frequency and the Q-factor and bandwidth, especially in relation to other coils. We swept a 5V sine wave through each coil and a known value resistor at frequencies from 1kHz to 5MHz in 1001 steps, taking the average at each point over a 500ms excitation. We performed impedance analysis for a variety of palm-sized coils, nail-sized coils, and spherical coils. Figure 58 presents the Q vs. frequency for our three types of coils.

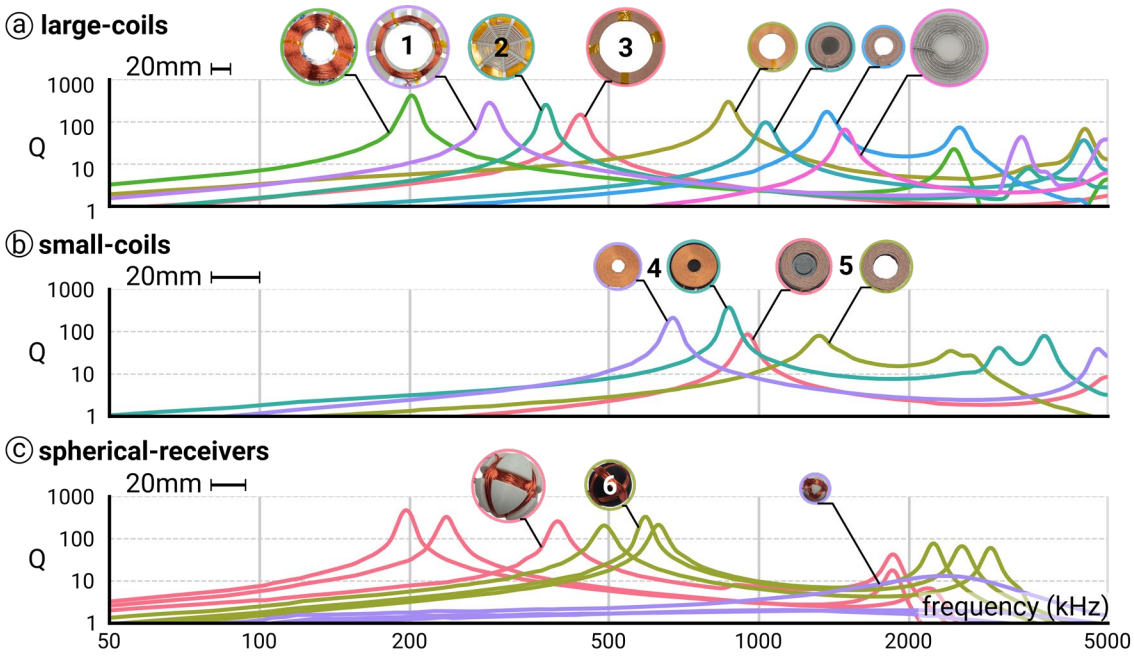

Figure 58. Quality factor with respect to frequency for (a) large-coils, (b) small-coils, & (c) spherical-receivers.

Impedance analysis yields insight into the coils that perform efficiently at our wearable transmitter's effective frequency range (50-900kHz). In each of our applications, we select coils with *Q-factor* greater than 95 for our selected transmitter frequency to support increased efficiency. In a similar effort to increase efficiency, we pair transmitting and receiving coils with similar resonant frequencies/bandwidths so that both perform maximally. In the following subsections, we further evaluate pairs of coils (individual coils labeled in Figure 58) following this principle. Generally, we find that large-coils have lower resonant frequencies and greater *Q-factor* than small-coils. This trend is highlighted by our spherical coils, where, for the same number of turns, decreasing coil diameter led to higher resonant frequencies and reduced *Q-factor*. As such, to maximize efficiency, we often aim to use the largest coils that an application permits. Finally, we found that ferrite backings shifted the resonant peaks. In the following subsection, we further investigate how ferrite backings can affect the power transfer efficiency.

Power Transfer with respect to Distance and Alignment

Next, we measure the power transfer efficiency for pairs of coils with respect to distance and alignment. This gives us a view of the types of devices we can power with different form factors, coil spacings, and affordances. We built a test apparatus using a pegboard with a grid of holes (7.5mm spacing) and adjustable height; we 3D-printed jigs that fixed the relative position between pairs of coils as shown in Figure 59. By sampling (4MHz sampling rate) the transmitted and received power over points in the grid at different heights, we can construct a 3D view of the power transfer. Here, we measured the "end-to-end" power transfer, i.e., we monitored the DC power draw of our transmission circuit and the rectified DC power through a load (250ohm) of our receiver circuit. All coils were tuned to the selected transmission frequency. Following these results in air, sections 6.4 and 6.5 investigate efficiency when coils are worn on the hand.

Large-coils. We tested the power transfer of coils 1 (transmitter) and 2 (receiver) at 320kHz. Figure 59 shows the 3D plot of efficiency and received power. We found a peak efficiency of 55% when coils were well-aligned and separated by 5mm; this corresponds to 2.2W received for this pair of coils. Our efficiency is comparable to other wireless power approaches within HCI, e.g., Meander Coil++ and TouchPower had end-to-end efficiencies of 25% and 46%, respectively [241, 300]. Given our aim to pass power through to the palm from the back of the hand, as well as enabling hovering, we are also interested in the performance at greater distances. For example, at 25mm gap (approximately the thickness of a hand) and no offset, the received power was 1.03W, suggesting that higher power devices (e.g., motors) can be powered through the thickness of the hand. At 45mm gap, the received power was 38mW; modern microcontrollers (e.g., nrf52840 used in our tags) consume well below this power even without entering power-efficient modes, suggesting that *Power-on-Touch* can power microcontrollers upon hovering [312]. Additionally,

we found that the received power was maximal when coils were aligned and decreased as the offset reached approximately the coils' radius.

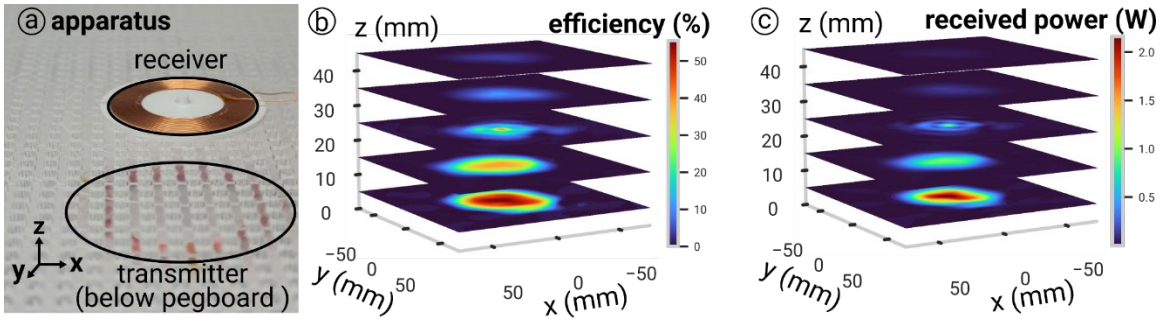

Figure 59. (a) Our pegboard apparatus for controlling 3D alignment between coils. Power transfer with respect to distance and alignment for a pair of large-coils: (b) efficiency and (c) received power.

Small-coils. We tested the power transfer of coils 4 (transmitter) and 5 (receiver) at 640kHz. Specifically, we aimed to determine whether ferrous backing, which typically is used in commercial wireless chargers to improve coupling, is beneficial for small-coils, which typically exhibit worse efficiencies than larger coils. As such, we tested our small-coils both without any ferrous backing (Figure 60a) and with ferrous backing (Figure 60b) to determine their effect. We found that the peak received power nearly doubled when ferrous backing was used (no ferrous backing peak received power: 0.87W; ferrous backing peak received power: 1.63W). At approximately finger thickness (15mm), ferrous backing also led to greater received power (no ferrous backing peak received power: 121mW; ferrous backing peak received power: 88.4mW). As such, we use ferrous backings on our small coil pairs to boost their efficiency.

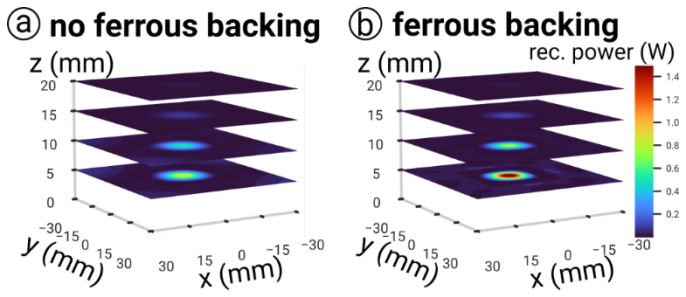

Figure 60. Power transfer with respect to distance and alignment for a pair of small-coils (a) without ferrous backing and (b) with ferrous backing.

Robustness to Angles

While flat coils are compact and very effective when aligned angularly, their efficiency drops as the angular difference increases [53, 79]. As such, to ensure robustness to different angles of touch, especially in applications where the angle of touch is expected to vary, we implement and characterize spherical-receivers designed to receive power in multiple dimensions. We performed this evaluation by rotating a spherical-receiver (coil 3) 360 degrees about its three axes while measuring the power received from a transmission coil (coil 6) at 15-degree increments. The z-spacing of the coils was set to 30mm and we tested both when the coils were axially-aligned and offset by the transmitting coil's radius. Figure 61 shows the average received power for each axis and alignment. As shown, the average received power for each axis is similar, indicating that spherical-receivers can be expected to receive power omnidirectionally. When the coils are axially-aligned, we found an average received power of about 130mW, enough to power a small vibration motor. As expected, the received power decreases with axial misalignment, but the received power is still roughly equal across the three axes. It is important to note that this test was performed with a 25mm diameter sphere, which strikes a compromise between compact size for embedding into objects and power transfer efficiency. Increasing the size of the sphere and decreasing the gap between coils both lead to increased power when designing applications.

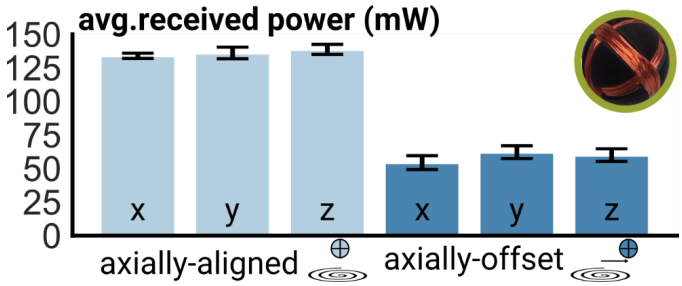

Figure 61. Average received power (mW) rotated about three axes of our spherical coils.

Characterizing Performance in Real Devices

Up to this point, we have characterized our system within a lab; however, real-world objects and environments often do not align with the ideals of the lab. As such, we now evaluate our system using real devices and interactions (e.g., grasping, touching, hovering) to measure the power transfer and the time to charge to produce useful outputs (e.g., sending a signal or driving a motor). To inform the likeliness of an interaction pose, we leverage the ContactDB dataset [26], which contains data on grasping 50 common objects (e.g., doorknob, cellphone, etc.) from 50 participants to create heatmaps of contact likeliness. In this study, we mimic likely touches from three of these objects (shown in Figure 62), as well as test alternative, less-likely touches while interacting with our devices.

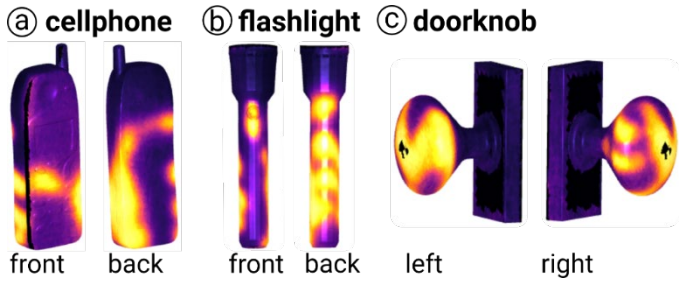

Figure 62. Contact likeliness heatmaps from ContactDB [26] that we used to inform touch interactions during characterization.

TV Remote. First, we tested a TV remote, from which we removed the batteries and converted to being powered by our receiver tag and two coils, as shown in Figure 63. First, we measured the

power consumed by the remote. As shown in Figure 63a, the remote consumes very little power when idle, but wakes upon a button press, followed by sending short a transmission signal, with a peak power of about 34mW (and total energy consumption of 0.9mJ).

To inform our touches, we refer to the heatmaps from the ContactDB dataset [26] for a similarly shaped device with similar buttons for interaction, a cellphone. We mimic the likely touch from the dataset's heatmaps, as well as our own, alternative touch which rotates the hand 180 degrees from the likely touch, as shown in Figure 63c. Figure 63d presents the received power in both interactions. We found that the likely touch resulted in 100mW of received power, while the alternative touch resulted in 40mW. Given the remote's peak power draw of 34mW, both touches can sufficiently power the remote. In fact, the spare power during the likely touch can even be used to *add haptic feedback* to the remote; as shown in Figure 63b, we added a vibration motor to augment the remote with eyes-free feedback and notifications.

Figure 63e shows the supercapacitor's charge over time starting at picking up the dead remote in the likely touch (rapid increase in supercapacitor charge indicates initiating pickup). As shown, the tag's microcontroller wakes about two seconds after the remote is picked up; the remote can then immediately function as though it were powered by batteries. Moreover, we demonstrate augmenting the remote with vibration feedback, which results in a brief supercapacitor voltage drop, followed by a rapid rise upon ceasing vibration.

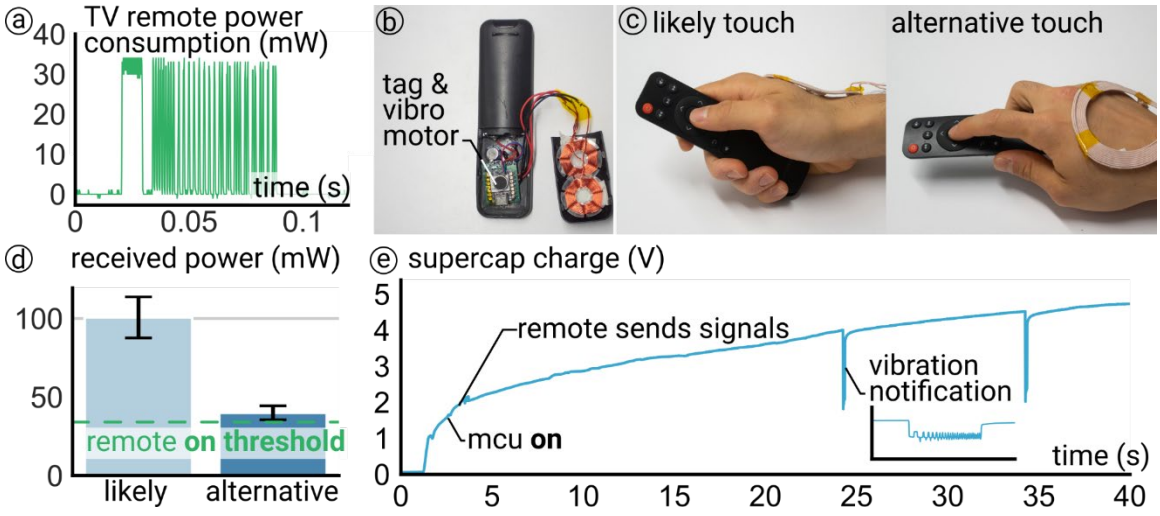

Figure 63. (a) Measured power consumption of the TV remote during a button press. (b) Our modified, battery-free remote, including two receiver coils and a vibration motor. (c) Our mimicry of the likely touch and our alternative touch. (d) The measured received power for both the likely and alternative touch (five repetitions). (e) Supercapacitor charge vs. time in the likely pose, detailing the microcontroller's waking, sending signals upon button press, and added vibration notifications.

Karaoke Mic. Second, we tested a karaoke microphone, from which we removed the batteries and converted to being powered by our receiver tag and a spherical-coil, as shown in Figure 64. We measured the karaoke microphone's power draw, which consists of powering the microphone transducer, streaming audio over BLE, and a small OLED display. Figure 64a plots this power draw along with a moving average. The microphone's average power consumption was 60mW, with spikes up to 130mW.

To inform our touches, we refer to the heatmaps from the ContactDB dataset [26] for a similar, cylindrical device with similar buttons, a flashlight. We mimic the likely touch from the dataset's heatmaps, as well as an alternative touch in which the microphone is held lower, increasing the misalignment between the coils, as shown in Figure 64c. Figure 64d illustrates the received power in both interactions. We found that the likely touch resulted in 138mW of received power, while the alternative touch resulted in 73mW. Thus, both touches exceed the average power draw of the

microphone. However, spikes in power draw may exceed the instantaneous received power. This is where the benefits of our tags' supercapacitor become clear: the supercapacitor stores energy when there is an excess and can help compensate the instantaneous received power when the power draw spikes.

Figure 64e plots the supercapacitor's charge over time beginning with picking up the dead microphone in the likely touch. As shown, the tag's microcontroller wakes about two seconds after the microphone is picked up. As the supercapacitor charges, more functionalities become available, such as the screen turning on at six seconds and streaming audio over BLE at seven seconds. After this initial charging from 0V, the microphone functions stably.

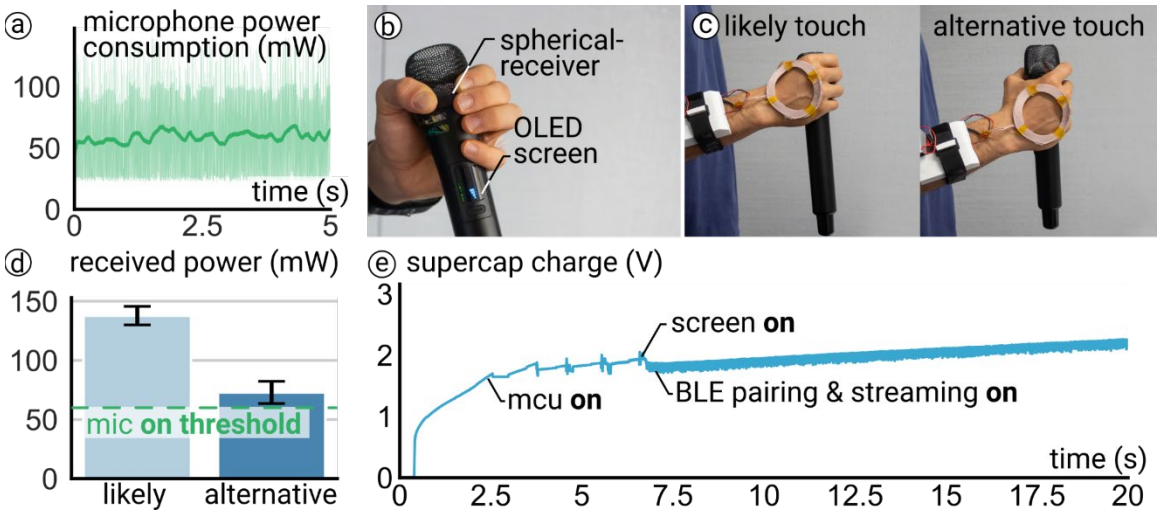

Figure 64. (a) Measured power consumption of the microphone. (b) Our modified, battery-free microphone including our spherical-coil. (c) Our mimicry of the likely touch and our alternative touch. (d) The measured received power for both the likely and alternative touch (five repetitions). (e) Supercapacitor charge vs. time in the likely pose.

Doorknob (with motor-controlled lock). Finally, we directly adapted an object from the ContactDB dataset [26]; we 3D-printed the studied doorknob from the dataset and hollowed it to embed a receiver coil directly inside, as shown in Figure 65. To illustrate how our approach enables powering actuators without batteries during interaction, we made a motorized latch that locks and

unlocks a cabinet to which we attached the doorknob. Figure 65a shows the power draw of the latch's motor, which exceeds 600mW for 350ms.

Again, we mimic the likely touch from ContactDB, as well as an alternative, looser touch in which the palm doesn't touch the knob, as shown in Figure 65c. Figure 65d shows the received power for both touches, where the likely and alternative touches resulted in 548mW and 83mW, respectively. While each of these is below the instantaneous power draw of the motor, our supercapacitor again aids by charging until it has stored sufficient energy to drive the motor. As shown in Figure 65e, this only takes about two seconds after grabbing the doorknob since the circuit's idle power consumption is low.

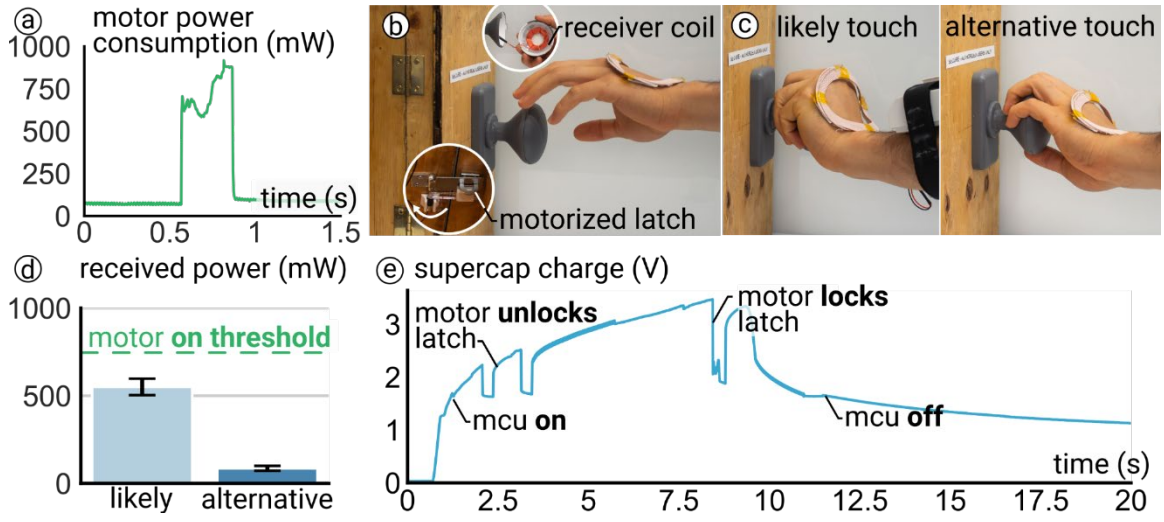

Figure 65. (a) Measured power consumption of the motorized latch. (b) Our cabinet features a battery-free, motorized latch that triggers upon doorknob touch. (c) Our mimicry of the likely touch and our alternative touch. (d) The received power for both the likely and alternative touch (five repetitions). (e) Supercapacitor charge in the likely pose while the user opens/closes the cabinet.

Discussion: Design Strategies for Specific Applications

While we used the same circuit components in our technical evaluation to reduce complexity, our tags' supercapacitor circuit can be tailored to each specific application. Each of the examples in our technical evaluation were designed to be complex to demonstrate the high-power capabilities

of our approach. For example, TV remotes are not normally augmented with vibrotactile feedback, thus their power demands are much lower and would therefore not require a large supercapacitor (or even a supercapacitor at all). In fact, if both the required power and the received power have been determined, the supercapacitor and its series resistor (determines charge/discharge rate) can be selected to to speed up the device's time to turn on. In cases where the delay may impact experience, analog circuits that give indication to the user that the device is receiving power and will turn on soon can mitigate uncertainty. As an example, an LED can be placed after the power is rectified, in a way that its brightness signals the power is being transferred. Moreover, additional LED or other forms of user feedback (e.g., the vibrations we use in some of our examples) can be controlled by a microcontroller to signal to the user that the device is now fully charged and operational. Ultimately, Power-on-Touch can take advantage of many design patterns used in modern devices to signal their readiness to their user.

Safety and Thermal Performance

Finally, we perform a safety and thermal analysis to validate that our wearable system transmits safe levels of electromagnetic field and does not significantly heat the skin. The IEC 60601-2-33 guideline defines the safe specific absorption rate of radiated energy in extremities (e.g., hands) at 20W/kg during occupational exposure and 4W/kg during general public exposure [310]. To determine the specific absorption rate of our system, we designed an experiment based on prior biomedical work on wearable wireless power [16]. We placed a transmitter coil on the back of the hand and aligned it to a receiving coil on the palm while measuring the received power. We then measured the received power across the same distance and angle in air, while keeping the transmitted power the same (4.5W). The difference between the received power in air and through the hand indicates the amount of power being absorbed by the hand. This was repeated five times

for each condition. Figure 66a shows the received power for each condition. We found that efficiency decreased by 0.82% and received power by 0.04W when transmitting through the hand. Considering the weight of a human hand is about 400 grams [54], the absorbed power averages ~0.1W/kg for a 4.5W transmission. Thus, our system is ~40x below the suggested limit, which suggests a factor of safety below the safe absorption rate.

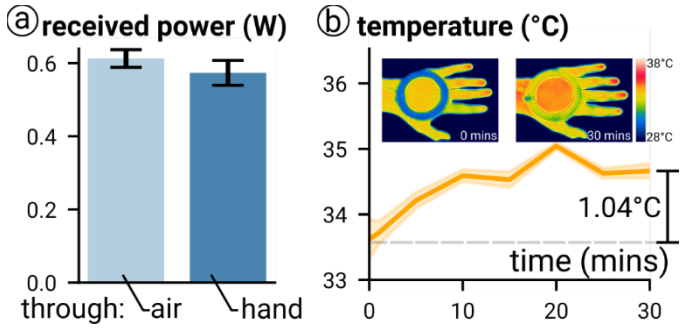

Figure 66. Safety and thermal performance of a 4.5W transmitter on the back of the hand: (a) Received power through the hand and through the same distance in air. (b) Skin temperature vs. time. Shaded error denotes 95% confidence interval.

While specific absorption rate is one measure of safety, thermal performance is also of interest as tissue heating can occur even at levels below absorption rate limits. As such, we measured the change in surface temperature of the back of the hand while wearing a 4.5W transmitter for 30 minutes, as shown in Figure 66b. Over the course of the experiment, we found that the skin temperature increased by only 1°C while the coil's temperature warmed to equilibrium with the skin. Given that our designed interactions are brief, on-demand, and well below 30 minutes of constant transmission, we can conclude that our particular implementation (i.e., transmitting at <1MHz) is safe when considering tissue heating. Note that there are additional safety cases that should be evaluated before deployment to a wide audience, such as characterizing potential interference with safety-critical devices like pacemakers [29].

Additional Applications

To illustrate the versatility of our approach, we demonstrate a wide range of applications, where we use *Power-on-Touch* to propose new opportunities for battery-free, interactive devices in ubiquitous environments. We implemented nine applications, including the three presented in our *Technical Evaluation*.

Communal Devices

Communal devices that are shared among users can be retrofitted into *Power-on-Touch* devices, so that the devices receive power directly from the user, without needing additional maintenance (changing/charging batteries).

Digital calipers. We retrofitted a battery-powered digital caliper with our receiver-tag and coil, making it batteryless. The receiver coil is attached to the outer case where users typically hold. The user, who wears our nail-type transmitter on their finger, will power on the caliper by simply picking it up.

Digital body scale. We retrofitted a battery-powered digital scale with our receiver-tag and coil. The receiver coil is attached to the top surface of the scale. This allows a user, who wears shoes with our transmitter coil embedded in the insole, to power the scale upon stepping on it.

Thermostat. We created a batteryless thermostat that works upon the touch from the user. Utilizing a small transmitter coil, the thermostat can draw power from the user to power on the microcontroller with a temperature sensor, an e-ink display, and buttons for control.

Figure 67. (a) A digital caliper is powered while the user holds it. (b) A digital body scale is powered on when the user, wearing shoes embedded with transmitter coil, steps on it. (c) A batteryless thermostat that contains an ink display and a thermistor.

Quick/disposable Interactions

Power-on-Touch can be made into devices that offer quick or disposable interactions.

Service button. We showcase a batteryless service button that can be used in restaurant settings. When the user's finger, wearing a transmitter coil, **hovers** over the button with an embedded receiver coil, the microcontroller inside is powered up and lights up an LED to indicate it is "on." When the user presses the button (to call for service), a buzzer beeps and the microcontroller sends out a wireless message through BLE containing the table number to the staff.

Actuated surprise box. We created a surprise box with an automatic-opening mechanism. When a user, wearing the palm-mounted transmitter coil, touches the box, the geared motor inside the box is powered on and lifts the lid to reveal a surprise figure.

Interactive birthday card. Since our receiving-tag is slim, it can be embedded into a birthday card, making it interactive. When the card receiver, wearing the transmitter coil on their palm opens the card, they power up the circuit inside the card, play a melody through the speaker, and light up LEDs.

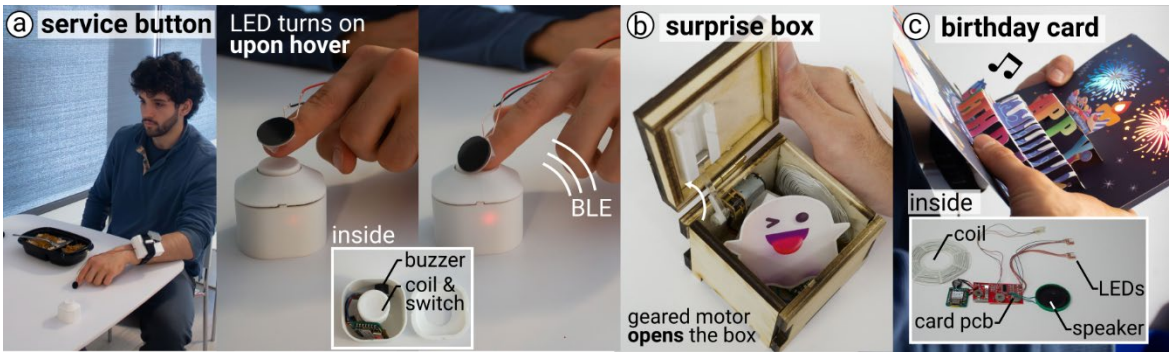

Figure 68. (a) A user in a restaurant uses a batteryless service button equipped with our receiver coil to call for service. (b) A surprise box opens automatically when touched by the user wearing a coil. (c) A birthday card that plays a melody and lights up when held.

Conclusion

We introduced *Power-on-Touch*, a novel method for powering devices *during* interaction using wireless power transfer between a user-worn coil and object-embedded coils. To enable many possible interactions with our novel concept, we performed technical characterizations (e.g., impedance and 3D-efficiency analysis) to reveal which coils best support a wide range of interactions (e.g., grasping, touching, hovering). On the technical side, this technical approach can inspire ubiquitous computing with new ways to scale up the number and diversity of battery-free devices, not just sensors (µWatts) but also actuators (Watts). We believe that future researchers in HCI equipped with our approach can improve our approach's efficiency with dynamic impedance matching/capacitive tuning as well as its range via alternative coil architectures to unlock further interactions.

We tend to think of Power-on-Touch not as an end-product but as a design technique that will inspire the creation of a new type of battery-free interactive devices that can even unlock new use cases. Thus, we have published the detailed fabrication process, hardware schematics and code as open-source to accelerate future research (see Chapter 1, Contributions).

Conclusion

This dissertation explored new approaches to enable actuation at scale in ubiquitous computing environments. While sensors have become ubiquitous, actuators have lagged behind, primarily due to their high power requirements. Through four technical implementations, we demonstrated how moving power sources to wearable devices can enable scalable actuation while minimizing the burden of battery maintenance. However, these implementations are not the end goal, but rather provocations that open new questions and opportunities at the intersection of energy and sustainability, materials science, and interaction design.

The Future of Ubiquitous Actuation

Our work reveals several key challenges and opportunities for the future of ubiquitous actuation:

Energy and Sustainability

The vision of ubiquitous actuation presents a fundamental challenge of scale: as we deploy more actuators throughout our environments, their cumulative energy consumption becomes a major concern. While this dissertation reduced the number of batteries to a single wearable power source per user, we must confront deeper questions about sustainability in ubiquitous computing.

Current battery technology, particularly lithium-ion batteries, has enabled the mobile computing revolution but comes with severe environmental costs: the energy required to produce them is immense, they have severe environmental consequences, and recycling them remains difficult [81, 180, 230]. Because actuation inherently costs more energy than sensing, making it ubiquitous has significant ramifications for sustainability.

Our work points toward several promising directions for more sustainable ubiquitous actuation:

Energy Harvesting and Sharing

A whole energy economy is emerging around devices harvesting and exchanging energy. For example, in 2016, PowerShake [281] demonstrated sharing energy between devices like phones and watches, a feature now available in modern commercial devices. More recent work like Power-over-skin [118] showed how energy could be transmitted through the skin from a central battery to power batteryless, peripheral wearables.

There has also been growing focus on more natural ways to charge wearable batteries, whether through daily interactions with kinetic objects in the environment [288] or through wearables that harvest energy directly from the user [252]. These methods are exciting because they complement our work. Power-on-Touch may charge its battery by harvesting or sharing power, then transfer that energy back to other devices as needed.

Rather than relying solely on batteries, this emerging energy economy suggests a future where power flows dynamically between users, wearables, and environmental devices. Our technical approach enables this by reducing power requirements to a single wearable source that may both receive shared energy and distribute it to passive elements in the environment.

Efficient/Sustainable Power

While our approach of placing the power source on the user rather than in the environment reduces the total number of batteries needed, it represents just one step toward more sustainable ubiquitous actuation. By enabling a single wearable power source to drive many passive elements, we reduce not only the number of batteries that need to be manufactured and maintained but also minimize electronic waste from replacing batteries in environmental devices.

However, this approach still depends on battery technology. For actuation to truly become part of our daily lives, we need new, eco-friendly energy storage solutions. The battery technology we

have today, while functional, requires enormous energy to produce and creates significant environmental impact through mining and manufacturing. The electricity used to charge these batteries should ideally come from sustainable sources, a transition that will require changes not just in technology, but in infrastructure.

The path toward *sustainable* ubiquitous actuation requires addressing several open challenges:

- Developing efficient actuators that operate with less power while maintaining effectiveness
- Engineering better energy harvesting techniques that can generate useful amounts of power from everyday activities
- Designing interactions that make users aware of and engaged with energy consumption

Materials and Integration

Right now, while the devices we demonstrated successfully provide haptics at scale, they are still distinct from Weiser's vision of being seamless: users are very aware they are wearing these devices and that they are the power source. Our ultimate vision lies at the intersection of Weiser's ubiquitous computing and human-computer integration: we want **actuators that integrate so well with people that they disappear into the background**.

Throughout this work, we have scratched the surface of new materials that could enable this vision (e.g., soft magnets in MagnetIO that conform to objects and body parts, conformal thermal conductors in ThermalGrasp that redirect heat while preserving natural interaction, stretchable wireless power coils in Power-on-Touch). However, when new materials emerge, integrating them into end applications is often difficult. This challenge manifests across our projects: How do we maintain magnetic strength while making magnets stretchable? How do we balance thermal conductivity with flexibility? How do we achieve efficient power transfer with deformable coils?

To achieve truly seamless integration, new materials and wearable form factors that function more like clothing or jewelry will be needed. This is not just about making devices smaller or more flexible, but about fundamentally rethinking how materials can serve both technical and aesthetic functions. Future actuators might be woven into fabric, embedded in jewelry, or even applied directly to the skin.

We also need better tools to aid in materials design, as demonstrated by our work on ThermalRouter [149]. While not central to this dissertation, ThermalRouter showed how computational tools can help users work with novel materials by simulating and optimizing their properties. Similar tools could help bridge the gap between new materials and practical applications, accelerating the development of more integrated actuators.

The path toward *integrated* ubiquitous actuation requires addressing several open challenges:

- Moving from rigid to soft/stretchable actuators: While we have demonstrated initial steps with soft magnets and flexible conductors, future work needs to push further toward materials that match the mechanical properties of clothing, skin, and natural movement.
- Developing tools that bridge prototyping and materials: As shown by ThermalRouter [149], we need better design tools that help users work with novel materials; not just simulating their properties but actively guiding design decisions about material selection and integration.
- Making power more wearable: Power sources themselves need to become more integrated, whether through stretchable batteries, conformable energy harvesters, or new materials that can store and transfer energy while maintaining the comfort and aesthetics of everyday wearables.

Interaction Design

The technical foundation for moving power sources to users opens up new questions about how we design interactions. While we have demonstrated that devices can share power during interaction, we need to think beyond just the technical capability: how do we make these interactions meaningful?

Take Power-on-Touch as an example: right now, users need to deliberately touch or grasp objects to power them. Could this instead become as natural as a handshake? Could the act of sharing power become a more expressive interaction rather than the utilitarian "can I borrow your charger?" we are all familiar with today? Several key questions emerge for interaction designers:

- How do we communicate power availability and transfer to users without adding cognitive burden?
- How do we design devices to have affordances that naturally enable power transfer?
- What is the threshold of adoption where power sharing works well (i.e., does everyone need to wear Power-on-Touch, or can energy be shared democratically even at lower adoption levels)?
- What social protocols might emerge around sharing power between people and devices?
- How do we design interactions that gracefully handle varying power availability without disrupting user experience?

Our work suggests some initial directions; however, there is still much to explore. Should devices indicate when they need power? How do we handle cases where multiple users might power the same device? What happens when power runs low: should devices degrade gracefully or simply stop working? These questions will become increasingly important as we move toward environments filled with battery-free, interaction-powered devices.

The challenge ahead is to make power transfer fade into the background of interaction while still maintaining user agency and understanding of affordances. Just as we do not think about the mechanics of touching a doorknob to open a door, future users should not have to think about powering the devices with which they interact (unless explicitly intended to provoke awareness of power use).

Open Challenges and Future Work

Looking ahead, several key challenges remain:

- Developing more sustainable power solutions for ubiquitous actuation
- Creating truly seamless wearable form factors
- Designing meaningful interactions around power sharing
- Bridging the gap between technical capability and practical deployment

While this dissertation has demonstrated the potential of user-worn power sources for enabling actuation at scale, it represents just the beginning of a broader transformation in how we think about powering ubiquitous interactive devices. As we continue to advance in materials, energy technology, and interaction design, we move closer to Weiser's vision of computing that truly weaves itself into the fabric of everyday life.

Bibliography

[1] Yuki Abe, Yu Someya, Mitsuhiko Shimomura, Task Ohmori, Seki Inoue, Masahiro Fujiwara, Yasutoshi Makino, and Hiroyuki Shinoda. 2022. Remote Friction Reduction on Polystyrene Foam Surface by Focused Airborne Ultrasound. *IEEE Trans. Haptics* (2022), 1–1. https://doi.org/10.1109/TOH.2022.3148004

[2] Kenneth Abrams, Jeff D Harvell, David Shriner, Philip Wertz, Hilda Maibach, Howard I Maibach, and S J Rehfeld. 1993. Effect of Organic Solvents on In Vitro Human Skin Water Barrier Function. *Journal of Investigative Dermatology* 101, 4 (October 1993), 609–613. https://doi.org/10.1111/1523-1747.ep12366068

[3] Michael J. Adams, Simon A. Johnson, Philippe Lefèvre, Vincent Lévesque, Vincent Hayward, Thibaut André, and Jean-Louis Thonnard. 2013. Finger pad friction and its role in grip and touch. *J. R. Soc. Interface.* 10, 80 (March 2013), 20120467. https://doi.org/10.1098/rsif.2012.0467

[4] Nathaniel Agharese, Tyler Cloyd, Laura H. Blumenschein, Michael Raitor, Elliot W. Hawkes, Heather Culbertson, and Allison M. Okamura. 2018. HapWRAP: Soft Growing Wearable Haptic Device. In *2018 IEEE International Conference on Robotics and Automation (ICRA)*, May 2018. IEEE, Brisbane, QLD, 5466–5472. https://doi.org/10.1109/ICRA.2018.8460891

[5] Asma Akther, Jasmine O. Castro, Seyed Ali Mousavi Shaegh, Amgad R. Rezk, and Leslie Y. Yeo. 2019. Miniaturised acoustofluidic tactile haptic actuator. *Soft Matter* 15, 20 (2019), 4146–4152. https://doi.org/10.1039/C9SM00479C

[6] Jason Alexander, Anne Roudaut, Jürgen Steimle, Kasper Hornbæk, Miguel Bruns Alonso, Sean Follmer, and Timothy Merritt. 2018. Grand Challenges in Shape-Changing Interface Research. In *Proceedings of the 2018 CHI Conference on Human Factors in Computing Systems - CHI '18*, 2018. ACM Press, Montreal QC, Canada, 1–14. https://doi.org/10.1145/3173574.3173873

[7] Abdullah S. Almansouri, Nouf A. Alsharif, Mohammed A. Khan, Liam Swanepoel, Altynay Kaidarova, Khaled N. Salama, and Jurgen Kosel. 2019. An Imperceptible Magnetic Skin. *Adv. Mater. Technol.* (August 2019), 1900493. https://doi.org/10.1002/admt.201900493

[8] Hideyuki Ando, Takeshi Miki, Masahiko Inami, and Taro Maeda. 2002. SmartFinger: nail-mounted tactile display. In *ACM SIGGRAPH 2002 conference abstracts and applications* (*SIGGRAPH '02*), 21 2002. Association for Computing Machinery, New York, NY, USA, 78. https://doi.org/10.1145/1242073.1242113

[9] Abul Al Arabi, Xue Wang, Yang Zhang, and Jeeeun Kim. 2023. E3D: Harvesting Energy from Everyday Kinetic Interactions Using 3D Printed Attachment Mechanisms. *Proc. ACM Interact. Mob. Wearable Ubiquitous Technol.* 7, 3 (September 2023), 1–31. https://doi.org/10.1145/3610897

[10] Shuhei Asano, Shogo Okamoto, and Yoji Yamada. 2015. Vibrotactile Stimulation to Increase and Decrease Texture Roughness. *IEEE Transactions on Human-Machine Systems* 45, 3 (June 2015), 393–398. https://doi.org/10.1109/THMS.2014.2376519

[11] Ronald T. Azuma. 1997. A Survey of Augmented Reality. *Presence: Teleoperators & Virtual Environments* 6, 4 (August 1997), 355–385. https://doi.org/10.1162/pres.1997.6.4.355

[12] Akash Badshah, Sidhant Gupta, Gabe Cohn, Nicolas Villar, Steve Hodges, and Shwetak N. Patel. 2011. Interactive generator: a self-powered haptic feedback device. In *Proceedings of the SIGCHI Conference on Human Factors in Computing Systems* (*CHI '11*), May 07, 2011. Association for Computing Machinery, New York, NY, USA, 2051–2054. https://doi.org/10.1145/1978942.1979240

[13] Je-Hyeong Bahk, Haiyu Fang, Kazuaki Yazawa, and Ali Shakouri. Flexible thermoelectric materials and device optimization for wearable energy harvesting. *Journal of Materials Chemistry C*, 45.

[14] Konstantinos B. Baltzis. 2010. The finite element method magnetics (FEMM) freeware package: May it serve as an educational tool in teaching electromagnetics? *Educ Inf Technol* 15, 1 (March 2010), 19–36. https://doi.org/10.1007/s10639-008-9082-8

[15] Erik Bardy, Joseph Mollendorf, and David Pendergast. 2005. Thermal conductivity and compressive strain of foam neoprene insulation under hydrostatic pressure. *J. Phys. D: Appl. Phys.* 38, 20 (October 2005), 3832–3840. https://doi.org/10.1088/0022-3727/38/20/009

[16] Juan Barreto, Gianfranco Perez, Abdul-Sattar Kaddour, and Stavros V. Georgakopoulos. 2021. A Study of Wearable Wireless Power Transfer Systems on the Human Body. *IEEE Open J. Antennas Propag.* 2, (2021), 86–94. https://doi.org/10.1109/OJAP.2020.3043579

[17] Michael D. Bartlett, Andrew Fassler, Navid Kazem, Eric J. Markvicka, Pratiti Mandal, and Carmel Majidi. 2016. Stretchable, High- *k* Dielectric Elastomers through Liquid-Metal Inclusions. *Adv. Mater.* 28, 19 (May 2016), 3726–3731. https://doi.org/10.1002/adma.201506243

[18] Cagatay Basdogan, Frederic Giraud, Vincent Levesque, and Seungmoon Choi. 2020. A Review of Surface Haptics: Enabling Tactile Effects on Touch Surfaces. *IEEE Trans. Haptics* 13, 3 (July 2020), 450–470. https://doi.org/10.1109/TOH.2020.2990712

[19] Olivier Bau and Ivan Poupyrev. 2012. REVEL: tactile feedback technology for augmented reality. *ACM Trans. Graph.* 31, 4 (August 2012), 1–11. https://doi.org/10.1145/2185520.2185585

[20] Olivier Bau, Ivan Poupyrev, Ali Israr, and Chris Harrison. 2010. TeslaTouch: electrovibration for touch surfaces. In *Proceedings of the 23nd annual ACM symposium on User interface software and technology - UIST '10*, 2010. ACM Press, New York, New York, USA, 283. https://doi.org/10.1145/1866029.1866074

[21] J.J Bikerman. 1947. The fundamentals of tackiness and adhesion. *Journal of Colloid Science* 2, 1 (February 1947), 163–175. https://doi.org/10.1016/0095-8522(47)90017-2

[22] Robert D. Blevins. 2001. *Formulas for natural frequency and mode shape* (Reprint ed ed.). Krieger Publishing, Malabar, Florida.

[23] Alberto Boem and Giovanni Maria Troiano. 2019. Non-Rigid HCI: A Review of Deformable Interfaces and Input. In *Proceedings of the 2019 on Designing Interactive Systems Conference - DIS '19*, 2019. ACM Press, San Diego, CA, USA, 885–906. https://doi.org/10.1145/3322276.3322347

[24] Roger Boldu, Sambhav Jain, Juan Pablo Forero Cortes, Haimo Zhang, and Suranga Nanayakkara. 2019. M-Hair: Creating Novel Tactile Feedback by Augmenting the Body Hair to Respond to Magnetic Field. In *Proceedings of the 32nd Annual ACM Symposium on User Interface Software and Technology - UIST '19*, 2019. ACM Press, New Orleans, LA, USA, 323–328. https://doi.org/10.1145/3332165.3347955

[25] Hugh Boys, Gabriele Frediani, Michele Ghilardi, Stefan Poslad, James C. Busfield, and Federico Carpi. 2018. Soft wearable non-vibratory tactile displays. In *2018 IEEE International Conference on Soft Robotics (RoboSoft)*, April 2018. IEEE, Livorno, Italy, 270–275. https://doi.org/10.1109/ROBOSOFT.2018.8404931

[26] Samarth Brahmbhatt, Cusuh Ham, Charles C. Kemp, and James Hays. 2019. ContactDB: Analyzing and Predicting Grasp Contact via Thermal Imaging. In *2019 IEEE/CVF Conference on Computer Vision and Pattern Recognition (CVPR)*, June 2019. IEEE, Long Beach, CA, USA, 8701–8711. https://doi.org/10.1109/CVPR.2019.00891

[27] Jas Brooks, Steven Nagels, and Pedro Lopes. 2020. Trigeminal-based Temperature Illusions. In *Proceedings of the 2020 CHI Conference on Human Factors in Computing Systems*, April 21, 2020. ACM, Honolulu HI USA, 1–12. https://doi.org/10.1145/3313831.3376806

[28] Shaoyu Cai, Pingchuan Ke, Takuji Narumi, and Kening Zhu. 2020. ThermAirGlove: A Pneumatic Glove for Thermal Perception and Material Identification in Virtual Reality. In *2020 IEEE Conference on Virtual Reality and 3D User Interfaces (VR)*, March 2020. IEEE, Atlanta, GA, USA, 248–257. https://doi.org/10.1109/VR46266.2020.00044

[29] Tommaso Campi, Silvano Cruciani, Valerio De Santis, and Mauro Feliziani. 2016. EMF Safety and Thermal Aspects in a Pacemaker Equipped With a Wireless Power Transfer System Working at Low Frequency. *IEEE Trans. Microwave Theory Techn.* (2016), 1–8. https://doi.org/10.1109/TMTT.2015.2514087

[30] Matthew J. Chabalko, Mohsen Shahmohammadi, and Alanson P. Sample. 2017. Quasistatic Cavity Resonance for Ubiquitous Wireless Power Transfer. *PLoS ONE* 12, 2 (February 2017), e0169045. https://doi.org/10.1371/journal.pone.0169045

[31] Somodyuti Chandra and Anupam Das. 2019. The science of nail polish, nail polish remover, and nail moisturizers. In *Nail Disorders* (1st ed.), Archana Singal, Shekhar Neema and Piyush Kumar (eds.). CRC Press, Boca Raton : Taylor & Francis, a CRC title, part of the Taylor & Francis imprint, a member of the Taylor & Francis Group, the academic division of T&F Informa, plc, 2018., 497–501. https://doi.org/10.1201/9781351139724-35

[32] Yi-Wen Chang, Wei Hung, Hong-Wen Wu, Yen-Chen Chiu, and Horng-Chaung Hsu. 2010. Measurements of Foot Arch in Standing, Level Walking, Vertical Jump and Sprint Start. 2, (2010), 8.

[33] Lung-Pan Cheng, Eyal Ofek, Christian Holz, Hrvoje Benko, and Andrew D. Wilson. 2017. Sparse Haptic Proxy: Touch Feedback in Virtual Environments Using a General Passive Prop. In *Proceedings of the 2017 CHI Conference on Human Factors in Computing Systems*, May 02, 2017. ACM, Denver Colorado USA, 3718–3728. https://doi.org/10.1145/3025453.3025753

[34] Changhyun Choi, Yuan Ma, Xinyi Li, Sitangshu Chatterjee, Sneha Sequeira, Rebecca F. Friesen, Jonathan R. Felts, and M. Cynthia Hipwell. 2022. Surface haptic rendering of virtual

shapes through change in surface temperature. *Sci. Robot.* 7, 63 (February 2022), eabl4543. https://doi.org/10.1126/scirobotics.abl4543

[35] Hyejin Choi, Seongwon Cho, Sunghwan Shin, Hojin Lee, and Seungmoon Choi. 2018. Data-driven thermal rendering: An initial study. In *2018 IEEE Haptics Symposium (HAPTICS)*, March 2018. IEEE, San Francisco, CA, 344–350. https://doi.org/10.1109/HAPTICS.2018.8357199

[36] Inrak Choi, Heather Culbertson, Mark R. Miller, Alex Olwal, and Sean Follmer. 2017. Grabity: A Wearable Haptic Interface for Simulating Weight and Grasping in Virtual Reality. In *Proceedings of the 30th Annual ACM Symposium on User Interface Software and Technology* (*UIST '17*), 2017. ACM, New York, NY, USA, 119–130. https://doi.org/10.1145/3126594.3126599

[37] Inrak Choi and Sean Follmer. 2016. Wolverine: A Wearable Haptic Interface for Grasping in VR. In *Proceedings of the 29th Annual Symposium on User Interface Software and Technology* (*UIST '16 Adjunct*), 2016. ACM, New York, NY, USA, 117–119. https://doi.org/10.1145/2984751.2985725

[38] Jaeyoo Choi, Chaochao Dun, Carlos Forsythe, Madeleine P. Gordon, and Jeffrey J. Urban. 2021. Lightweight wearable thermoelectric cooler with rationally designed flexible heatsink consisting of phase-change material/graphite/silicone elastomer. *J. Mater. Chem. A* 9, 28 (2021), 15696–15703. https://doi.org/10.1039/D1TA01911B

[39] Seungmoon Choi and Katherine J. Kuchenbecker. 2013. Vibrotactile Display: Perception, Technology, and Applications. *Proc. IEEE* 101, 9 (September 2013), 2093–2104. https://doi.org/10.1109/JPROC.2012.2221071

[40] Xiang Cui, Hao Zhou, JiaLin Deng, Wangqiu Zhou, Xing Guo, and Yu Gu. 2022. Mag-E4E: Trade Efficiency for Energy in Magnetic MIMO Wireless Power Transfer System. In *IEEE INFOCOM 2022 - IEEE Conference on Computer Communications*, May 02, 2022. IEEE, London, United Kingdom, 440–449. https://doi.org/10.1109/INFOCOM48880.2022.9796771

[41] A. K. Dąbrowska, G.-M. Rotaru, S. Derler, F. Spano, M. Camenzind, S. Annaheim, R. Stämpfli, M. Schmid, and R. M. Rossi. 2016. Materials used to simulate physical properties of human skin. *Skin Res Technol* 22, 1 (February 2016), 3–14. https://doi.org/10.1111/srt.12235

[42] Kiran Dandekar, Balasundar I. Raju, and Mandayam A. Srinivasan. 2003. 3-D Finite-Element Models of Human and Monkey Fingertips to Investigate the Mechanics of Tactile Sense. *Journal of Biomechanical Engineering* 125, 5 (October 2003), 682–691. https://doi.org/10.1115/1.1613673

[43] Nick J. Davis. 2020. *Water-immersion finger-wrinkling improves grip efficiency in handling wet objects*. Neuroscience. https://doi.org/10.1101/2020.11.07.372631

[44] Danilo De Rossi, F. Carpi, N. Carbonaro, A. Tognetti, and E. P. Scilingo. 2011. Electroactive polymer patches for wearable haptic interfaces. In *2011 Annual International Conference of the IEEE Engineering in Medicine and Biology Society*, August 2011. IEEE, Boston, MA, 8369–8372. https://doi.org/10.1109/IEMBS.2011.6092064

[45] Jasper De Winkel, Vito Kortbeek, Josiah Hester, and Przemysław Pawełczak. 2020. Battery-Free Game Boy. *Proc. ACM Interact. Mob. Wearable Ubiquitous Technol.* 4, 3 (September 2020), 1–34. https://doi.org/10.1145/3411839

[46] Ayoub Ben Dhiab and Charles Hudin. 2019. Confinement of Vibrotactile Stimuli in Narrow Plates. In *2019 IEEE World Haptics Conference (WHC)*, July 2019. IEEE, Tokyo, Japan, 431–436. https://doi.org/10.1109/WHC.2019.8816081

[47] Aashish Dhungana and Eyuphan Bulut. 2020. Peer-to-peer energy sharing in mobile networks: Applications, challenges, and open problems. *Ad Hoc Networks* 97, (February 2020), 102029. https://doi.org/10.1016/j.adhoc.2019.102029

[48] Tim Duente, Justin Schulte, Max Pfeiffer, and Michael Rohs. 2018. MuscleIO: Muscle-Based Input and Output for Casual Notifications. *Proc. ACM Interact. Mob. Wearable Ubiquitous Technol.* 2, 2 (July 2018), 64:1-64:21. https://doi.org/10.1145/3214267

[49] Brygida M. Dzidek, Michael J. Adams, James W. Andrews, Zhibing Zhang, and Simon A. Johnson. 2017. Contact mechanics of the human finger pad under compressive loads. *J. R. Soc. Interface.* 14, 127 (February 2017), 20160935. https://doi.org/10.1098/rsif.2016.0935

[50] A Abo El-Nasr and S M El-Haggar. Effective thermal conductivity of heat pipes. 5.

[51] Bettina Eska, Jeff-Owens Iyalekhue, Sebastian Günther, Jasmin Niess, and Florian Müller. 2023. ThermoFeet: Assessing On-Foot Thermal Stimuli for Directional Cues. In *Proceedings of the 22nd International Conference on Mobile and Ubiquitous Multimedia*, December 03, 2023. ACM, Vienna Austria, 166–171. https://doi.org/10.1145/3626705.3627974

[52] Jerry Alan Fails and Dan Olsen. Light Widgets: Interacting in Every-day Spaces. 7.

[53] Junjie Feng, Qiang Li, Fred C. Lee, and Minfan Fu. 2019. Transmitter Coils Design for Free-Positioning Omnidirectional Wireless Power Transfer System. *IEEE Trans. Ind. Inf.* 15, 8 (August 2019), 4656–4664. https://doi.org/10.1109/TII.2019.2908217

[54] Elisa R. Ferrè, Jonathan Joel, Denise Cadete, and Matthew R. Longo. 2023. Systematic underestimation of human hand weight. *Current Biology* 33, 14 (July 2023), R758–R759. https://doi.org/10.1016/j.cub.2023.05.041

[55] Anton Franzluebbers and Kyle Johnsen. 2018. Performance Benefits of High-Fidelity Passive Haptic Feedback in Virtual Reality Training. In *Proceedings of the Symposium on Spatial User Interaction*, October 13, 2018. ACM, Berlin Germany, 16–24. https://doi.org/10.1145/3267782.3267790

[56] Nan-Wei Gong, Jürgen Steimle, Simon Olberding, Steve Hodges, Nicholas Edward Gillian, Yoshihiro Kawahara, and Joseph A. Paradiso. 2014. PrintSense: a versatile sensing technique to support multimodal flexible surface interaction. In *Proceedings of the 32nd annual ACM conference on Human factors in computing systems - CHI '14*, 2014. ACM Press, Toronto, Ontario, Canada, 1407–1410. https://doi.org/10.1145/2556288.2557173

[57] Daniel Gooch and Leon Watts. 2012. YourGloves, hothands and hotmits: devices to hold hands at a distance. In *Proceedings of the 25th annual ACM symposium on User interface software and technology - UIST '12*, 2012. ACM Press, Cambridge, Massachusetts, USA, 157. https://doi.org/10.1145/2380116.2380138

[58] Hesam Sadeghi Gougheri and Mehdi Kiani. 2016. Optimal wireless receiver structure for omnidirectional inductive power transmission to biomedical implants. In *2016 38th Annual International Conference of the IEEE Engineering in Medicine and Biology Society (EMBC)*, August 2016. IEEE, Orlando, FL, USA, 1975–1978. https://doi.org/10.1109/EMBC.2016.7591111

[59] Daniel Groeger, Martin Feick, Anusha Withana, and Jürgen Steimle. 2019. Tactlets: Adding Tactile Feedback to 3D Objects Using Custom Printed Controls. In *Proceedings of the 32nd Annual ACM Symposium on User Interface Software and Technology*, October 17, 2019. ACM, New Orleans LA USA, 923–936. https://doi.org/10.1145/3332165.3347937

[60] Daniel Groeger and Jürgen Steimle. 2018. ObjectSkin: Augmenting Everyday Objects with Hydroprinted Touch Sensors and Displays. *Proc. ACM Interact. Mob. Wearable Ubiquitous Technol.* 1, 4 (January 2018), 1–23. https://doi.org/10.1145/3161165

[61] L. Grunberg and A. H. Nissan. 1949. The energies of vaporisation, viscosity and cohesion and the structure of liquids. *Trans. Faraday Soc.* 45, (1949), 125. https://doi.org/10.1039/tf9494500125

[62] David Gueorguiev, Séréna Bochereau, André Mouraux, Vincent Hayward, and Jean-Louis Thonnard. 2016. Touch uses frictional cues to discriminate flat materials. *Sci Rep* 6, 1 (July 2016), 25553. https://doi.org/10.1038/srep25553

[63] David Gueorguiev, Eric Vezzoli, André Mouraux, Betty Lemaire-Semail, and Jean-Louis Thonnard. 2017. The tactile perception of transient changes in friction. *J. R. Soc. Interface.* 14, 137 (December 2017), 20170641. https://doi.org/10.1098/rsif.2017.0641

[64] Steve Guest, Francis McGlone, Andrew Hopkinson, Zachary A. Schendel, Kevin Blot, and Greg Essick. 2013. Perceptual and Sensory-Functional Consequences of Skin Care Products. *JCDSA* 03, 01 (2013), 66–78. https://doi.org/10.4236/jcdsa.2013.31A010

[65] Steve Guest, Anahit Mehrabyan, Greg Essick, Nicola Phillips, Andrew Hopkinson, and Francis Mcglone. 2012. PHYSICS AND TACTILE PERCEPTION OF FLUID-COVERED SURFACES: PHYSICS AND TACTILE PERCEPTION OF FLUIDS. *Journal of Texture Studies* 43, 1 (February 2012), 77–93. https://doi.org/10.1111/j.1745-4603.2011.00318.x

[66] Jeremy Gummeson, James Mccann, Chouchang (JACK) Yang, Damith Ranasinghe, Scott Hudson, and Alanson Sample. 2017. RFID Light Bulb: Enabling Ubiquitous Deployment of Interactive RFID Systems. *Proc. ACM Interact. Mob. Wearable Ubiquitous Technol.* 1, 2 (June 2017), 1–16. https://doi.org/10.1145/3090077

[67] Sebastian Günther, Florian Müller, Dominik Schön, Omar Elmoghazy, Max Mühlhäuser, and Martin Schmitz. 2020. Therminator: Understanding the Interdependency of Visual and On-Body Thermal Feedback in Virtual Reality. In *Proceedings of the 2020 CHI Conference on Human Factors in Computing Systems*, April 21, 2020. ACM, Honolulu HI USA, 1–14. https://doi.org/10.1145/3313831.3376195

[68] C. S. Haines, M. D. Lima, N. Li, G. M. Spinks, J. Foroughi, J. D. W. Madden, S. H. Kim, S. Fang, M. Jung de Andrade, F. Goktepe, O. Goktepe, S. M. Mirvakili, S. Naficy, X. Lepro, J. Oh, M. E. Kozlov, S. J. Kim, X. Xu, B. J. Swedlove, G. G. Wallace, and R. H. Baughman. 2014. Artificial Muscles from Fishing Line and Sewing Thread. *Science* 343, 6173 (February 2014), 868–872. https://doi.org/10.1126/science.1246906

[69] Jonna Häkkilä and Ashley Colley. 2016. Towards a Design Space for Liquid User Interfaces. In *Proceedings of the 9th Nordic Conference on Human-Computer Interaction*, October 23, 2016. ACM, Gothenburg Sweden, 1–4. https://doi.org/10.1145/2971485.2971537

[70] Takumi Hamazaki, Miku Kaneda, Jianyao Zhang, Seitaro Kaneko, and Hiroyuki Kajimoto. 2022. Chemical-induced Thermal Grill Illusion. In *2022 IEEE Haptics Symposium (HAPTICS)*, March 21, 2022. IEEE, Santa Barbara, CA, USA, 1–6. https://doi.org/10.1109/HAPTICS52432.2022.9765569

[71] Nur Al-huda Hamdan, Adrian Wagner, Simon Voelker, Jürgen Steimle, and Jan Borchers. 2019. Springlets: Expressive, Flexible and Silent On-Skin Tactile Interfaces. In *Proceedings of the 2019 CHI Conference on Human Factors in Computing Systems - CHI '19*, 2019. ACM Press, Glasgow, Scotland Uk, 1–14. https://doi.org/10.1145/3290605.3300718

[72] Teng Han, Fraser Anderson, Pourang Irani, and Tovi Grossman. 2018. HydroRing: Supporting Mixed Reality Haptics Using Liquid Flow. In *The 31st Annual ACM Symposium on User Interface Software and Technology - UIST '18*, 2018. ACM Press, 913–925. https://doi.org/10.1145/3242587.3242667

[73] Teng Han, Fraser Anderson, Pourang Irani, and Tovi Grossman. 2018. HydroRing: Supporting Mixed Reality Haptics Using Liquid Flow. In *The 31st Annual ACM Symposium on User Interface Software and Technology - UIST '18*, 2018. ACM Press, Berlin, Germany, 913–925. https://doi.org/10.1145/3242587.3242667

[74] Teng Han, Shubhi Bansal, Xiaochen Shi, Yanjun Chen, Baogang Quan, Feng Tian, Hongan Wang, and Sriram Subramanian. 2020. HapBead: On-Skin Microfluidic Haptic Interface using Tunable Bead. In *Proceedings of the 2020 CHI Conference on Human Factors in Computing Systems*, April 21, 2020. ACM, Honolulu HI USA, 1–10. https://doi.org/10.1145/3313831.3376190

[75] Teng Han, Qian Han, Michelle Annett, Fraser Anderson, Da-Yuan Huang, and Xing-Dong Yang. 2017. Frictio: Passive Kinesthetic Force Feedback for Smart Ring Output. In *Proceedings of the 30th Annual ACM Symposium on User Interface Software and Technology - UIST '17*, 2017. ACM Press, Québec City, QC, Canada, 131–142. https://doi.org/10.1145/3126594.3126622

[76] Chris Harrison, Hrvoje Benko, and Andrew D. Wilson. 2011. OmniTouch: wearable multitouch interaction everywhere. In *Proceedings of the 24th annual ACM symposium on User interface software and technology*, October 16, 2011. ACM, Santa Barbara California USA, 441–450. https://doi.org/10.1145/2047196.2047255

[77] Chris Harrison and Scott E. Hudson. 2008. Scratch input: creating large, inexpensive, unpowered and mobile finger input surfaces. In *Proceedings of the 21st annual ACM symposium on User interface software and technology - UIST '08*, 2008. ACM Press, Monterey, CA, USA, 205. https://doi.org/10.1145/1449715.1449747

[78] Chris Harrison, Robert Xiao, and Scott Hudson. 2012. Acoustic barcodes: passive, durable and inexpensive notched identification tags. In *Proceedings of the 25th annual ACM symposium on User interface software and technology - UIST '12*, 2012. ACM Press, Cambridge, Massachusetts, USA, 563. https://doi.org/10.1145/2380116.2380187

[79] Nam Ha-Van, Yining Liu, Prasad Jayathurathnage, Constantin R. Simovski, and Sergei A. Tretyakov. 2022. Cylindrical Transmitting Coil for Two-Dimensional Omnidirectional Wireless Power Transfer. *IEEE Trans. Ind. Electron.* 69, 10 (October 2022), 10045–10054. https://doi.org/10.1109/TIE.2022.3151961

[80] Tess Hellebrekers, Oliver Kroemer, and Carmel Majidi. 2019. Soft Magnetic Skin for Continuous Deformation Sensing. *Advanced Intelligent Systems* 1, 4 (August 2019), 1900025. https://doi.org/10.1002/aisy.201900025

[81] Josiah Hester and Jacob Sorber. 2017. The Future of Sensing is Batteryless, Intermittent, and Awesome. In *Proceedings of the 15th ACM Conference on Embedded Network Sensor Systems*, November 06, 2017. ACM, Delft Netherlands, 1–6. https://doi.org/10.1145/3131672.3131699

[82] Josiah Hester, Kevin Storer, and Jacob Sorber. 2017. Timely Execution on Intermittently Powered Batteryless Sensors. In *Proceedings of the 15th ACM Conference on Embedded Network Sensor Systems*, November 06, 2017. ACM, Delft Netherlands, 1–13. https://doi.org/10.1145/3131672.3131673

[83] John S. Hibbard, Gayle K. Mulberry, and Ann R. Brady. 2002. A Clinical Study Comparing the Skin Antisepsis and Safety of ChloraPrep, 70% Isopropyl Alcohol, and 2% Aqueous Chlorhexidine: *Journal of Infusion Nursing* 25, 4 (July 2002), 244–249. https://doi.org/10.1097/00129804-200207000-00007

[84] Uwe Hiller. 1968. Untersuchungen zum Feinbau und zur Funktion der Haftborsten von Reptilien. *Z. Morph. Tiere* 62, 4 (1968), 307–362. https://doi.org/10.1007/BF00401561

[85] Ronan Hinchet, Velko Vechev, Herbert Shea, and Otmar Hilliges. 2018. DextrES: Wearable Haptic Feedback for Grasping in VR via a Thin Form-Factor Electrostatic Brake. In *Proceedings of the 31st Annual ACM Symposium on User Interface Software and Technology* (*UIST '18*), October 11, 2018. Association for Computing Machinery, New York, NY, USA, 901–912. https://doi.org/10.1145/3242587.3242657

[86] K. Hinckley, R. Pausch, J. Goble, and N. Kassell. 1994. Passive real-world interface props for neurosurgical visualization. In *Proceedings of the SIGCHI conference on Human factors in computing systems*, April 1994. 452–458. https://doi.org/10.1145/191666.191821

[87] Steve Hodges. 2013. Batteries Not Included: Powering the Ubiquitous Computing Dream. *Computer* 46, 4 (April 2013), 90–93. https://doi.org/10.1109/MC.2013.125

[88] Simon Holland, David R. Morse, and Henrik Gedenryd. 2002. Direct Combination: A New User Interaction Principle for Mobile and Ubiquitous HCI. In *Human Computer Interaction with Mobile Devices*, Fabio Paternò (ed.). Springer Berlin Heidelberg, Berlin, Heidelberg, 108–122. https://doi.org/10.1007/3-540-45756-9_10

[89] Wenqi Hu, Guo Zhan Lum, Massimo Mastrangeli, and Metin Sitti. 2018. Small-scale soft-bodied robot with multimodal locomotion. *Nature* 554, 7690 (February 2018), 81–85. https://doi.org/10.1038/nature25443

[90] Thomas Hulin, Michael Rothammer, Isabel Tannert, Suraj Subramanyam Giri, Benedikt Pleintinger, Harsimran Singh, Bernhard Weber, and Christian Ott. 2020. FingerTac – A Wearable Tactile Thimble for Mobile Haptic Augmented Reality Applications. In *Virtual, Augmented and Mixed Reality. Design and Interaction* (*Lecture Notes in Computer Science*),

2020. Springer International Publishing, Cham, 286–298. https://doi.org/10.1007/978-3-030-49695-1_19

[91] María Ibañez-Puy, Javier Bermejo-Busto, César Martín-Gómez, Marina Vidaurre-Arbizu, and José Antonio Sacristán-Fernández. 2017. Thermoelectric cooling heating unit performance under real conditions. *Applied Energy* 200, (August 2017), 303–314. https://doi.org/10.1016/j.apenergy.2017.05.020

[92] IoT.Business.News. 2024. State of IoT 2024: Number of connected IoT devices growing 13% to 18.8 billion globally. *IoT Business News*. Retrieved December 5, 2024 from https://iotbusinessnews.com/2024/09/04/26399-state-of-iot-2024-number-of-connected-iot-devices-growing-13-to-18-8-billion-globally/

[93] Yasha Iravantchi, Mayank Goel, and Chris Harrison. 2020. Digital Ventriloquism: Giving Voice to Everyday Objects. In *Proceedings of the 2020 CHI Conference on Human Factors in Computing Systems*, April 21, 2020. ACM, Honolulu HI USA, 1–10. https://doi.org/10.1145/3313831.3376503

[94] Yoshitaka Ishihara, Yuichi Itoh, Ryo Shirai, Kazuyuki Fujita, Kazuki Takashima, and Takao Onoye. 2020. StickyTouch: A Tactile Display with Changeable Adhesive Distribution. In *2020 IEEE Haptics Symposium (HAPTICS)*, March 2020. IEEE, Crystal City, VA, USA, 842–847. https://doi.org/10.1109/HAPTICS45997.2020.ras.HAP20.4.b5d4a51b

[95] Ken Ito, Shogo Okamoto, Yoji Yamada, and Hiroyuki Kajimoto. 2019. Tactile Texture Display with Vibrotactile and Electrostatic Friction Stimuli Mixed at Appropriate Ratio Presents Better Roughness Textures. *ACM Trans. Appl. Percept.* 16, 4 (October 2019), 1–15. https://doi.org/10.1145/3340961

[96] Vikram Iyer, Justin Chan, and Shyamnath Gollakota. 2017. 3D printing wireless connected objects. *ACM Trans. Graph.* 36, 6 (November 2017), 1–13. https://doi.org/10.1145/3130800.3130822

[97] Yvonne Jansen, Thorsten Karrer, and Jan Borchers. 2010. MudPad: localized tactile feedback on touch surfaces. In *Proceedings of the 23nd Annual ACM Symposium on User Interface Software and Technology*, 2010. 385–386. https://doi.org/10.1145/1866218.1866232

[98] Seungwoo Je, Hyunseung Lim, Kongpyung Moon, Shan-Yuan Teng, Jas Brooks, Pedro Lopes, and Andrea Bianchi. 2021. Elevate: A Walkable Pin-Array for Large Shape-Changing Terrains. In *Proceedings of the 2021 CHI Conference on Human Factors in Computing Systems*, May 06, 2021. ACM, Yokohama Japan, 1–11. https://doi.org/10.1145/3411764.3445454

[99] Per Jenmalm and Roland S. Johansson. 1997. Visual and Somatosensory Information about Object Shape Control Manipulative Fingertip Forces. *J. Neurosci.* 17, 11 (June 1997), 4486–4499. https://doi.org/10.1523/JNEUROSCI.17-11-04486.1997

[100] Nathan Seongheon Jeong and Francesco Carobolante. 2017. Wireless Charging of a Metal-Body Device. *IEEE Transactions on Microwave Theory and Techniques* 65, 4 (April 2017), 1077–1086. https://doi.org/10.1109/TMTT.2017.2673820

[101] Chutian Jiang, Yanjun Chen, Mingming Fan, Liuping Wang, Luyao Shen, Nianlong Li, Wei Sun, Yu Zhang, Feng Tian, and Teng Han. 2021. Douleur: Creating Pain Sensation with

Chemical Stimulant to Enhance User Experience in Virtual Reality. *Proc. ACM Interact. Mob. Wearable Ubiquitous Technol.* 5, 2 (June 2021), 1–26. https://doi.org/10.1145/3463527

[102] Arata Jingu, Nihar Sabnis, Paul Strohmeier, and Jürgen Steimle. 2024. Shaping Compliance: Inducing Haptic Illusion of Compliance in Different Shapes with Electrotactile Grains. In *Proceedings of the CHI Conference on Human Factors in Computing Systems*, May 11, 2024. ACM, Honolulu HI USA, 1–13. https://doi.org/10.1145/3613904.3641907

[103] L.A. Jones and H.-N. Ho. 2008. Warm or Cool, Large or Small? The Challenge of Thermal Displays. *IEEE Transactions on Haptics* 1, 1 (January 2008), 53–70. https://doi.org/10.1109/TOH.2008.2

[104] Hsin-Liu (Cindy) Kao, Miren Bamforth, David Kim, and Chris Schmandt. 2018. Skinmorph: texture-tunable on-skin interface through thin, programmable gel. In *Proceedings of the 2018 ACM International Symposium on Wearable Computers*, October 08, 2018. ACM, Singapore Singapore, 196–203. https://doi.org/10.1145/3267242.3267262

[105] Masayuki Kato and Katsuhiro Hirata. 2018. Characteristic Evaluation of Linear Resonant Actuator Utilizing Electrical Resonance. *IEEJ Journal IA* 7, 2 (2018), 175–180. https://doi.org/10.1541/ieejjia.7.175

[106] Anzu Kawazoe, Massimiliano Di Luca, and Yon Visell. 2019. Tactile Echoes: A Wearable System for Tactile Augmentation of Objects. In *2019 IEEE World Haptics Conference (WHC)*, July 2019. 359–364. https://doi.org/10.1109/WHC.2019.8816099

[107] Kazunobu Sumiya, Kazunobu Sumiya, Takuya Sasatani, Takuya Sasatani, Yuki Nishizawa, Yuki Nishizawa, Kenji Tsushio, Kenji Tsushio, Yoshiaki Narusue, Yoshiaki Narusue, Yoshihiro Kawahara, and Yoshihiro Kawahara. 2019. Alvus: A Reconfigurable 2-D Wireless Charging System. 3, 2 (June 2019), 68. https://doi.org/10.1145/3332533

[108] Sadeque Reza Khan and Marc P.Y. Desmulliez. 2019. Towards a Miniaturized 3D Receiver WPT System for Capsule Endoscopy. *Micromachines* 10, 8 (August 2019), 545. https://doi.org/10.3390/mi10080545

[109] Sadeque Reza Khan, Sumanth Kumar Pavuluri, Gerard Cummins, and Marc P. Y. Desmulliez. 2019. Miniaturized 3-D Cross-Type Receiver for Wirelessly Powered Capsule Endoscopy. *IEEE Trans. Microwave Theory Techn.* 67, 5 (May 2019), 1985–1993. https://doi.org/10.1109/TMTT.2019.2893204

[110] Hwan Kim, Minhwan Kim, and Woohun Lee. 2016. HapThimble: A Wearable Haptic Device Towards Usable Virtual Touch Screen. In *Proceedings of the 2016 CHI Conference on Human Factors in Computing Systems* (*CHI '16*), 2016. ACM, New York, NY, USA, 3694–3705. https://doi.org/10.1145/2858036.2858196

[111] Hwan Kim, HyeonBeom Yi, Hyein Lee, and Woohun Lee. 2018. HapCube: A Wearable Tactile Device to Provide Tangential and Normal Pseudo-Force Feedback on a Fingertip. In *Proceedings of the 2018 CHI Conference on Human Factors in Computing Systems*, April 21, 2018. ACM, Montreal QC Canada, 1–13. https://doi.org/10.1145/3173574.3174075

[112] Lawrence H. Kim, Pablo Castillo, Sean Follmer, and Ali Israr. 2019. VPS Tactile Display: Tactile Information Transfer of Vibration, Pressure, and Shear. *Proc. ACM Interact. Mob. Wearable Ubiquitous Technol.* 3, 2 (June 2019), 1–17. https://doi.org/10.1145/3328922

[113] Seung-Won Kim. 2020. Thermal display glove for interacting with virtual reality. *Scientific Reports* (2020), 12.

[114] Seyeong Kim, Yea-kyung Row, and Tek-Jin Nam. 2018. Thermal Interaction with a Voice-based Intelligent Agent. In *Extended Abstracts of the 2018 CHI Conference on Human Factors in Computing Systems*, April 20, 2018. ACM, Montreal QC Canada, 1–6. https://doi.org/10.1145/3170427.3188656

[115] Martin Hartwig Kirschner, Reinhold Andreas Lang, Burkhard Breuer, Marion Breuer, Corinna Schulze Gronover, Thomas Zwingers, Johannes Georg Böttrich, Andreas Arndt, Ute Brauer, Matthias Hintzpeter, Marc-Alexander Burmeister, and Jan-Dirk Fauteck. 2009. Transdermal resorption of an ethanol- and 2-propanol-containing skin disinfectant. *Langenbecks Arch Surg* 394, 1 (January 2009), 151–157. https://doi.org/10.1007/s00423-007-0237-7

[116] Lina K. Klein, Guido Maiello, Roland W. Fleming, and Dimitris Voudouris. 2021. Friction is preferred over grasp configuration in precision grip grasping. *Journal of Neurophysiology* 125, 4 (2021), 1330–1338. https://doi.org/10.1152/jn.00021.2021

[117] Ben Kleinsman-Leusink-Hill, John Bronlund, and Gourab Sen Gupta. 2018. Thermal and haptic interface design: Adding sensory feedback to VR/AR. In *2018 IEEE International Instrumentation and Measurement Technology Conference (I2MTC)*, May 2018. IEEE, Houston, TX, USA, 1–6. https://doi.org/10.1109/I2MTC.2018.8409733

[118] Andy Kong, Daehwa Kim, and Chris Harrison. 2024. Power-over-Skin: Full-Body Wearables Powered By Intra-Body RF Energy. In *Proceedings of the 37th Annual ACM Symposium on User Interface Software and Technology*, October 13, 2024. ACM, Pittsburgh PA USA, 1–13. https://doi.org/10.1145/3654777.3676394

[119] Michinari Kono, Hiromi Nakamura, and Jun Rekimoto. 2017. Intentiō: power distribution through a potentialized human body. In *Proceedings of the 8th Augmented Human International Conference*, March 16, 2017. ACM, Silicon Valley California USA, 1–10. https://doi.org/10.1145/3041164.3041175

[120] Michinari Kono, Takumi Takahashi, Hiromi Nakamura, Takashi Miyaki, and Jun Rekimoto. 2018. Design Guideline for Developing Safe Systems that Apply Electricity to the Human Body. *ACM Trans. Comput.-Hum. Interact.* 25, 3 (June 2018), 1–36. https://doi.org/10.1145/3184743

[121] R. Kötz and M. Carlen. 2000. Principles and applications of electrochemical capacitors. *Electrochimica Acta* 45, 15–16 (May 2000), 2483–2498. https://doi.org/10.1016/S0013-4686(00)00354-6

[122] Robert Kovacs, Eyal Ofek, Mar Gonzalez Franco, Alexa Fay Siu, Sebastian Marwecki, Christian Holz, and Mike Sinclair. 2020. Haptic PIVOT: On-Demand Handhelds in VR. In *Proceedings of the 33rd Annual ACM Symposium on User Interface Software and Technology*. Association for Computing Machinery, New York, NY, USA, 1046–1059. Retrieved June 28, 2021 from https://doi.org/10.1145/3379337.3415854

[123] Sven Kratz and Tony Dunnigan. 2017. ThermoTouch: a New Scalable Hardware Design for Thermal Displays. In *Proceedings of the 2017 ACM International Conference on*

Interactive Surfaces and Spaces, October 17, 2017. ACM, Brighton United Kingdom, 132–141. https://doi.org/10.1145/3132272.3134133

[124] Daniel J. Kucherhan, Miriam Goubran, Vinicius P. da Fonseca, Thiago E. Alves de Oliveira, Emil M. Petriu, and Voicu Groza. 2018. Object Recognition Through Manipulation Using Tactile Enabled Prosthetic Fingers and Feedback Glove - Experimental Study. In *2018 IEEE International Symposium on Medical Measurements and Applications (MeMeA)*, June 2018. IEEE, Rome, 1–6. https://doi.org/10.1109/MeMeA.2018.8438757

[125] Julien van Kuilenburg, Marc A Masen, and Emile van der Heide. 2015. A review of fingerpad contact mechanics and friction and how this affects tactile perception. *Proceedings of the Institution of Mechanical Engineers, Part J: Journal of Engineering Tribology* 229, 3 (March 2015), 243–258. https://doi.org/10.1177/1350650113504908

[126] André Kurs, Aristeidis Karalis, Robert Moffatt, J. D. Joannopoulos, Peter Fisher, and Marin Soljačić. 2007. Wireless Power Transfer via Strongly Coupled Magnetic Resonances. *Science* 317, 5834 (July 2007), 83–86. https://doi.org/10.1126/science.1143254

[127] Jinwoo Lee, Heayoun Sul, Wonha Lee, Kyung Rok Pyun, Inho Ha, Dongkwan Kim, Hyojoon Park, Hyeonjin Eom, Yeosang Yoon, Jinwook Jung, Dongjun Lee, and Seung Hwan Ko. 2020. Stretchable Skin-Like Cooling/Heating Device for Reconstruction of Artificial Thermal Sensation in Virtual Reality. *Adv. Funct. Mater.* 30, 29 (July 2020), 1909171. https://doi.org/10.1002/adfm.201909171

[128] Vincent Levesque, Louise Oram, Karon MacLean, Andy Cockburn, Nicholas D. Marchuk, Dan Johnson, J. Edward Colgate, and Michael A. Peshkin. 2011. Enhancing physicality in touch interaction with programmable friction. In *Proceedings of the SIGCHI Conference on Human Factors in Computing Systems*, May 07, 2011. ACM, Vancouver BC Canada, 2481–2490. https://doi.org/10.1145/1978942.1979306

[129] Jiahao Li, Jeeeun Kim, and Xiang "Anthony" Chen. 2019. Robiot: A Design Tool for Actuating Everyday Objects with Automatically Generated 3D Printable Mechanisms. In *Proceedings of the 32nd Annual ACM Symposium on User Interface Software and Technology*, October 17, 2019. ACM, New Orleans LA USA, 673–685. https://doi.org/10.1145/3332165.3347894

[130] Jiamin Li, Yilong Dong, Jeong Hoan Park, and Jerald Yoo. 2021. Body-coupled power transmission and energy harvesting. 4, 7 (June 2021), 530–538. https://doi.org/10.1038/s41928-021-00592-y

[131] Jonghyun Lim and Sung Jin Kim. 2018. Fabrication and experimental evaluation of a polymer-based flexible pulsating heat pipe. *Energy Conversion and Management* 156, (January 2018), 358–364. https://doi.org/10.1016/j.enconman.2017.11.022

[132] Rongzhou Lin, Han-Joon Kim, Sippanat Achavananthadith, Selman A. Kurt, Shawn C. C. Tan, Haicheng Yao, Benjamin C. K. Tee, Jason K. W. Lee, and John S. Ho. 2020. Wireless battery-free body sensor networks using near-field-enabled clothing. *Nat Commun* 11, 1 (January 2020), 444. https://doi.org/10.1038/s41467-020-14311-2

[133] Xun Liu. 2015. Qi Standard Wireless Power Transfer Technology Development Toward Spatial Freedom. *IEEE Circuits and Systems Magazine* 15, 2 (2015), 32–39. https://doi.org/10.1109/MCAS.2015.2419011

[134] H. Löffler, G. Kampf, D. Schmermund, and H.I. Maibach. 2007. How irritant is alcohol? *Br J Dermatol* 157, 1 (July 2007), 74–81. https://doi.org/10.1111/j.1365-2133.2007.07944.x

[135] John E. Logsdon and Richard A. Loke. 2000. Isopropyl Alcohol. In *Kirk-Othmer Encyclopedia of Chemical Technology* (1st ed.), Kirk-Othmer (ed.). Wiley. https://doi.org/10.1002/0471238961.0919151612150719.a01

[136] Pedro Lopes and Patrick Baudisch. 2013. Muscle-propelled force feedback: bringing force feedback to mobile devices. In *Proceedings of the SIGCHI Conference on Human Factors in Computing Systems* (*CHI '13*), April 27, 2013. Association for Computing Machinery, New York, NY, USA, 2577–2580. https://doi.org/10.1145/2470654.2481355

[137] Pedro Lopes, Alexandra Ion, and Patrick Baudisch. 2015. Impacto: Simulating Physical Impact by Combining Tactile Stimulation with Electrical Muscle Stimulation. In *Proceedings of the 28th Annual ACM Symposium on User Interface Software & Technology* (*UIST '15*), 2015. ACM, New York, NY, USA, 11–19. https://doi.org/10.1145/2807442.2807443

[138] Pedro Lopes, Ricardo Jota, and Joaquim A. Jorge. 2011. Augmenting touch interaction through acoustic sensing. In *Proceedings of the ACM International Conference on Interactive Tabletops and Surfaces - ITS '11*, 2011. ACM Press, Kobe, Japan, 53. https://doi.org/10.1145/2076354.2076364

[139] Jasmine Lu, Ziwei Liu, Jas Brooks, and Pedro Lopes. 2021. Chemical Haptics: Rendering Haptic Sensations via Topical Stimulants. In *The 34th Annual ACM Symposium on User Interface Software and Technology*, October 10, 2021. ACM, Virtual Event USA, 239–257. https://doi.org/10.1145/3472749.3474747

[140] Guo Zhan Lum, Zhou Ye, Xiaoguang Dong, Hamid Marvi, Onder Erin, Wenqi Hu, and Metin Sitti. 2016. Shape-programmable magnetic soft matter. *Proc Natl Acad Sci USA* 113, 41 (October 2016), E6007–E6015. https://doi.org/10.1073/pnas.1608193113

[141] William E. Luttrell and Austin L. LaGrow. 2014. Acetone. *J. Chem. Health Saf.* 21, 3 (May 2014), 29–31. https://doi.org/10.1016/j.jchas.2014.03.006

[142] Tomosuke Maeda and Tetsuo Kurahashi. 2019. TherModule: Wearable and Modular Thermal Feedback System based on a Wireless Platform. In *Proceedings of the 10th Augmented Human International Conference 2019*, March 11, 2019. ACM, Reims France, 1–8. https://doi.org/10.1145/3311823.3311826

[143] Amal Ibrahim Mahmood, Sadik Kamel Gharghan, Mohamed A. A. Eldosoky, Mustafa Falah Mahmood, and Ahmed M. Soliman. 2021. Wireless Power Transfer Based on Spider Web–Coil for Biomedical Implants. *IEEE Access* 9, (2021), 167674–167686. https://doi.org/10.1109/ACCESS.2021.3136817

[144] Nicolai Marquardt, Miguel A. Nacenta, James E. Young, Sheelagh Carpendale, Saul Greenberg, and Ehud Sharlin. 2009. The Haptic Tabletop Puck: tactile feedback for interactive tabletops. In *Proceedings of the ACM International Conference on Interactive Tabletops and Surfaces*, November 23, 2009. ACM, Banff Alberta Canada, 85–92. https://doi.org/10.1145/1731903.1731922

[145] Alex Mazursky, Jas Brooks, Beza Desta, and Pedro Lopes. 2024. ThermalGrasp: Enabling Thermal Feedback even while Grasping and Walking. In *2024 IEEE Conference Virtual*

Reality and 3D User Interfaces (VR), March 16, 2024. IEEE, Orlando, FL, USA, 342–353. https://doi.org/10.1109/VR58804.2024.00056

[146] Alex Mazursky, Aryan Gupta, Andre de la Cruz, and Pedro Lopes. 2025. Power-on-Touch: Powering Actuators, Sensors, and Devices during Interaction. 2025. .

[147] Alex Mazursky, Jeong-Hoi Koo, and Tae-Heon Yang. 2019. Design, modeling, and evaluation of a slim haptic actuator based on electrorheological fluid. *Journal of Intelligent Material Systems and Structures* (March 2019), 1045389X1983617. https://doi.org/10.1177/1045389X19836172

[148] Alex Mazursky, Jeong-Hoi Koo, and Tae-Heon Yang. 2020. A compact and compliant electrorheological actuator for generating a wide range of haptic sensations. *Smart Mater. Struct.* (January 2020). https://doi.org/10.1088/1361-665X/ab710c

[149] Alex Mazursky, Borui Li, Shan-Yuan Teng, Daria Shifrina, Joyce E Passananti, Svitlana Midianko, and Pedro Lopes. 2023. ThermalRouter: Enabling Users to Design Thermally-Sound Devices. In *Proceedings of the 36th Annual ACM Symposium on User Interface Software and Technology*, October 29, 2023. ACM, San Francisco CA USA, 1–14. https://doi.org/10.1145/3586183.3606747

[150] Alex Mazursky, Jacob Serfaty, and Pedro Lopes. 2024. Stick&Slip: Altering Fingerpad Friction via Liquid Coatings. In *Proceedings of the CHI Conference on Human Factors in Computing Systems*, May 11, 2024. ACM, Honolulu HI USA, 1–14. https://doi.org/10.1145/3613904.3642299

[151] Alex Mazursky, Shan-Yuan Teng, Romain Nith, and Pedro Lopes. 2021. MagnetIO: Passive yet Interactive Soft Haptic Patches Anywhere. In *Proceedings of the 2021 CHI Conference on Human Factors in Computing Systems - CHI '21*, 2021. ACM Press, Yokohama, Japan, 1–15.

[152] Alex Mazursky, Shan-Yuan Teng, Romain Nith, and Pedro Lopes. 2021. MagnetIO: Passive yet Interactive Soft Haptic Patches Anywhere. In *Proceedings of the 2021 CHI Conference on Human Factors in Computing Systems*, May 06, 2021. ACM, Yokohama Japan, 1–15. https://doi.org/10.1145/3411764.3445543

[153] Jess McIntosh, Paul Strohmeier, Jarrod Knibbe, Sebastian Boring, and Kasper Hornbæk. 2019. Magnetips: Combining Fingertip Tracking and Haptic Feedback for Around-Device Interaction. In *Proceedings of the 2019 CHI Conference on Human Factors in Computing Systems - CHI '19*, 2019. ACM Press, Glasgow, Scotland Uk, 1–12. https://doi.org/10.1145/3290605.3300638

[154] Rochdi Merzouki (Ed.). 2013. *Intelligent mechatronic systems: modeling, control and diagnosis*. Springer, London ; New York.

[155] David J. Meyer, Michael Wiertlewski, Michael A. Peshkin, and J. Edward Colgate. 2014. Dynamics of ultrasonic and electrostatic friction modulation for rendering texture on haptic surfaces. In *2014 IEEE Haptics Symposium (HAPTICS)*, February 2014. IEEE, Houston, TX, USA, 63–67. https://doi.org/10.1109/HAPTICS.2014.6775434

[156] Viktor Miruchna, Robert Walter, David Lindlbauer, Maren Lehmann, Regine von Klitzing, and Jörg Müller. 2015. GelTouch: Localized Tactile Feedback Through Thin, Programmable Gel. In *Proceedings of the 28th Annual ACM Symposium on User Interface Software &*

Technology - UIST '15, 2015. ACM Press, Daegu, Kyungpook, Republic of Korea, 3–10. https://doi.org/10.1145/2807442.2807487

[157] Abhijeet Mishra, Piyush Kumar, Jainendra Shukla, and Aman Parnami. 2022. HaptiDrag: A Device with the Ability to Generate Varying Levels of Drag (Friction) Effects on Real Surfaces. *Proc. ACM Interact. Mob. Wearable Ubiquitous Technol.* 6, 3 (September 2022), 1–26. https://doi.org/10.1145/3550310

[158] Noor Mohammed, Rui Wang, Robert W. Jackson, Yeonsik Noh, Jeremy Gummeson, and Sunghoon Ivan Lee. 2021. ShaZam: Charge-Free Wearable Devices via Intra-Body Power Transfer from Everyday Objects. *Proc. ACM Interact. Mob. Wearable Ubiquitous Technol.* 5, 2 (June 2021), 1–25. https://doi.org/10.1145/3463505

[159] Jocelyn Monnoyer, Laurence Willemet, and Michaël Wiertlewski. 2023. Rapid change of friction causes the illusion of touching a receding surface. *J. R. Soc. Interface.* 20, 199 (February 2023), 20220718. https://doi.org/10.1098/rsif.2022.0718

[160] J. L. Monteith. 1981. Evaporation and surface temperature: EVAPORATION and SURFACE TEMPERATURE. *Q.J.R. Meteorol. Soc.* 107, 451 (January 1981), 1–27. https://doi.org/10.1002/qj.49710745102

[161] Rafael Morales González, Asier Marzo, Euan Freeman, William Frier, and Orestis Georgiou. 2021. UltraPower: Powering Tangible & Wearable Devices with Focused Ultrasound. In *Proceedings of the Fifteenth International Conference on Tangible, Embedded, and Embodied Interaction*, February 14, 2021. ACM, Salzburg Austria, 1–13. https://doi.org/10.1145/3430524.3440620

[162] Adiyan Mujibiya. 2015. Haptic feedback companion for Body Area Network using body-carried electrostatic charge. In *2015 IEEE International Conference on Consumer Electronics (ICCE)*, January 2015. IEEE, Las Vegas, NV, USA, 571–572. https://doi.org/10.1109/ICCE.2015.7066530

[163] Takaki Murakami, Tanner Person, Charith Lasantha Fernando, and Kouta Minamizawa. 2017. Altered touch: miniature haptic display with force, thermal and tactile feedback for augmented haptics. In *ACM SIGGRAPH 2017 Emerging Technologies*, July 30, 2017. ACM, Los Angeles California, 1–2. https://doi.org/10.1145/3084822.3084836

[164] Arshad Nasser, Taizhou Chen, Can Liu, Kening Zhu, and PVM Rao. 2020. FingerTalkie: Designing a Low-Cost Finger-Worn Device for Interactive Audio Labeling of Tactile Diagrams. In *Human-Computer Interaction. Multimodal and Natural Interaction* (*Lecture Notes in Computer Science*), 2020. Springer International Publishing, Cham, 475–496. https://doi.org/10.1007/978-3-030-49062-1_32

[165] Arshad Nasser, Kexin Zheng, and Kening Zhu. 2021. ThermEarhook: Investigating Spatial Thermal Haptic Feedback on the Auricular Skin Area. In *Proceedings of the 2021 International Conference on Multimodal Interaction*, October 18, 2021. ACM, Montréal QC Canada, 662–672. https://doi.org/10.1145/3462244.3479922

[166] Narihiro Nishimura, Daniel Leonardis, Massimiliano Solazzi, Antonio Frisoli, and Hiroyuki Kajimoto. 2014. Wearable encounter-type haptic device with 2-DoF motion and vibration for presentation of friction. In *2014 IEEE Haptics Symposium (HAPTICS)*,

February 2014. IEEE, Houston, TX, USA, 1–1. https://doi.org/10.1109/HAPTICS.2014.6775537

[167] Romain Nith, Shan-Yuan Teng, Pengyu Li, Yujie Tao, and Pedro Lopes. 2021. DextrEMS: Achieving Dexterity in Electrical Muscle Stimulation by Combining it with Brakes. In *Proceedings of the 34th Annual Symposium on User Interface Software and Technology* (*UIST '21*), October 10, 2021. Association for Computing Machinery, Virtual Event USA. Retrieved September 9, 2021 from https://programs.sigchi.org/uist/2021/program/content/61368

[168] Aditya Shekhar Nittala, Arshad Khan, Klaus Kruttwig, Tobias Kraus, and Jürgen Steimle. PhysioSkin: Rapid Fabrication of Skin-Conformal Physiological Interfaces. 10.

[169] Aditya Shekhar Nittala, Klaus Kruttwig, Jaeyeon Lee, Roland Bennewitz, Eduard Arzt, and Jürgen Steimle. 2019. Like A Second Skin: Understanding How Epidermal Devices Affect Human Tactile Perception. In *Proceedings of the 2019 CHI Conference on Human Factors in Computing Systems - CHI '19*, 2019. ACM Press, Glasgow, Scotland Uk, 1–16. https://doi.org/10.1145/3290605.3300610

[170] Aditya Shekhar Nittala, Anusha Withana, Narjes Pourjafarian, and Jürgen Steimle. 2018. Multi-Touch Skin: A Thin and Flexible Multi-Touch Sensor for On-Skin Input. In *Proceedings of the 2018 CHI Conference on Human Factors in Computing Systems - CHI '18*, 2018. ACM Press, Montreal QC, Canada, 1–12. https://doi.org/10.1145/3173574.3173607

[171] Katherine Nolan and Ellen Marmur. 2012. Moisturizers: Reality and the skin benefits: Moisturizers: reality and the skin benefits. *Dermatol Ther* 25, 3 (May 2012), 229–233. https://doi.org/10.1111/j.1529-8019.2012.01504.x

[172] Abigail Nolin, Kelly Pierson, Rainer Hlibok, Chun-Yuan Lo, Laure V. Kayser, and Charles Dhong. 2022. Controlling fine touch sensations with polymer tacticity and crystallinity. *Soft Matter* 18, 20 (2022), 3928–3940. https://doi.org/10.1039/D2SM00264G

[173] Yoshimune Nonomura, Takaharu Fujii, Yuichiro Arashi, Taku Miura, Takashi Maeno, Kaoru Tashiro, Yasuhisa Kamikawa, and Rie Monchi. 2009. Tactile impression and friction of water on human skin. *Colloids and Surfaces B: Biointerfaces* 69, 2 (March 2009), 264–267. https://doi.org/10.1016/j.colsurfb.2008.11.024

[174] Simon Olberding, Sergio Soto Ortega, Klaus Hildebrandt, and Jürgen Steimle. 2015. Foldio: Digital Fabrication of Interactive and Shape-Changing Objects With Foldable Printed Electronics. In *Proceedings of the 28th Annual ACM Symposium on User Interface Software & Technology - UIST '15*, 2015. ACM Press, Daegu, Kyungpook, Republic of Korea, 223–232. https://doi.org/10.1145/2807442.2807494

[175] Makoto Ono, Buntarou Shizuki, and Jiro Tanaka. 2013. Touch & activate: adding interactivity to existing objects using active acoustic sensing. In *Proceedings of the 26th annual ACM symposium on User interface software and technology - UIST '13*, 2013. ACM Press, St. Andrews, Scotland, United Kingdom, 31–40. https://doi.org/10.1145/2501988.2501989

[176] Jun Oohara, Hiroshi Kato, Yuki Hashimoto, and Hiroyuki Kajimoto. 2010. Presentation of Positional Information by Heat Phantom Sensation. In *Haptics: Generating and Perceiving*

Tangible Sensations, Astrid M. L. Kappers, Jan B. F. van Erp, Wouter M. Bergmann Tiest and Frans C. T. van der Helm (eds.). Springer Berlin Heidelberg, Berlin, Heidelberg, 445–450. https://doi.org/10.1007/978-3-642-14075-4_66

[177] Yukiko Osawa and Seiichiro Katsura. 2018. Wearable Thermal Interface for Sharing Palm Heat Conduction. In *IECON 2018 - 44th Annual Conference of the IEEE Industrial Electronics Society*, October 2018. IEEE, D.C., DC, USA, 3310–3315. https://doi.org/10.1109/IECON.2018.8591352

[178] Christopher Oshman, Qian Li, Li-Anne Liew, Ronggui Yang, Victor M Bright, and Y C Lee. 2013. Flat flexible polymer heat pipes. *J. Micromech. Microeng.* 23, 1 (January 2013), 015001. https://doi.org/10.1088/0960-1317/23/1/015001

[179] J. A. Paradiso, K. Hsiao, J. Strickon, J. Lifton, and A. Adler. 2000. Sensor systems for interactive surfaces. *IBM Syst. J.* 39, 3.4 (2000), 892–914. https://doi.org/10.1147/sj.393.0892

[180] J.A. Paradiso and T. Starner. 2005. Energy Scavenging for Mobile and Wireless Electronics. *IEEE Pervasive Comput.* 4, 1 (January 2005), 18–27. https://doi.org/10.1109/MPRV.2005.9

[181] Kaushik Parida, Hyunwoo Bark, and Pooi See Lee. 2021. Emerging Thermal Technology Enabled Augmented Reality. *Adv. Funct. Mater.* (February 2021), 2007952. https://doi.org/10.1002/adfm.202007952

[182] Fabrizio Pece, Juan Jose Zarate, Velko Vechev, Nadine Besse, Olexandr Gudozhnik, Herbert Shea, and Otmar Hilliges. 2017. MagTics: Flexible and Thin Form Factor Magnetic Actuators for Dynamic and Wearable Haptic Feedback. In *Proceedings of the 30th Annual ACM Symposium on User Interface Software and Technology - UIST '17*, 2017. ACM Press, Quebec City, QC, Canada, 143–154. https://doi.org/10.1145/3126594.3126609

[183] Fabrizio Pece, Juan Jose Zarate, Velko Vechev, Nadine Besse, Olexandr Gudozhnik, Herbert Shea, and Otmar Hilliges. 2017. MagTics: Flexible and Thin Form Factor Magnetic Actuators for Dynamic and Wearable Haptic Feedback. In *Proceedings of the 30th Annual ACM Symposium on User Interface Software and Technology - UIST '17*, 2017. ACM Press, Québec City, QC, Canada, 143–154. https://doi.org/10.1145/3126594.3126609

[184] Roshan Lalintha Peiris, Liwei Chan, and Kouta Minamizawa. 2018. LiquidReality: Wetness Sensations on the Face for Virtual Reality. In *Haptics: Science, Technology, and Applications*, Domenico Prattichizzo, Hiroyuki Shinoda, Hong Z. Tan, Emanuele Ruffaldi and Antonio Frisoli (eds.). Springer International Publishing, Cham, 366–378. https://doi.org/10.1007/978-3-319-93399-3_32

[185] Roshan Lalintha Peiris, Wei Peng, Zikun Chen, Liwei Chan, and Kouta Minamizawa. 2017. ThermoVR: Exploring Integrated Thermal Haptic Feedback with Head Mounted Displays. In *Proceedings of the 2017 CHI Conference on Human Factors in Computing Systems - CHI '17*, 2017. ACM Press, Denver, Colorado, USA, 5452–5456. https://doi.org/10.1145/3025453.3025824

[186] Roshan Lalitha Peiris, Yuan-Ling Feng, Liwei Chan, and Kouta Minamizawa. 2019. ThermalBracelet: Exploring Thermal Haptic Feedback Around the Wrist. In *Proceedings of*

the 2019 CHI Conference on Human Factors in Computing Systems, May 02, 2019. ACM, Glasgow Scotland Uk, 1–11. https://doi.org/10.1145/3290605.3300400

[187] Siina Pekkanen, Jani Väyrynen, Tuomas Lappalainen, Ashley Colley, and Jonna Häkkilä. 2019. Liquid slider: evaluating the experience of liquid on a touch input surface. In *Proceedings of the 18th International Conference on Mobile and Ubiquitous Multimedia*, November 26, 2019. ACM, Pisa Italy, 1–5. https://doi.org/10.1145/3365610.3368408

[188] Evan Pezent, Ali Israr, Majed Samad, Shea Robinson, Priyanshu Agarwal, Hrvoje Benko, and Nick Colonnese. 2019. Tasbi: Multisensory Squeeze and Vibrotactile Wrist Haptics for Augmented and Virtual Reality. In *2019 IEEE World Haptics Conference (WHC)*, July 2019. 1–6. https://doi.org/10.1109/WHC.2019.8816098

[189] Claudio S Pinhanez, Frederik C Kjeldsen, Anthony Levas, Gopal S Pingali, Mark E Podlaseck, and Paul B Chou. Ubiquitous Interactive Graphics.

[190] Sima Pirmoradi, Beth Ferguson, Gozde Goncu Berk, and Katia Vega. 2021. CJ-2050: Body Cooling Wearable Technology. In *2021 International Symposium on Wearable Computers*, September 21, 2021. ACM, Virtual USA, 207–210. https://doi.org/10.1145/3460421.3478826

[191] Valentin L. Popov. 2010. *Contact Mechanics and Friction*. Springer Berlin Heidelberg, Berlin, Heidelberg. https://doi.org/10.1007/978-3-642-10803-7

[192] Ivan Poupyrev and Shigeaki Maruyama. 2003. Tactile Interfaces for Small Touch Screens. In *Proceedings of the 16th annual ACM symposium on User interface software and technology*, 2003. 217–220.

[193] Ivan Poupyrev and Shigeaki Maruyama. 2003. Tactile interfaces for small touch screens. In *Proceedings of the 16th annual ACM symposium on User interface software and technology*, November 02, 2003. ACM, Vancouver Canada, 217–220. https://doi.org/10.1145/964696.964721

[194] Ivan Poupyrev, Shigeaki Maruyama, and Jun Rekimoto. 2002. Ambient touch: designing tactile interfaces for handheld devices. In *Proceedings of the 15th annual ACM symposium on User interface software and technology*, 2002. 51–60. https://doi.org/10.1145/571985.571993

[195] Pornthep Preechayasomboon and Eric Rombokas. 2021. Haplets: Finger-Worn Wireless and Low-Encumbrance Vibrotactile Haptic Feedback for Virtual and Augmented Reality. *Frontiers in Virtual Reality* 2, (2021), 121. https://doi.org/10.3389/frvir.2021.738613

[196] Thomas Preindl, Cedric Honnet, Andreas Pointner, Roland Aigner, Joseph A. Paradiso, and Michael Haller. 2020. Sonoflex: Embroidered Speakers Without Permanent Magnets. In *Proceedings of the 33rd Annual ACM Symposium on User Interface Software and Technology*, October 20, 2020. ACM, Virtual Event USA, 675–685. https://doi.org/10.1145/3379337.3415888

[197] W.R. Provancher and N.D. Sylvester. 2009. Fingerpad Skin Stretch Increases the Perception of Virtual Friction. *IEEE Trans. Haptics* 2, 4 (October 2009), 212–223. https://doi.org/10.1109/TOH.2009.34

[198] Purnendu, Jess Hartcher-O'Brien, Vatsal Mehta, Nicholas Colonnese, Aakar Gupta, Carson J. Bruns, and Priyanshu Agarwal. 2023. Fingertip Wearable High-resolution Electrohydraulic Interface for Multimodal Haptics. In *2023 IEEE World Haptics Conference (WHC)*, July 10, 2023. IEEE, Delft, Netherlands, 299–305. https://doi.org/10.1109/WHC56415.2023.10224383

[199] Isabel P. S. Qamar, Rainer Groh, David Holman, and Anne Roudaut. 2018. HCI meets material science: a literature review of morphing materials for the design of shape-changing interfaces. In *Proceedings of the 2018 CHI Conference on Human Factors in Computing Systems - CHI '18*, 2018. 1–23. https://doi.org/10.1145/3173574.3173948

[200] Kirill Ragozin, Dingding Zheng, George Chernyshov, and Danny Hynds. 2020. Sophroneo: Fear not. A VR Horror Game with Thermal Feedback and Physiological Signal Loop. In *Extended Abstracts of the 2020 CHI Conference on Human Factors in Computing Systems*, April 25, 2020. ACM, Honolulu HI USA, 1–6. https://doi.org/10.1145/3334480.3381659

[201] Ramesh Raskar, Greg Welch, Kok-Lim Low, and Deepak Bandyopadhyay. 2001. Shader Lamps: Animating Real Objects With Image-Based Illumination. In *Rendering Techniques 2001*, Steven J. Gortler and Karol Myszkowski (eds.). Springer Vienna, Vienna, 89–102. https://doi.org/10.1007/978-3-7091-6242-2_9

[202] Bradley A. Reese and Charles R. Sullivan. 2017. Litz wire in the MHz range: Modeling and improved designs. In *2017 IEEE 18th Workshop on Control and Modeling for Power Electronics (COMPEL)*, July 2017. 1–8. https://doi.org/10.1109/COMPEL.2017.8013391

[203] Jun Rekimoto. 2014. Traxion: a tactile interaction device with virtual force sensation. In *ACM SIGGRAPH 2014 Emerging Technologies*, July 27, 2014. ACM, Vancouver Canada, 1–1. https://doi.org/10.1145/2614066.2614079

[204] R. F. Remler. 1923. The Solvent Properties of Acetone. *Ind. Eng. Chem.* 15, 7 (July 1923), 717–720. https://doi.org/10.1021/ie50163a023

[205] Hendrik Richter, Doris Hausen, Sven Osterwald, and Andreas Butz. Reproducing materials of virtual elements on touchscreens using supplemental thermal feedback. 8.

[206] Hendrik Richter, Felix Manke, and Moriel Seror. 2013. LiquiTouch: liquid as a medium for versatile tactile feedback on touch surfaces. In *Proceedings of the 7th International Conference on Tangible, Embedded and Embodied Interaction*, February 10, 2013. ACM, Barcelona Spain, 315–318. https://doi.org/10.1145/2460625.2460678

[207] Robert Rissmann, Marion H. M. Oudshoorn, Wim E. Hennink, Maria Ponec, and Joke A. Bouwstra. 2009. Skin barrier disruption by acetone: observations in a hairless mouse skin model. *Arch Dermatol Res* 301, 8 (September 2009), 609–613. https://doi.org/10.1007/s00403-009-0946-6

[208] Rocco Rizzo, Antonino Musolino, and Lynette A. Jones. 2018. Shape Localization and Recognition Using a Magnetorheological-Fluid Haptic Display. *IEEE Trans. Haptics* 11, 2 (April 2018), 317–321. https://doi.org/10.1109/TOH.2017.2771420

[209] Steeven Villa Salazar, Claudio Pacchierotti, Xavier de Tinguy, Anderson Maciel, and Maud Marchal. 2020. Altering the Stiffness, Friction, and Shape Perception of Tangible

Objects in Virtual Reality Using Wearable Haptics. *IEEE Trans. Haptics* 13, 1 (January 2020), 167–174. https://doi.org/10.1109/TOH.2020.2967389

[210] Alanson P. Sample, Benjamin H. Waters, Scott T. Wisdom, and Joshua R. Smith. 2013. Enabling Seamless Wireless Power Delivery in Dynamic Environments. *Proc. IEEE* 101, 6 (June 2013), 1343–1358. https://doi.org/10.1109/JPROC.2013.2252453

[211] Mine Sarac, Allison M. Okamura, and Massimiliano Di Luca. 2019. Effects of Haptic Feedback on the Wrist during Virtual Manipulation. *arXiv:1911.02104 [cs]* (November 2019). Retrieved March 23, 2022 from http://arxiv.org/abs/1911.02104

[212] Takuya Sasatani, Chouchang Jack Yang, Matthew J. Chabalko, Yoshihiro Kawahara, and Alanson P. Sample. 2018. Room-Wide Wireless Charging and Load-Modulation Communication via Quasistatic Cavity Resonance. *Proc. ACM Interact. Mob. Wearable Ubiquitous Technol.* 2, 4 (December 2018), 1–23. https://doi.org/10.1145/3287066

[213] Katsunari Sato. 2016. Augmentation of Thermal Sensation on Finger Pad Using Stimuli for Finger Side. In *Haptics: Perception, Devices, Control, and Applications*, 2016. Springer International Publishing, Cham, 512–520.

[214] Katsunari Sato, Takashi Maeno, and Keio University, 4-1-1 Hiyoshi, Kohoku-ku, Yokohama 223-8526, Japan. 2013. Presentation of Rapid Temperature Change Using Spatially Divided Hot and Cold Stimuli. *J. Robot. Mechatron.* 25, 3 (June 2013), 497–505. https://doi.org/10.20965/jrm.2013.p0497

[215] Katsunari Sato and Susumu Tachi. 2010. Design of electrotactile stimulation to represent distribution of force vectors. In *2010 IEEE Haptics Symposium*, March 2010. IEEE, Waltham, MA, USA, 121–128. https://doi.org/10.1109/HAPTIC.2010.5444666

[216] Munehiko Sato, Ivan Poupyrev, and Chris Harrison. 2012. Touché: enhancing touch interaction on humans, screens, liquids, and everyday objects. In *Proceedings of the 2012 ACM annual conference on Human Factors in Computing Systems - CHI '12*, 2012. ACM Press, Austin, Texas, USA, 483. https://doi.org/10.1145/2207676.2207743

[217] M. Satyanarayanan. 2001. Pervasive computing: vision and challenges. *IEEE Pers. Commun.* 8, 4 (August 2001), 10–17. https://doi.org/10.1109/98.943998

[218] Valkyrie Savage, Xiaohan Zhang, and Björn Hartmann. 2012. Midas: fabricating custom capacitive touch sensors to prototype interactive objects. In *Proceedings of the 25th annual ACM symposium on User interface software and technology - UIST '12*, 2012. ACM Press, Cambridge, Massachusetts, USA, 579. https://doi.org/10.1145/2380116.2380189

[219] Samuel Benjamin Schorr and Allison M. Okamura. 2017. Three-Dimensional Skin Deformation as Force Substitution: Wearable Device Design and Performance During Haptic Exploration of Virtual Environments. *IEEE Trans. Haptics* 10, 3 (July 2017), 418–430. https://doi.org/10.1109/TOH.2017.2672969

[220] Y. Sekiguchi, K. Hirota, and M. Hirose. 2005. The Design and Implementation of Ubiquitous Haptic Device. In *First Joint Eurohaptics Conference and Symposium on Haptic Interfaces for Virtual Environment and Teleoperator Systems*, 2005. IEEE, Pisa, Italy, 527–528. https://doi.org/10.1109/WHC.2005.128

[221] Lixin Shi, Zachary Kabelac, Dina Katabi, and David Perreault. 2015. Wireless Power Hotspot that Charges All of Your Devices. In *Proceedings of the 21st Annual International Conference on Mobile Computing and Networking*, September 07, 2015. ACM, Paris France, 2–13. https://doi.org/10.1145/2789168.2790092

[222] Rishi Shukla, Neev Kiran, Rui Wang, Jeremy Gummeson, and Sunghoon Ivan Lee. 2019. SkinnyPower: enabling batteryless wearable sensors via intra-body power transfer. In *Proceedings of the 17th Conference on Embedded Networked Sensor Systems*, November 10, 2019. ACM, New York New York, 68–82. https://doi.org/10.1145/3356250.3360034

[223] Craig D. Shultz, Michael A. Peshkin, and J. Edward Colgate. 2015. Surface haptics via electroadhesion: Expanding electrovibration with Johnsen and Rahbek. In *2015 IEEE World Haptics Conference (WHC)*, June 2015. IEEE, Evanston, IL, 57–62. https://doi.org/10.1109/WHC.2015.7177691

[224] Craig D. Shultz, Michael A. Peshkin, and J. Edward Colgate. 2018. On the electrical characterization of electroadhesive displays and the prominent interfacial gap impedance associated with sliding fingertips. In *2018 IEEE Haptics Symposium (HAPTICS)*, March 2018. IEEE, San Francisco, CA, 151–157. https://doi.org/10.1109/HAPTICS.2018.8357168

[225] Yatharth Singhal, Haokun Wang, Hyunjae Gil, and Jin Ryong Kim. 2021. Mid-Air Thermo-Tactile Feedback using Ultrasound Haptic Display. In *Proceedings of the 27th ACM Symposium on Virtual Reality Software and Technology*, December 08, 2021. ACM, Osaka Japan, 1–11. https://doi.org/10.1145/3489849.3489889

[226] Mel Slater and Sylvia Wilbur. 1997. A Framework for Immersive Virtual Environments (FIVE): Speculations on the Role of Presence in Virtual Environments. *Presence: Teleoperators & Virtual Environments* 6, 6 (December 1997), 603–616. https://doi.org/10.1162/pres.1997.6.6.603

[227] Cem Som and Michael De Rooij. 2019. *Trilogy of wireless power transfer: basic principles, WPT Systems and application* (1st edition ed.). Swiridoff Verlag, Künzelsau.

[228] Hyungki Son, Inwook Hwang, Tae-Heon Yang, Seungmoon Choi, Sang-Youn Kim, and Jin Ryong Kim. 2019. RealWalk: Haptic Shoes Using Actuated MR Fluid for Walking in VR. In *2019 IEEE World Haptics Conference (WHC)*, July 2019. IEEE, Tokyo, Japan, 241–246. https://doi.org/10.1109/WHC.2019.8816165

[229] Gábor Sörös, Stephan Semmler, Luc Humair, and Otmar Hilliges. 2015. Fast blur removal for wearable QR code scanners. In *Proceedings of the 2015 ACM International Symposium on Wearable Computers - ISWC '15*, 2015. ACM Press, Osaka, Japan, 117–124. https://doi.org/10.1145/2802083.2808390

[230] T.E. Starner. 2003. Powerful change. 1. Batteries and possible alternatives for the mobile market. *IEEE Pervasive Comput.* 2, 4 (October 2003), 86–88. https://doi.org/10.1109/MPRV.2003.1251172

[231] Jürgen Steimle. 2009. Designing pen-and-paper user interfaces for interaction with documents. In *Proceedings of the 3rd International Conference on Tangible and Embedded Interaction - TEI '09*, 2009. ACM Press, Cambridge, United Kingdom, 197. https://doi.org/10.1145/1517664.1517707

[232] Charalampos A. Stergiou and Vassilis Zaspalis. 2016. Impact of Ferrite Shield Properties on the Low-Power Inductive Power Transfer. *IEEE Trans. Magn.* 52, 8 (August 2016), 1–9. https://doi.org/10.1109/TMAG.2016.2536669

[233] Robert S Stormont, Gareth R Davies, P James Ross, David J Lurie, and Lionel M Broche. 2023. A flexible 8.5 MHz litz wire receive array for field-cycling imaging. *Phys. Med. Biol.* 68, 5 (March 2023), 055016. https://doi.org/10.1088/1361-6560/acb9d0

[234] Patrick L. Strandholt, Oana A. Dogaru, Niels C. Nilsson, Rolf Nordahl, and Stefania Serafin. 2020. Knock on Wood: Combining Redirected Touching and Physical Props for Tool-Based Interaction in Virtual Reality. In *Proceedings of the 2020 CHI Conference on Human Factors in Computing Systems*, April 21, 2020. ACM, Honolulu HI USA, 1–13. https://doi.org/10.1145/3313831.3376303

[235] Evan Strasnick, Jackie Yang, Kesler Tanner, Alex Olwal, and Sean Follmer. 2017. shiftIO: Reconfigurable Tactile Elements for Dynamic Affordances and Mobile Interaction. In *Proceedings of the 2017 CHI Conference on Human Factors in Computing Systems - CHI '17*, 2017. ACM Press, Denver, Colorado, USA, 5075–5086. https://doi.org/10.1145/3025453.3025988

[236] Paul Strohmeier and Jess McIntosh. 2020. Novel Input and Output opportunities using an Implanted Magnet. In *Proceedings of the Augmented Humans International Conference*, March 16, 2020. ACM, Kaiserslautern Germany, 1–5. https://doi.org/10.1145/3384657.3384785

[237] Yuning Su, Yuhua Jin, Zhengqing Wang, Yonghao Shi, Da-Yuan Huang, Teng Han, and Xing-Dong Yang. 2023. Laser-Powered Vibrotactile Rendering. *Proc. ACM Interact. Mob. Wearable Ubiquitous Technol.* 7, 4 (December 2023), 1–25. https://doi.org/10.1145/3631449

[238] D. Tabor. 1981. The Role of Surface and Intermolecular Forces in Thin Film Lubrication. In *Tribology Series*. Elsevier, 651–682. https://doi.org/10.1016/S0167-8922(08)70913-1

[239] Ryo Takahashi, Masaaki Fukumoto, Changyo Han, Takuya Sasatani, Yoshiaki Narusue, and Yoshihiro Kawahara. 2020. TelemetRing: A Batteryless and Wireless Ring-shaped Keyboard using Passive Inductive Telemetry. In *Proceedings of the 33rd Annual ACM Symposium on User Interface Software and Technology*, October 20, 2020. ACM, Virtual Event USA, 1161–1168. https://doi.org/10.1145/3379337.3415873

[240] Ryo Takahashi, Wakako Yukita, Takuya Sasatani, Tomoyuki Yokota, Takao Someya, and Yoshihiro Kawahara. 2021. Twin Meander Coil: Sensitive Readout of Battery-free On-body Wireless Sensors Using Body-scale Meander Coils. *Proc. ACM Interact. Mob. Wearable Ubiquitous Technol.* 5, 4 (December 2021), 1–21. https://doi.org/10.1145/3494996

[241] Ryo Takahashi, Wakako Yukita, Tomoyuki Yokota, Takao Someya, and Yoshihiro Kawahara. 2022. Meander Coil++: A Body-scale Wireless Power Transmission Using Safe-to-body and Energy-efficient Transmitter Coil. In *CHI Conference on Human Factors in Computing Systems*, April 29, 2022. ACM, New Orleans LA USA, 1–12. https://doi.org/10.1145/3491102.3502119

[242] Daniel W. Tan, Matthew A. Schiefer, Michael W. Keith, James Robert Anderson, Joyce Tyler, and Dustin J. Tyler. 2014. A neural interface provides long-term stable natural touch

perception. *Sci. Transl. Med.* 6, 257 (October 2014). https://doi.org/10.1126/scitranslmed.3008669

[243] Yujie Tao, Shan-Yuan Teng, and Pedro Lopes. 2021. Altering Perceived Softness of Real Rigid Objects by Restricting Fingerpad Deformation. In *The 34th Annual ACM Symposium on User Interface Software and Technology*, October 10, 2021. ACM, Virtual Event USA, 985–996. https://doi.org/10.1145/3472749.3474800

[244] Ramona Tasar, Cornelia Wiegand, and Peter Elsner. 2021. How irritant are n-propanol and isopropanol? – A systematic review. *Contact Dermatitis* 84, 1 (January 2021), 1–14. https://doi.org/10.1111/cod.13722

[245] Craig L. Taylor and Robert J. Schwartz. 1955. The Anatomy and Mechanics of the Human Hand. *Artificial Limbs* 2, 2 (1955), 22–35.

[246] Chin-Hung Teng and Bing-Shiun Wu. 2012. Developing QR Code Based Augmented Reality Using SIFT Features. In *2012 9th International Conference on Ubiquitous Intelligence and Computing and 9th International Conference on Autonomic and Trusted Computing*, September 2012. IEEE, Fukuoka, Japan, 985–990. https://doi.org/10.1109/UIC-ATC.2012.56

[247] Shan-Yuan Teng, Tzu-Sheng Kuo, Chi Wang, Chi-huan Chiang, Da-Yuan Huang, Liwei Chan, and Bing-Yu Chen. 2018. PuPoP: Pop-up Prop on Palm for Virtual Reality. In *The 31st Annual ACM Symposium on User Interface Software and Technology - UIST '18*, 2018. ACM Press, Berlin, Germany, 5–17. https://doi.org/10.1145/3242587.3242628

[248] Shan-Yuan Teng, Tzu-Sheng Kuo, Chi Wang, Chi-huan Chiang, Da-Yuan Huang, Liwei Chan, and Bing-Yu Chen. 2018. PuPoP: Pop-up Prop on Palm for Virtual Reality. In *The 31st Annual ACM Symposium on User Interface Software and Technology - UIST '18*, 2018. ACM Press, Berlin, Germany, 5–17. https://doi.org/10.1145/3242587.3242628

[249] Shan-Yuan Teng, Pengyu Li, Romain Nith, Joshua Fonseca, and Pedro Lopes. 2021. Touch&Fold: A Foldable Haptic Actuator for Rendering Touch in Mixed Reality. In *Proceedings of the 2021 CHI Conference on Human Factors in Computing Systems* (*CHI '21*), 6 2021. Association for Computing Machinery, New York, NY, USA, 1–14. https://doi.org/10.1145/3411764.3445099

[250] Shan-Yuan Teng, Cheng-Lung Lin, Chi-huan Chiang, Tzu-Sheng Kuo, Liwei Chan, Da-Yuan Huang, and Bing-Yu Chen. 2019. TilePoP: Tile-type Pop-up Prop for Virtual Reality. In *Proceedings of the 32nd Annual ACM Symposium on User Interface Software and Technology*, October 17, 2019. ACM, New Orleans LA USA, 639–649. https://doi.org/10.1145/3332165.3347958

[251] Shan-Yuan Teng, K. D. Wu, Jacqueline Chen, and Pedro Lopes. 2022. Prolonging VR Haptic Experiences by Harvesting Kinetic Energy from the User. In *Proceedings of the 35th Annual ACM Symposium on User Interface Software and Technology*, October 29, 2022. ACM, Bend OR USA, 1–18. https://doi.org/10.1145/3526113.3545635

[252] Shan-Yuan Teng, K. D. Wu, Jacqueline Chen, and Pedro Lopes. 2022. Prolonging VR Haptic Experiences by Harvesting Kinetic Energy from the User. In *Proceedings of the 35th Annual ACM Symposium on User Interface Software and Technology*, October 29, 2022. ACM, Bend OR USA, 1–18. https://doi.org/10.1145/3526113.3545635

[253] Thoams Guthrie Zimmerman, T. G. Zimmerman, and Thomas G. Zimmerman. 1996. Personal area networks: near-field intrabody communication. *Ibm Systems Journal* 35, 3 (September 1996), 609–617. https://doi.org/10.1147/sj.353.0609

[254] Chih-An Tsao, Tzu-Chun Wu, Hsin-Ruey Tsai, Tzu-Yun Wei, Fang-Ying Liao, Sean Chapman, and Bing-Yu Chen. 2022. FrictShoes: Providing Multilevel Nonuniform Friction Feedback on Shoes in VR. *IEEE Transactions on Visualization and Computer Graphics* 28, 5 (May 2022), 2026–2036. https://doi.org/10.1109/TVCG.2022.3150492

[255] Jessica Tsimeris, Colin Dedman, Michael Broughton, and Tom Gedeon. 2013. ForceForm: a dynamically deformable interactive surface. In *Proceedings of the 2013 ACM international conference on Interactive tabletops and surfaces - ITS '13*, 2013. ACM Press, St. Andrews, Scotland, United Kingdom, 175–178. https://doi.org/10.1145/2512349.2512807

[256] Muhammad Umair, Corina Sas, and Miquel Alfaras. 2020. ThermoPixels: Toolkit for Personalizing Arousal-based Interfaces through Hybrid Crafting. In *Proceedings of the 2020 ACM Designing Interactive Systems Conference*, July 03, 2020. ACM, Eindhoven Netherlands, 1017–1032. https://doi.org/10.1145/3357236.3395512

[257] Unknown. 2003. The actuated workbench: computer-controlled actuation in tabletop tangible interfaces. In *ACM SIGGRAPH 2003 Papers on - SIGGRAPH '03*, 2003. ACM Press, San Diego, California, 699. https://doi.org/10.1145/1201775.882330

[258] Keigo Ushiyama and Pedro Lopes. 2023. FeetThrough: Electrotactile Foot Interface that Preserves Real-World Sensations. In *Proceedings of the 36th Annual ACM Symposium on User Interface Software and Technology*, October 29, 2023. ACM, San Francisco CA USA, 1–11. https://doi.org/10.1145/3586183.3606808

[259] Virag Varga, Gergely Vakulya, Alanson Sample, and Thomas R. Gross. 2018. Enabling Interactive Infrastructure with Body Channel Communication. *Proc. ACM Interact. Mob. Wearable Ubiquitous Technol.* 1, 4 (January 2018), 1–29. https://doi.org/10.1145/3161180

[260] Amit Vasudevan and Sagar Chaki. 2018. Have Your PI and Eat it Too: Practical Security on a Low-Cost Ubiquitous Computing Platform. In *2018 IEEE European Symposium on Security and Privacy (EuroS&P)*, April 2018. IEEE, London, 183–198. https://doi.org/10.1109/EuroSP.2018.00021

[261] Marynel Vázquez, Eric Brockmeyer, Ruta Desai, Chris Harrison, and Scott E. Hudson. 2015. 3D Printing Pneumatic Device Controls with Variable Activation Force Capabilities. In *Proceedings of the 33rd Annual ACM Conference on Human Factors in Computing Systems - CHI '15*, 2015. ACM Press, Seoul, Republic of Korea, 1295–1304. https://doi.org/10.1145/2702123.2702569

[262] Velko Vechev, Juan Zarate, David Lindlbauer, Ronan Hinchet, Herbert Shea, and Otmar Hilliges. 2019. TacTiles: Dual-Mode Low-Power Electromagnetic Actuators for Rendering Continuous Contact and Spatial Haptic Patterns in VR. Spring 2019. 312–320. https://doi.org/10.1109/VR.2019.8797921

[263] Ronald T. Verrillo. 1992. Vibration Sensation in Humans. *Music Perception* 9, 3 (April 1992), 281–302. https://doi.org/10.2307/40285553

[264] Dries van Wageningen and Toine Staring. 2010. The Qi wireless power standard. In *Proceedings of 14th International Power Electronics and Motion Control Conference EPE-*

PEMC 2010, September 2010. S15-25-S15-32. https://doi.org/10.1109/EPEPEMC.2010.5606673

[265] Feng Wang and Xiangshi Ren. 2009. Empirical evaluation for finger input properties in multi-touch interaction. In *Proceedings of the 27th international conference on Human factors in computing systems - CHI 09*, 2009. ACM Press, Boston, MA, USA, 1063. https://doi.org/10.1145/1518701.1518864

[266] Ruican Wang and Richard W. Hartel. 2021. Understanding stickiness in sugar-rich food systems: A review of mechanisms, analyses, and solutions of adhesion. *Comprehensive Reviews in Food Science and Food Safety* 20, 6 (November 2021), 5901–5937. https://doi.org/10.1111/1541-4337.12833

[267] R. Want. 2004. Enabling ubiquitous sensing with RFID. *Computer* 37, 4 (April 2004), 84–86. https://doi.org/10.1109/MC.2004.1297315

[268] Benjamin H. Waters, Brody J. Mahoney, Gunbok Lee, and Joshua R. Smith. 2014. Optimal coil size ratios for wireless power transfer applications. In *2014 IEEE International Symposium on Circuits and Systems (ISCAS)*, June 2014. IEEE, Melbourne VIC, Australia, 2045–2048. https://doi.org/10.1109/ISCAS.2014.6865567

[269] Martin Weigel, Tong Lu, Gilles Bailly, Antti Oulasvirta, Carmel Majidi, and Jürgen Steimle. 2015. iSkin: Flexible, Stretchable and Visually Customizable On-Body Touch Sensors for Mobile Computing. In *Proceedings of the 33rd Annual ACM Conference on Human Factors in Computing Systems - CHI '15*, 2015. ACM Press, Seoul, Republic of Korea, 2991–3000. https://doi.org/10.1145/2702123.2702391

[270] Mark Weiser. 1999. The computer for the 21 st century. *SIGMOBILE Mob. Comput. Commun. Rev.* 3, 3 (July 1999), 3–11. https://doi.org/10.1145/329124.329126

[271] Mark Weiser. The Computer for the 21st Century. 8.

[272] Malte Weiss, Chat Wacharamanotham, Simon Voelker, and Jan Borchers. 2011. FingerFlux: near-surface haptic feedback on tabletops. In *Proceedings of the 24th annual ACM symposium on User interface software and technology - UIST '11*, 2011. ACM Press, Santa Barbara, California, USA, 615. https://doi.org/10.1145/2047196.2047277

[273] Michael Wessely, Ticha Sethapakdi, Carlos Castillo, Jackson C. Snowden, Ollie Hanton, Isabel P. S. Qamar, Mike Fraser, Anne Roudaut, and Stefanie Mueller. 2020. Sprayable User Interfaces: Prototyping Large-Scale Interactive Surfaces with Sensors and Displays. In *Proceedings of the 2020 CHI Conference on Human Factors in Computing Systems*, April 21, 2020. ACM, Honolulu HI USA, 1–12. https://doi.org/10.1145/3313831.3376249

[274] Reto Wettach, Christian Behrens, Adam Danielsson, and Thomas Ness. 2007. A thermal information display for mobile applications. In *Proceedings of the 9th international conference on Human computer interaction with mobile devices and services - MobileHCI '07*, 2007. ACM Press, Singapore, 182–185. https://doi.org/10.1145/1377999.1378004

[275] Michael White, James Gain, Ulysse Vimont, and Daniel Lochner. 2019. The Case for Haptic Props: Shape, Weight and Vibro-tactile Feedback. In *Motion, Interaction and Games*, October 28, 2019. ACM, Newcastle upon Tyne United Kingdom, 1–10. https://doi.org/10.1145/3359566.3360058

[276] Laurence Willemet, Khoubeib Kanzari, Jocelyn Monnoyer, Ingvars Birznieks, and Michaël Wiertlewski. 2021. Initial contact shapes the perception of friction. *Proc Natl Acad Sci USA* 118, 49 (December 2021), e2109109118. https://doi.org/10.1073/pnas.2109109118

[277] Raphael Wimmer and Patrick Baudisch. 2011. Modular and deformable touch-sensitive surfaces based on time domain reflectometry. In *Proceedings of the 24th annual ACM symposium on User interface software and technology - UIST '11*, 2011. ACM Press, Santa Barbara, California, USA, 517. https://doi.org/10.1145/2047196.2047264

[278] Laura Winfield, John Glassmire, J. Edward Colgate, and Michael Peshkin. 2007. T-PaD: Tactile Pattern Display through Variable Friction Reduction. In *Second Joint EuroHaptics Conference and Symposium on Haptic Interfaces for Virtual Environment and Teleoperator Systems (WHC'07)*, March 2007. IEEE, Tsukuba, Japan, 421–426. https://doi.org/10.1109/WHC.2007.105

[279] Anusha Withana, Daniel Groeger, and Jürgen Steimle. 2018. Tacttoo: A Thin and Feel-Through Tattoo for On-Skin Tactile Output. In *The 31st Annual ACM Symposium on User Interface Software and Technology - UIST '18*, 2018. ACM Press, Berlin, Germany, 365–378. https://doi.org/10.1145/3242587.3242645

[280] Paul Worgan and Mike Fraser. 2017. CoilMove: An Actuated to-body Energy Transfer System. In *Proceedings of the 2017 Conference on Designing Interactive Systems*, June 10, 2017. ACM, Edinburgh United Kingdom, 791–795. https://doi.org/10.1145/3064663.3064693

[281] Paul Worgan, Jarrod Knibbe, Mike Fraser, and Diego Martinez Plasencia. 2016. PowerShake: Power Transfer Interactions for Mobile Devices. In *Proceedings of the 2016 CHI Conference on Human Factors in Computing Systems*, May 07, 2016. ACM, San Jose California USA, 4734–4745. https://doi.org/10.1145/2858036.2858569

[282] Robert Xiao, Chris Harrison, and Scott E Hudson. WorldKit: Rapid and Easy Creation of Ad-hoc Interactive Applications on Everyday Surfaces. 10.

[283] Zhi-Wei Xing, Miao Yu, Jie Fu, Yuan Wang, and Lu-Jie Zhao. 2015. A laminated magnetorheological elastomer bearing prototype for seismic mitigation of bridge superstructures. *Journal of Intelligent Material Systems and Structures* 26, 14 (September 2015), 1818–1825. https://doi.org/10.1177/1045389X15577654

[284] Xinge Yu, Xinge Yu, Zhaoqian Xie, Zhaoqian Xie, Yang Yu, Yang Yu, Jungyup Lee, Jungyup Lee, Abraham Vázquez-Guardado, Abraham Vázquez-Guardado, Haiwen Luan, Haiwen Luan, Jasper Ruban, Jasper Ruban, Xin Ning, Xin Ning, Aadeel Akhtar, Aadeel Akhtar, Dengfeng Li, Dengfeng Li, Bowen Ji, Bowen Ji, Bowen Ji, Yiming Liu, Yiming Liu, Rujie Sun, Rujie Sun, Jingyue Cao, Jingyue Cao, Qingze Huo, Qingze Huo, Yuncheng Zhong, Yishan Zhong, Chan Mi Lee, ChanMi Lee, Chan Mi Lee, Seung Yeop Kim, Seung Yeop Kim, Philipp Gutruf, Philipp Gutruf, Changxing Zhang, Changxing Zhang, Changxing Zhang, Changxing Zhang, Yeguang Xue, Yeguang Xue, Qinglei Guo, Qinglei Guo, Aditya Chempakasseril, Aditya Chempakasseril, Peilin Tian, Peilin Tian, Wei Lü, Wei Lu, Ji Yoon Jeong, JiYoon Jeong, Ji Yoon Jeong, Yong Yu, Yongjoon Yu, Yong Joon Yu, Jesse Cornman, Jesse Cornman, Chee Sim Tan, Chee Sim Tan, Bong Hoon Kim, BongHoon Kim, Bong Hoon Kim, Kun Hyuk Lee, Kun Hyuk Lee, Xue Feng, Xue Feng, Xue Feng, Yonggang Huang, Yonggang Huang, Jinghua Li, and John A. Rogers. 2019. Skin-integrated wireless

haptic interfaces for virtual and augmented reality. *Nature* 575, 7783 (November 2019), 473–479. https://doi.org/10.1038/s41586-019-1687-0

[285] Tianqi Xu, Jiachen Zhang, Mohammad Salehizadeh, Onaizah Onaizah, and Eric Diller. 2019. Millimeter-scale flexible robots with programmable three-dimensional magnetization and motions. *Sci. Robot.* 4, 29 (April 2019), eaav4494. https://doi.org/10.1126/scirobotics.aav4494

[286] Chao Yang, Chengyi Song, Wen Shang, Peng Tao, and Tao Deng. 2015. Flexible heat pipes with integrated bioinspired design. *Progress in Natural Science: Materials International* 25, 1 (February 2015), 51–57. https://doi.org/10.1016/j.pnsc.2015.01.011

[287] Tae Heon Yang and Jeong Hoi Koo. 2017. Experimental evaluation of a miniature MR device for a wide range of human perceivable haptic sensations. *Smart Materials and Structures* 26, 12 (2017), 1–12. https://doi.org/10.1088/1361-665X/aa934a

[288] Xiaoying Yang, Jacob Sayono, Jess Xu, and Yang Zhang. 2024. Interaction-Power Stations: Turning Environments into Ubiquitous Power Stations for Charging Wearables. In *Extended Abstracts of the CHI Conference on Human Factors in Computing Systems*, May 02, 2024. ACM, Honolulu HI USA, 1–8. https://doi.org/10.1145/3613905.3650769

[289] Kentaro Yasu. 2017. Magnetic Plotter: A Macrotexture Design Method Using Magnetic Rubber Sheets. In *Proceedings of the 2017 CHI Conference on Human Factors in Computing Systems - CHI '17*, 2017. ACM Press, Denver, Colorado, USA, 4983–4993. https://doi.org/10.1145/3025453.3025702

[290] Kentaro Yasu. 2019. Magnetact: Magnetic-sheet-based Haptic Interfaces for Touch Devices. (2019), 8.

[291] Kentaro Yasu and Yuichiro Katsumoto. 2015. Bump ahead: easy-to-design haptic surface using magnet array. In *SIGGRAPH Asia 2015 Emerging Technologies on - SA '15*, 2015. ACM Press, Kobe, Japan, 1–3. https://doi.org/10.1145/2818466.2818478

[292] Koji Yatani and Khai Nhut Truong. 2009. SemFeel: a user interface with semantic tactile feedback for mobile touch-screen devices. In *Proceedings of the 22nd annual ACM symposium on User interface software and technology - UIST '09*, 2009. ACM Press, Victoria, BC, Canada, 111. https://doi.org/10.1145/1622176.1622198

[293] Huizhong Ye, Chi-Jung Lee, Te-Yen Wu, Xing-Dong Yang, Bing-Yu Chen, and Rong-Hao Liang. 2022. Body-Centric NFC: Body-Centric Interaction with NFC Devices Through Near-Field Enabled Clothing. In *Designing Interactive Systems Conference*, June 13, 2022. ACM, Virtual Event Australia, 1626–1639. https://doi.org/10.1145/3532106.3534569

[294] Vibol Yem and Hiroyuki Kajimoto. 2017. Wearable tactile device using mechanical and electrical stimulation for fingertip interaction with virtual world. In *2017 IEEE Virtual Reality (VR)*, March 2017. 99–104. https://doi.org/10.1109/VR.2017.7892236

[295] Sang Ho Yoon, Siyuan Ma, Woo Suk Lee, Shantanu Thakurdesai, Di Sun, Flávio P. Ribeiro, and James D. Holbery. 2019. HapSense: A Soft Haptic I/O Device with Uninterrupted Dual Functionalities of Force Sensing and Vibrotactile Actuation. In *Proceedings of the 32nd Annual ACM Symposium on User Interface Software and Technology*, October 17, 2019. ACM, New Orleans LA USA, 949–961. https://doi.org/10.1145/3332165.3347888

[296] Andre Zenner, Kristin Ullmann, and Antonio Kruger. 2021. Combining Dynamic Passive Haptics and Haptic Retargeting for Enhanced Haptic Feedback in Virtual Reality. *IEEE Trans. Visual. Comput. Graphics* 27, 5 (May 2021), 2627–2637. https://doi.org/10.1109/TVCG.2021.3067777

[297] Zhenishbek Zhakypov and Allison M. Okamura. 2022. FingerPrint: A 3-D Printed Soft Monolithic 4-Degree-of-Freedom Fingertip Haptic Device with Embedded Actuation. In *2022 IEEE 5th International Conference on Soft Robotics (RoboSoft)*, April 04, 2022. IEEE, Edinburgh, United Kingdom, 938–944. https://doi.org/10.1109/RoboSoft54090.2022.9762107

[298] Bowen Zhang and Misha Sra. 2021. PneuMod: A Modular Haptic Device with Localized Pressure and Thermal Feedback. In *Proceedings of the 27th ACM Symposium on Virtual Reality Software and Technology*, December 08, 2021. ACM, Osaka Japan, 1–7. https://doi.org/10.1145/3489849.3489857

[299] Pengcheng Zhang, Qingxin Yang, Xian Zhang, Yang Li, and Yongjian Li. 2017. Comparative Study of Metal Obstacle Variations in Disturbing Wireless Power Transmission System. *IEEE Transactions on Magnetics* 53, 6 (June 2017), 1–4. https://doi.org/10.1109/TMAG.2017.2657517

[300] Tengxiang Zhang, Xin Yi, Chun Yu, Yuntao Wang, Nicholas Becker, and Yuanchun Shi. 2017. TouchPower: Interaction-based Power Transfer for Power-as-needed Devices. *Proc. ACM Interact. Mob. Wearable Ubiquitous Technol.* 1, 3 (September 2017), 1–20. https://doi.org/10.1145/3130986

[301] Yang Zhang, Yasha Iravantchi, Haojian Jin, Swarun Kumar, and Chris Harrison. 2019. Sozu: Self-Powered Radio Tags for Building-Scale Activity Sensing. In *Proceedings of the 32nd Annual ACM Symposium on User Interface Software and Technology*, October 17, 2019. ACM, New Orleans LA USA, 973–985. https://doi.org/10.1145/3332165.3347952

[302] Yang Zhang, Gierad Laput, and Chris Harrison. 2017. Electrick: Low-Cost Touch Sensing Using Electric Field Tomography. In *Proceedings of the 2017 CHI Conference on Human Factors in Computing Systems - CHI '17*, 2017. ACM Press, Denver, Colorado, USA, 1–14. https://doi.org/10.1145/3025453.3025842

[303] Yang Zhang, Chouchang (Jack) Yang, Scott E. Hudson, Chris Harrison, and Alanson Sample. 2018. Wall++: Room-Scale Interactive and Context-Aware Sensing. In *Proceedings of the 2018 CHI Conference on Human Factors in Computing Systems - CHI '18*, 2018. ACM Press, Montreal QC, Canada, 1–15. https://doi.org/10.1145/3173574.3173847

[304] Huichan Zhao, Aftab M. Hussain, Ali Israr, Daniel M. Vogt, Mihai Duduta, David R. Clarke, and Robert J. Wood. 2020. A Wearable Soft Haptic Communicator Based on Dielectric Elastomer Actuators. *Soft Robotics* (January 2020), soro.2019.0113. https://doi.org/10.1089/soro.2019.0113

[305] Clement Zheng and Ellen Yi-Luen Do. 2018. Mechamagnets: Tactile Mechanisms with Embedded Magnets. In *Proceedings of the Twelfth International Conference on Tangible, Embedded, and Embodied Interaction - TEI '18*, 2018. ACM Press, Stockholm, Sweden, 57–64. https://doi.org/10.1145/3173225.3173268

[306] Clement Zheng, Jeeeun Kim, Daniel Leithinger, Mark D. Gross, and Ellen Yi-Luen Do. 2019. Mechamagnets: Designing and Fabricating Haptic and Functional Physical Inputs with Embedded Magnets. In *Proceedings of the Thirteenth International Conference on Tangible, Embedded, and Embodied Interaction - TEI '19*, 2019. ACM Press, Tempe, Arizona, USA, 325–334. https://doi.org/10.1145/3294109.3295622

[307] Kening Zhu, Simon Perrault, Taizhou Chen, Shaoyu Cai, and Roshan Lalintha Peiris. 2019. A sense of ice and fire: Exploring thermal feedback with multiple thermoelectric-cooling elements on a smart ring. *International Journal of Human-Computer Studies* 130, (October 2019), 234–247. https://doi.org/10.1016/j.ijhcs.2019.07.003

[308] Oldrich Zmeskal, Lucie Marackova, Tereza Lapcikova, Premysl Mencik, and Radek Prikryl. 2020. Thermal properties of samples prepared from polylactic acid by 3D printing. 2020. Smolenice, Slovakia, 020022. https://doi.org/10.1063/5.0033857

[309] 1988. Sampling and Analytical Methods, Chemical Sampling Information for Acetone. Retrieved from https://www.osha.gov/sites/default/files/methods/osha-69.pdf

[310] 2011. *IEC 60601-1-SER* ([Ed. var.] ed.). IEC, Geneva.

[311] F-TEM (Flexible-thermoelectric module) Part Number：DK-TEM es-02 Datasheet.

[312] https://infocenter.nordicsemi.com/pdf/nRF52840_PS_v1.1.pdf. Retrieved September 12, 2024 from https://infocenter.nordicsemi.com/pdf/nRF52840_PS_v1.1.pdf